

Aus dem Max-Planck-Institut für biophysikalische Chemie in Göttingen
Abteilung Zelluläre Biochemie
Direktor: Prof. Dr. Reinhard Lührmann

**Characterization of cytoplasmic bodies involved in
5' to 3' mRNA degradation in human cells**

Dissertation

zur Erlangung des Doktorgrades
der Mathematisch-Naturwissenschaftlichen Fakultäten
der Georg-August-Universität zu Göttingen

vorgelegt von

Maria Alexandra Andrei

Aus Bukarest, Rumänien

Göttingen 2007

D 7

Referent: Prof. Dr. Oliver Einsle

Korreferent: Prof. Dr. Reinhard Lührmann

Tag der mündlichen Prüfung: 4. Mai 2007

*To my family,
In loving memory of Bita and Tata*

Acknowledgements

I would like to express my most sincere appreciation to a number of people whose invaluable contributions have made this thesis possible.

I gratefully acknowledge Professor Reinhard Lührmann for providing me with the opportunity to complete this PhD work in his group, which proved to be a challenging and rewarding experience. I thank him for his support and giving me the great chance to grow with the young field of P bodies. Only owing to the trust he gave to me I am able to present this work today.

Special gratitude is expressed to Professor Detlef Doenecke for excellently chairing the GRK 521, through which this work was mainly financed. Without his positive attitude towards my research and constant encouragement in promoting these studies to a larger audience, this work might not have come to this end.

I wish to thank Prof. Oliver Einsle for kindly accepting to be my Doktorvater as well as to the other members of my committee: Prof. Michael Kessel, Prof. Gerhard Braus, Prof. Karen Hirsch-Ernst, Prof. Christiane Gatz and Prof. Ernst Wimmer.

To Dr. Rolando Rivera-Pomar I want to thank for nourishing my earliest interest in scientific research, for the inspiring optimism he conveyed.

At the end of my study, I wish to acknowledge the special mentoring I received from my university professors: Prof. Dana Iordachescu, Prof. Anca Dinischiotu, Prof. Marieta Costache, Prof. Radu Mester, who shaped my education, while in Bucharest. I owe many thanks to all members of AZB for the friendly working atmosphere and good tips throughout the years.

Particularly, this thesis benefited from the critical and constructive comments of Ira Lemm to whom I am thankful, in addition, for her readiness to answer all my queries.

To the head of the Mass Spectrometry Facility, Dr. Henning Urlaub, and to Uwe Pleßmann and Monika Raabe I thank for the mass spec work, which nevertheless added valuable information to my work.

I thank Markus Hossbach for patiently guiding my first steps in the cell culture lab and introducing RNA interference to me. To Gabriella Ficzi I am indebted for initiating me in the exiting technology of confocal microscopy. Jochen Deckert I thank for his willingness in sharing expertise in biochemical aspects of my work as

well as for his friendly help in solving many issues from the “Living in Germany” category. Gruss Gott!

I thank Markus Wahl, Mihaela Diaconu and Vlad Pena for helpful advice for protein expression and purification. To Reinhard Rauhut I thank for his immediate fixes to my computer problems.

I thank the “new generation” students, Elmar Wolf and Michael Grote for sustaining an optimistic atmosphere and making the time spent in the lab enjoyable. Keep so!

To the former members of our group, Dierk Ingelfinger and Nina Schaffert I want to thank for creating a stimulating working atmosphere.

I warmly thank my friends around the institute, Maria Doitsidou for her tremendous patience and understanding, for adding value to the leisure time here in Goettingen; my Romanian friends Mihaela Diaconu and Mara Pitulescu for all moments they were ready to share with me during these years and for helping me find the way out at many difficult times.

I want to thank my parents for the countless sacrifices they made to give me the best possible education. I am indebted to my mother for her persistent confidence and always standing behind me in all these years that I have been away from home. I dedicate this work to the memory of my dear grandmother and father with whom I would have so much wished to share this time.

I thank my brother Dan for his wit and for his cheerful spirit, I promise to keep working on that patent. Also, my great appreciation is for tanti Sanda who had gone together through most of the examinations I ever took. Thank you Andi, Alina for looking after me in those unforgettable trips to the Carpathians.

Thank you Baris for having enriched my life in more ways than you think. Seni öpüyorum.

Table of contents

1. Summary	1
2. Introduction.....	2
2.1 The many shapes of mRNA silencing	2
2.2 From protein composition to functional aspects of the P bodies	4
2.2.1 mRNA degradation pathways	6
2.2.2 RNA-dependent mRNA silencing	8
2.2.3 mRNA surveillance	11
2.3 The transition between mRNA translation and degradation.....	12
2.3.1 Translation initiation in eukaryotes.....	12
2.3.2. Coupling translation and mRNA turnover	13
2.3.3 Regulation of mRNA stability	16
3. Rationale	18
4. Materials and Methods.....	19
4.1 Materials	19
4.1.1 Equipment.....	19
4.1.2 Chemicals and consumables.....	20
4.1.3. Buffers and solutions.....	21
4.1.4 Growth media.....	21
4.1.5 Enzymes, antibodies and reaction kits	22
4.1.6 dsRNA synthetic oligonucleotides.....	23
4.1.7 DNA primers	24
4.1.8 DNA vectors	24
4.1.9 Software and World Wide Web resources	24
4.2 Methods	25
4.2.1 Microbiological methods	25
Culturing of bacteria.....	25
Preparation of chemically competent bacterial cells and transformation.....	25
4.2.2 Molecular biology methods.....	25
Isolation of plasmid DNA from bacteria.....	25
Isolation of total RNA from eukaryotic cells in culture	26
PCR and RT-PCR amplification.....	26
Site-directed mutagenesis.....	28
Molecular cloning	29
Sequencing of plasmid DNA	30
RNA Interference and validation of siRNA knockdown efficiencies.....	30
4.2.3 Cell biological methods.....	32
Cultivation of cell lines	32
Transfection of cell lines	33
TUNEL test for apoptosis detection	34
4.2.4 Biophysical methods	35
Immunofluorescence.....	35
Confocal laser scanning microscopy	35
Fluorescence recovery after photobleaching (FRAP).....	35
Fluorescence resonance energy transfer (FRET).....	36
4.2.5 Biochemical methods	37

Preparation of cytoplasmic extracts from eukaryotic cells in culture.....	37
HA- and Flag- Pull Down Assay	38
SDS polyacrylamide gel electrophoresis.....	39
Silver staining of protein gels.....	39
5. Results.....	41
5.1.1 The cap-binding translation initiation factor eIF4E is present in P bodies.....	41
5.1.1.1 The eIF4E Homologous Protein is present in P bodies.	42
5.1.2 Comparison of two cytoplasmic compartments- the Stress Granules and P bodies	43
5.1.3 The eIF4E-binding protein eIF4E-T is a component of P bodies	44
5.1.4 eIF4E interacts with eIF4E-T and rck/ p54 in P bodies.....	47
5.2. Factor requirements for the assembly of P bodies.....	49
5.2.1 Interdependence of degradation factors for accumulation in P bodies determined in an RNA interference screen	49
5.2.1.1 Validation of knockdown efficiency by real-time RT-PCR.....	49
5.2.1.2 Impact of the depletion of P body protein factors on their organization .	51
5.2.2 mRNA flux is required for the maintenance of P bodies	53
5.3 FRAP reveals a rapid exchange of P body components.	55
5.4 Intrinsic signals responsible for P body targeting and assembly.....	56
5.4.1 Mutagenesis analyses of eIF4E.....	57
5.4.2 Mutagenesis analyses of eIF4E-T	58
5.4.2.1 Implications of eIF4E-T interaction site mutagenesis on P body formation	58
5.4.2.2 Functional mapping of eIF4E-T domains.....	61
5.5 Biochemical investigations towards the elucidation of the P body composition	68
6. Discussion	71
6.1.1 The translation initiation factor eIF4E and the translation inhibitor eIF4E-T are P body residents.....	71
6.1.2 The translational repressor rck/ p54 is a P body resident.....	73
6.1.3 The eIF4E Homologous Protein is a P body resident.....	74
6.2.1 Depletion of P body proteins indicates a sequential assembly of the cytoplasmic structures and demonstrates the requirements for their assembly	75
6.2.2 Variation of the mRNA flux to the P bodies has immediate repercussion on the organization of the cytoplasmic structures	77
6.2.3 P bodies are dynamic but stable structures.....	78
6.3.1 Intact protein-protein interaction is vital for accurate targeting of the P body component eIF4E.....	78
6.3.2 P body destabilizing domains within eIF4E-T.....	80
6.4 Identification of novel P body components using biochemical purification coupled to MS analyses	80
7. References.....	82
Appendix	97
List of figures.....	97
List of tables.....	99
Curriculum vitae.....	100

1. Summary

In the context of gene expression regulation, discontinuing translation of mRNAs occurs by evolutionarily conserved mechanisms whose executors have been described to be associated with various types of cytoplasmic mRNA granules. Processing (P) bodies are such granules where mRNA co-localizes with effectors of the 5' to 3' mRNA degradation, RNA interference and Nonsense Mediated Decay pathways.

In this manuscript we demonstrate that the m⁷G cap-binding protein eIF4E and one of its interaction partners, eIF4E-Transporter, are also components of mammalian P bodies. We further show, by FRET, that they form a molecular complex with each other in P bodies in vivo. Additionally, eIF4E interacts with the translational repressor rck/p54. In contrast, other translation initiation factors such as eIF4G or components of the translation machinery were not detected in these cytoplasmic foci, ruling out the possibility that P bodies are sites where active translation can occur. It was possible to show that eIF4E requires that it is bound to the m⁷G cap of the mRNA and interact with eIF4E-T in order to be targeted to the P bodies. Altogether, eIF4E-T prevents the formation of a translationally active mRNP by interacting with eIF4E and thus plays a role in remodeling events that render mRNAs available for degradation. No particular sequence within eIF4E-T was found sufficient for its localization to the P bodies, but only the full-length eIF4E-T molecule could assemble inside these bodies.

Using RNAi-mediated knockdowns we observed that a subset of P body factors, including eIF4E-T, LSm1, rck/p54, and Ccr4 are required for the accumulation of each other and of eIF4E in P bodies. Furthermore, cycloheximide treatment of cells lead to disassembly of the entire structure, indicating that the accumulation of LSm1, eIF4E, eIF4E-T, and rck/p54 in P bodies also requires that an mRNA flux be available. These results suggest that these factors are targeted to P bodies as part of a larger mRNP complex and that they are essential for P body formation and function in mRNA processing. A block in the decay of the mRNA body upon depletion of the decapping enzyme Dcp2 or the exoribonuclease Xrn1, leads to an increase in the size and number of P bodies. A distinct hierarchy of remodeling steps and sequence of events can be inferred towards formation of the P bodies whereas early acting factors are represented by the deadenylase Ccr4, LSm1, eIF4E-T and rck/p54 and late joining factors include Dcp2 and Xrn1.

Mass spectrometric analyses helped to identify a novel RNA-binding protein residing in the P bodies, which has preference for Cytosine-rich elements and hints to a mechanism implying sequence-specific silencing of mRNAs inside the P bodies.

2. Introduction

Achieving control over the translational status and availability of messenger RNAs is a highly specific and efficient means of regulating gene expression. This includes tightly spatially and temporally regulated events that are needed in order to specify the intricate protein pattern required at any moment along the cellular cycle and within completion of the developmental programs in multicellular organisms, starting from a single cell. Discontinuing translation of the mRNAs occurs by evolutionarily conserved mechanisms and several ways by which this can be achieved have been described.

2.1 The many shapes of mRNA silencing

In different animal species cytoplasmic mRNA-protein granules have been observed and integrating the knowledge of their composition allowed for the understanding of their function. Thus, a suitable mean for controlling the space and time where and when a protein is to be expressed was for the cell to confine individual mRNAs within complexes containing regulatory proteins into distinct cytoplasmic domains. From these, mRNAs would be released or subjected to decay, as dictated by the environmental cues and in agreement with a distinct cellular program.

Morphological studies dating back to more than a century ago reported on the presence of polarized optical dense granules in insect larvae (Metschnikoff, 1865). From the numerous studies that followed it is known that these are specialized regions in the cytoplasm of eggs in a variety of organisms and they contain the determinant(s) responsible for the differentiation of germ cells. This so-called germ-plasm is organized into germline granules termed P granules in *Caenorhabditis elegans* (Strome and Wood, 1982), polar granules in *Drosophila melanogaster* (Mahowald, 1962) or germinal granules in *Xenopus laevis* (Czolowska, 1969). Their composition was intensively investigated and work of the past three decades established that they represent ribonucleoprotein (RNP) particles containing maternally synthesized mRNAs coated with a particular set of proteins, vastly overlapping among different

species. This protein combination is needed for the transport and precise localization of the mRNAs as well as for controlling the timing of their translational activation during oogenesis, oocyte maturation and early embryogenesis. Examples of factors conserved in different animals include the helicase CGH-1 (Navarro et al., 2001, Navarro and Blackwell, 2005), Me31B (Nakamura et al., 2001), Xp54 (Smillie and Sommerville, 2002) that was shown to be necessary for translational regulation and repression (Weston and Sommerville, 2006). Also, an RNA-binding protein Staufen is needed for the microtubule-dependent transport and localization as well as for translational derepression of maternal mRNA in oocytes (St. Johnston et al., 1992, Micklem et al., 2000).

Synaptic plasticity is achieved in the mammalian nervous system by controlling protein synthesis at specific time-points and subcellular locations within neurons. For this, mRNAs that are synthesized and accumulate in the neuronal cell body need to be transported via axons to their sites of translation, into dendrites. This translocation and correct positioning occurs in the shape of discrete motile structures referred to as neuronal RNA granules (Knowles et al., 1996, reviewed in Kiebler and Bassell, 2006). These macromolecular structures are responsible for the translational arrest of the resident mRNAs during transport, as suggested by the presence of the RNA-binding protein Staufen (Kiebler et al., 1999). Localized protein synthesis is only activated once they reach their destination in the dendrite, upon synaptic stimulation by specific signals (Krichevsky and Kosik, 2001). Further analyses of *Drosophila* neuronal granules have shown that they contain not only maternal translational control and RNA-transport molecules (Staufen, Barentz, Yps, eIF4E, Cup), but also factors of the miRNA (Argonaute-2), NMD (UPF1) and RNA degradation (DCP1, Pacman/ Xrn1, Me31B) pathways (Barbee et al., 2006).

Over a century ago a perinuclear cytoplasmic granule was observed in spermatogenic cells (Benda, 1891) and was named chromatoid body. This has a similar structure and composition to that of the *Drosophila* germplasm (nuage) and is also proposed to function in RNA processing and storage (Parvinen, 2005). Additionally, components of the miRNA pathway, as well as the decapping enzyme subunit Dcp1, the 5' to 3' exoribonuclease Xrn1 and the RNA-binding protein GW182 were identified to accumulate in the chromatoid body (Kotaja et al., 2006).

In mammalian cells that are exposed to various stress conditions, such as heat shock, UV irradiation or oxidative stress, translation of mRNAs is inhibited upon phosphorylation of eIF2 α subunit. In turn, this inhibits the addition of the initiator

tRNA^{Met} to the 48S pre-initiation complex. These mRNAs that are inactivated into stalled translation pre-initiation complexes in response to stress are sequestered in the cytoplasm within the stress granules (Kedersha and Anderson, 2002, Kimball et al., 2003).

But, not only stored mRNA destined for later (re)-activation is concentrated in such cytoplasmic granules. The youngest of the cytoplasmic mRNP granules studied so far are referred to as processing (P) bodies. Observations of the past decade could show that key factors of the 5' to 3' deadenylation dependent mRNA degradation pathway are enriched in distinct cytoplasmic foci of mammalian cells (Bashkirov et al., 1997, Ingelfinger et al., 2002, van Dijk et al., 2002). Similar foci in yeast were additionally shown to contain mRNA degradation intermediates suggesting that these foci are centers of active mRNA decay (Sheth and Parker, 2003, Cougot et al., 2004). Moreover, effector components of the RNAi machinery, the Argonaute proteins (Liu et al., 2005, Sen and Blau, 2005), together with miRNAs and their repressed mRNA targets also localize to P bodies (Pillai et al., 2005). These cytoplasmic speckles did not co-localize with markers for other known, membrane-bound cytoplasmic organelles, such as the Golgi apparatus, endosomes, lysosomes or peroxisomes (Eystathiou et al., 2002).

Taken together, these data point out that RNA granules with a similar core composition function in evolutionarily similar mechanisms that have evolved in order to control gene expression by concerted regulation of the localization and translational in/activation of selected or bulk mRNAs. This is attained through a complex and dynamic reshaping process of the mRNP particles.

2.2 From protein composition to functional aspects of the P bodies

Numerous research efforts in the recent years have aimed at deciphering the composition and the underlying mechanisms of the P bodies, which appear to be regular cytoplasmic components observed in various eukaryotic models, from *Saccharomyces* to mammalian cells. Compiled in table 2.1 are protein components of the P bodies identified in different organisms and listed according to the specific pathway in which they are involved. From this table, it becomes apparent that components of three major post-transcriptional regulatory pathways are physically interconnected in the P bodies, namely 5' to 3' mRNA degradation, RNA interference and mRNA surveillance (NMD).

P body component	Species	Function	Reference
CCR4 /NOT	<i>Hs, Sc</i>	Deadenylase complex	Cougot et al., 2004 Sheth & Parker, 2003
<i>Xrn1</i>	<i>Hs, Mm, Dm</i> (Pacman), <i>Sc</i> (Kem1)	5'to 3'exoribonuclease	Ingelfinger, et al, 2002 Bashkirov et al., 1997 Barbee et al., 2006
<i>Dcp1</i>	<i>Hs, Sc, Dm, Ce</i> (DCAP-1)	Decapping enzyme co-activator subunit	van Dijk et al., 2002 Sheth & Parker, 2003 Lall et al., 2005
<i>Dcp2</i>	<i>Hs, Sc, Dm, Ce</i> (DCAP-2)	Decapping enzyme	Same as for <i>Dcp1</i>
<i>RCK/p54</i>	<i>Hs, Sc</i> (Dhh1), <i>Ce</i> (CGH-1), <i>Dm</i> (Me31B)	Decapping co-activator helicase, translational regulator	Cougot et al., 2004 Sheth & Parker, 2003 Nakamura et al., 2001
LSm1-7	<i>Hs, Sc</i>	Decapping co-activator	Ingelfinger, et al., 2002 Sheth & Parker, 2003
Pat 1	<i>Hs, Sc, Dm</i> (CG5208)	Decapping co-activator	Unpublished observation Sheth & Parker, 2003 Eulalio et al., 2007
<i>LSm 14</i> (RAP55)	<i>Hs, Mm, Xl, Ce</i> (CAR-1), <i>Dm</i> (Tra1), <i>Sc</i> (Scd6p)	Translational repressor	Yang et al., 2006 Tanaka et al., 2006 Audhya et al., 2005 Barbee et al., 2006
LSm 16 (EDC3)	<i>Hs, Sc</i>	Enhancer of decapping (co-activator)	Kshirsagar & Parker, 2004
<i>eIF4E</i>	<i>Hs, Dm</i>	Cap-binding protein	Andrei et al., 2005 Barbee et al., 2006
<i>eIF4E-T</i>	<i>Hs, Dm</i> (Cup), <i>Mm</i> (Clast4)	eIF4E-binding, translational repression	Andrei et al., 2005 Wilhelm et al., 2003 Villaescusa et al., 2006
<i>CPEB</i>	<i>Hs, Xl</i>	Translational regulator	Wilczynska et al., 2004
<i>Staufen</i>	<i>Dm</i>	mRNA localization	Barbee et al., 2006
<i>Argonaute proteins</i>	<i>Hs, Ce, Dm</i>	Effectors in siRNA and miRNA silencing pathways	Liu et al., 2005a Barbee et al., 2006
<i>GW 182</i>	<i>Hs, Ce</i> (AIN-1), <i>Dm</i>	miRNA pathway	Eystathiou et al., 2002 Ding et al., 2005 Rehwinkel et al., 2005
SMG7, SMG5*	<i>Hs</i>	Non-sense mediated mRNA decay (NMD)	Unterholzner & Izaurralde, 2004
UPF1*	<i>Hs, Dm, Sc</i>	NMD	Unterholzner & Izaurralde, 2004
<i>TTP</i>	<i>Hs</i>	AU-rich element- mediated mRNA decay	Kedersha et al., 2005

Table 2.1. Protein composition of P bodies. Components in italics represent proteins that are additionally present in other types of RNA granules. *Hs* stands for *Homo sapiens*, *Sc* for *Saccharomyces cerevisiae*, *Ce* for *Caenorhabditis elegans*, *Dm* for *Drosophila melanogaster*, *Xl* for *Xenopus laevis*, *Rn* for *Rattus norvegicus*, *Mm* for *Mus musculus*. In brackets are indicated orthologs of the human proteins, as denominated in the different species (second column). *SMG5 and UPF1 localization to P bodies becomes apparent upon overexpression of SMG7. Modified from Eulalio et al., 2007.

2.2.1 mRNA degradation pathways

Deadenylation independent mRNA decay

In the deadenylation independent mechanism, it was shown that removal of the poly (A) tail is not a prerequisite for an initial internal cleavage of the mRNA by an endoribonuclease activity to take place, which labels the transcript for degradation. However, this pathway has been described to occur for only few mRNAs and it is probably a specific means to allow for a fast response which bypasses the general deadenylation dependent pathway (Wang and Kiledjian, 2000). In *Drosophila*, decay of non-sense transcripts was observed to initiate with an endonucleolytic cleavage followed by 5' to 3' and 3' to 5' exonucleolysis of the resulting two fragments (Gatfield and Izaurralde, 2004).

Deadenylation dependent mRNA decay

The deadenylation-dependent mRNA degradation can occur by two alternative pathways, namely the 3' to 5' or 5' to 3' decay.

The 3' to 5' exosomal mRNA decay

The 3' to 5' degradation of mRNAs is accomplished by the exosome which comprises ten 3' to 5' conserved exonucleases and is found in both the nucleus and the cytoplasm. The nuclear exosome complex is involved in 3' processing of the precursors to stable RNAs, surveillance and degradation of aberrant nuclear pre-mRNAs, pre-rRNAs or pre-tRNAs precursors (reviewed in Houseley et al., 2006). The cytoplasmic exosome performs the 3' degradation of normal mRNAs, as well as of those targeted by surveillance mechanisms. For example, mRNAs containing premature termination codons (PTCs) are removed in **Nonsense Mediated Decay** (reviewed in Amrani et al., 2006), whereas mRNAs that lack translation termination codons are eliminated in **Non Stop Decay** (Frischmeyer et al., 2002) with the participation of the exosomal activities. It was shown that the exosomal RNA decay is stimulated by AU-rich elements of the mRNA and was previously considered to be the main mRNA degradation pathway in human (Chen et al., 2001, Mukherjee et al., 2002).

The 5' to 3' mRNA decay

Over a decade ago, work done in bakers' yeast started to elucidate the scaffold of an mRNA decay machinery, which degrades the transcript in a deadenylation-dependent manner, in the 5' to 3' direction. Degradation of bulk mRNA is initiated by trimming of the poly (A) tail by the poly (A)-specific nuclease, PAN (Lowell et al., 1998). Then, deadenylation is completed by the primary cytoplasmic deadenylase Ccr4/Caf1p (Tucker et al., 2001). Since the 3' end poly (A) tail and the 5' end m⁷G cap structure are known to synergistically cooperate for enhancing translation (Sachs et al., 1997), deadenylation of the transcript is in turn a trigger for removal of the cap of the mRNA.

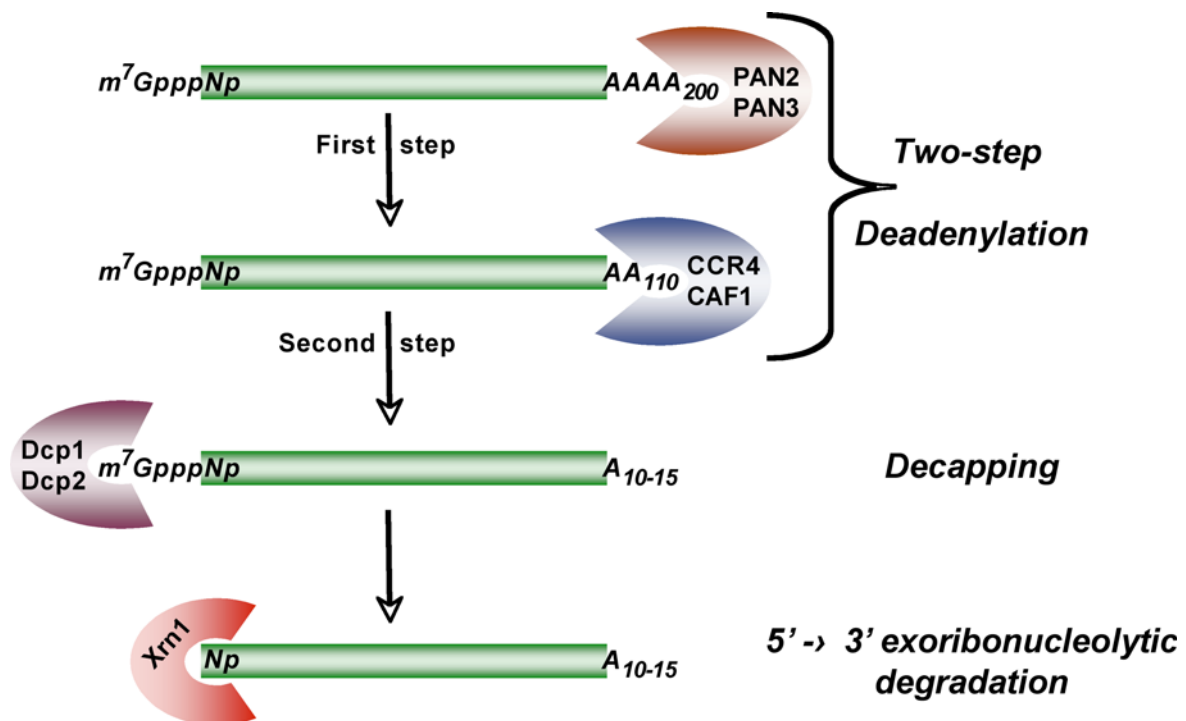


Figure 2.1. Current model of mammalian 5' to 3' mRNA degradation pathway. Degradation starts with deadenylation of the mRNA effected in two steps. An initial trimming of the poly(A) tail down to ~ 110 nt is performed by the poly(A) nuclease PAN2-PAN3 complex (Yamashita et al., 2005); in the second phase, PAN2-PAN3 is replaced by CCC4-CAF1 deadenylase complex which removes the rest of the poly(A) tail. Following removal of the m⁷G cap by the decapping enzyme subunits Dcp1-Dcp2, the mRNA body is susceptible to decay by the 5' to 3' exoribonuclease Xrn1. Modified from Mühlemann, 2005.

This is achieved by a complex consisting of Dcp1p and Dcp2p (La Grandeur and Parker, 1998, Dunckley and Parker, 1999). The 5' cap of the eukaryotic mRNAs is an important stability determinant as it protects the translationally competent transcripts against 5' exonucleolytic decay. Hence, decapping is a step where several regulatory factors act as translational repressors, in synergy with the decapping

enzymes. This is the case with the decapping activators Dhh1 and Pat1, which were shown to stimulate translational repression and promote degradation of the mRNA (Coller and Parker, 2005). A set of seven Sm-like proteins, Lsm1p-7p has been described to form a heteromeric ring complex, which interacts with deadenylated mRNAs (Bouveret et al. 2000). In addition, this complex is required for efficient mRNA decapping to take place (Tharun et al. 2000). It could be determined that decapping plays an important role as a determinant of an mRNA's half-life as short-lived mRNAs decap rapidly whereas longer-lived mRNAs decap more slowly (Muhlrad et al. 1994, 1995).

Following deadenylation and decapping, mRNAs are subject to 5' to 3' exonucleolytic degradation by a processive exoribonuclease, Xrn1p (Hsu and Stevens, 1993).

Mammalian homologues of most of these proteins, which are structurally and functionally similar to the yeast proteins, have been identified indicating that this mRNA degradation pathway is conserved in mammals: hCcr4 (Albert et al. 2000, Chen et al., 2002), hDcp1/2 (Lykke-Andersen, 2002, Wang et al., 2002), mXrn1 (Bashkirov et al., 1997), hLSm1-7 (Achsel et al., 1999).

Fluorescence microscopy observations revealed that the players of the 5' to 3' mRNA degradation pathway (hDcp1/2, hLSm1-7, hXrn1) are concentrated in distinct foci in the cytoplasm of human HEK, HeLa, monkey COS-7, and mouse 3T3 cells (Ingelfinger et al., 2002, van Dijk et al., 2002, Cougot et al., 2004). Furthermore, these foci contain at least one mRNP protein, GW182 (Eystathiou et al., 2003). Similar foci are observed in yeast, and by use of engineered transcripts that contain a strong secondary structure which puts a block to decay by the Xrn1 nuclease, it was possible to show that degradation intermediates accumulate in these structures, suggesting that they are mRNA processing centers (Sheth and Parker, 2003).

2.2.2 RNA-dependent mRNA silencing

Post-transcriptional gene silencing (PTGS) by non-coding RNAs through the RNA interference (RNAi) pathways represents a sequence-specific gene expression inhibition process that has been observed as an evolutionarily conserved phenomenon of eukaryotes, from fission yeast, plants and up to mammals. The

determinants of these gene-silencing events are nucleic acids, which initiate the assembly of repressor RNA-protein complexes and have been divided into two classes: the small interfering RNAs (siRNAs) and the microRNAs (miRNAs).

siRNAs are 21-nucleotide-long RNA regulators with perfect complementarity to an mRNA sequence that will be targeted for endonucleolytic cleavage (Elbashir et al., 2001), followed by degradation of the resulting fragments by the exosome and by Xrn1 (Orban and Izaurralde, 2005). miRNAs comprise a large family of 20 to 22-nucleotide-long regulatory RNAs expressed in plants and metazoan animals. In plants, the miRNAs have near perfect complementarity to RNA targets (Rhoades et al., 2002), mediate their cleavage, (Tang et al., 2003) and trigger degradation of the cognate mRNA, similarly to the siRNAs. In contrast, animal miRNAs exhibit limited complementarity to their targets and bind imperfectly to the 3' UTR of their target mRNA and inhibit protein synthesis by mechanisms which are still under debate.

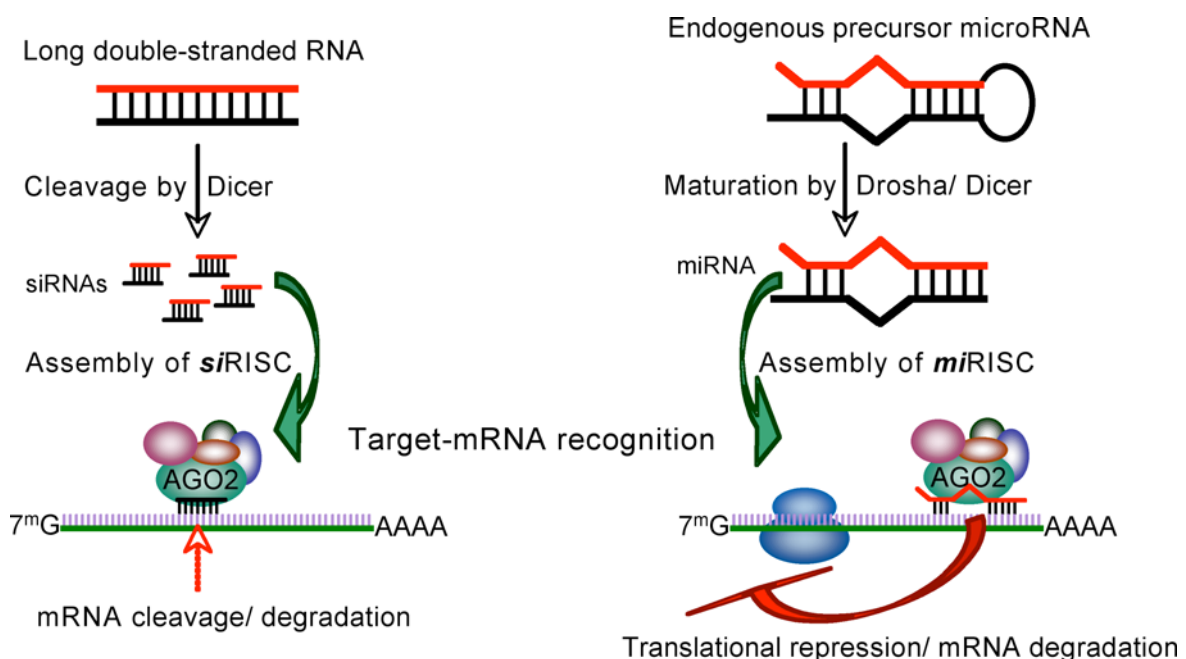


Figure 2.2. Biogenesis of and post-transcriptional gene regulation by siRNAs and miRNAs. Small interfering RNAs (siRNAs) are Dicer (RNase III-type enzyme) cleavage products generated from double-stranded RNA substrates (left picture). siRNAs are incorporated into RNA-Induced Silencing Complexes (RISC). Mature, activated siRISC contains the guide (antisense) RNA strand which binds to the complementary sequence in the target mRNA. Argonaute 2 protein (AGO2) of siRISC provides the catalytic activity for cleavage of the cognate mRNA, which will next be degraded. Precursor micro-RNAs (right picture) are cleaved in the nucleus by Drosha (RNase III-like enzyme). In the cytoplasm Dicer further processes the pre-miRNAs into mature miRNAs, which are subsequently loaded into miRISC. This silencing complex binds to several sites within the target mRNA and forms bulges and mismatches in the non-complementary region, resulting in translation inhibition and/or degradation of the cognate mRNA.

In spite of their different biogenesis and mechanisms employed for gene silencing, both siRNAs and miRNAs assemble into an Argonaute-containing effector RNP complex referred to as RNA-Induced Silencing Complex (siRISC or miRISC). RISC is responsible for recognition of the cognate mRNA sequence with the Argonaute proteins representing its core catalytic components (Bartel, 2004, Rivas et al., 2005) that were described to localize to the P bodies (Liu et al., 2005a). Argonaute family of proteins has been viewed as the molecular scaffold, which presents the guide-RNA molecules of RNA silencing pathways to their complementary targets (Parker and Barford, 2006). In *Drosophila*, distinct roles could be attributed to different Argonautes, such as in the RNAi pathway mediated by siRNAs where Argonaute 2 is catalyzing the cleavage of the transcript, while Argonaute 1 was shown to function in miRNA-mediated translational repression (Okamura et al., 2004).

Prior to the mi/siRNA:mRNA contact mediated by base-pairing of complementary regions, the interaction of RISC with the target mRNA may also be influenced by several Argonaute interaction partners. These include the RNA-binding protein GW182, the RNA helicase Rck/p54 as well as the decapping enzyme subunits Dcp1 and Dcp2 (Liu et al., 2005b, Chu and Rana, 2006, Liu et al., 2005a), which were found among components of known complexes residing in the P bodies. Particularly, depletion of GW182 in *Drosophila* resulted in an up-regulation of transcripts from to the category of predicted and validated miRNA targets, suggesting that GW182 plays a key role in the RISC-mediated silencing pathway (Behm-Ansmant et al., 2006). This is similar to results obtained upon depletion of Argonaute 1 (in *Drosophila*, Rehwinkel et al., 2005), or Argonaute 2 (in human HEK293 cells, Schmitter et al., 2006), indicating that Argonaute and GW182 act in the same silencing pathway. One way that miRNAs use to regulate gene expression is by targeting transcripts for decay (Bagga et al., 2005, Lim et al., 2005) and the fact that GW182 depletion lead to an increase in the level of transcripts which are common miRNA targets implicates GW182 in silencing by triggering decay of the mRNA by the 5' to 3' degradation pathway. Consistently, this mode of silencing could be reversed by depletion of the deadenylase subunits Caf1 and NOT1, as well as by depletion of the decapping enzyme subunits Dcp1 and Dcp2, whereby stabilization of a reporter target mRNA was achieved (Behm-Ansmant et al., 2006).

Another means by which miRNAs regulate mRNA expression is via inhibition of protein synthesis (Humphreys et al., 2005). miRNAs have been visualized, together with their target, translationally repressed mRNAs inside the P bodies and this is consistent with a role of these foci in maintaining an environment unfavorable for translation (Pillai et al., 2005). Interestingly, the P body component rck/p54 helicase, which was initially considered as a component of the 5' to 3' degradation machinery, was shown to be required for miRNA-mediated translational repression, as part of miRISC (Chu and Rana, 2006).

Despite the numerous recent reports that provide mechanistic insights to silencing by the RNA interference machinery, further analyses are required in order to be able to devise a unified model of the RNA-regulated mRNA metabolism.

2.2.3 mRNA surveillance

Elaborate mRNA quality control mechanisms operating both in the nucleus and the cytoplasm have evolved in order to ensure that only fully processed, error-free mRNAs become translated into proteins (Fasken and Corbett, 2005). Nonsense mediated decay (NMD) is an extensively characterized surveillance pathway responsible for the recognition and targeting for destruction of aberrant mRNAs that contain premature stop codons (PTC). The principal effectors of NMD are the conserved UPF1-3 proteins and their regulators SMG1 (catalyzing phosphorylation of UPF1), and SMG5-7 (mediating dephosphorylation of UPF1). Upon assembly of the NMD effectors to the mRNA undergoing premature translation termination, the surveillance complex recruits the enzymes of mRNA decay, ensuring for accelerated degradation of the abnormal transcript (Eulalio and Izaurralde, 2007). Following the observation that overexpression of SMG7 recruits UPF1 to P bodies in human cells (Unterholzner and Izaurralde, 2004), Sheth and Parker (2006) made use of reporter RNA harboring a PTC and showed that in yeast NMD involves targeting of PTC-containing substrates to P bodies in a UPF1-mediated fashion.

2.3 The transition between mRNA translation and degradation

2.3.1 Translation initiation in eukaryotes

A distinct feature of eukaryotic genes is that they are discontinuous and transcribed individually into monocistronic mRNAs. Following nuclear maturation events that include pre-mRNA capping, splicing and polyadenylation, mRNAs are exported into the cytoplasm where they are translated into proteins. Three steps can be distinguished during protein synthesis, namely initiation, elongation and termination. Compared to translation elongation and termination that are performed by a limited set of factors, the initiation step is assisted by a complex machinery and it is thus a level where intricate regulatory mechanisms act, including those which discontinue translation of the mRNA (reviewed in Gebauer and Hentze, 2004).

Translation initiation includes assembly of the 80S ribosome and its positioning on the AUG initiator codon. This includes events prior to the reaction by which the first peptide bond is formed. The most common, cap-dependent eukaryotic translation initiation system employs the m⁷G cap present at the 5' end of all cellular mRNAs as an anchor site for the translation initiation machinery (Shatkin, 1976). Initially, the translation initiation factor eIF4E binds to the m⁷G cap and further interacts with the eIF4A-bound eIF4G forming the eIF4F holoenzyme complex (Gingras et al., 1999) which mediates recruitment of the small ribosomal subunit to the 5' end of the mRNA. A 43S pre-initiation complex is formed by the small ribosomal subunit, 40S, the translation initiation factors 1, 1A, 3 and 5 as well as a ternary complex containing the GTP-bound initiation factor 2 and the initiator Methionine-tRNA (see Fig. 2.3). Docking onto the mRNA of the 43S particle is mediated by the contact of the initiation factor 3 with the translation initiation factor eIF4G (Lamphear et al., 1995). By processive 5' to 3' scanning through the 5' untranslated region, the small ribosomal subunit relocates to the translation initiator AUG codon. Upon pairing with the initiator AUG codon, a stable 48S pre-initiation complex is formed. In a GTP-dependent reaction, the 60S ribosomal subunit joins the 48S particle forming an 80S initiation complex that is ready to perform the polypeptide synthesis (Pestova et al., 2000).

2.3.2. Coupling translation and mRNA turnover

As it becomes apparent from Fig. 2.3, structural elements of the eukaryotic transcript located in the 3' and the 5' UTRs- the poly (A) tail and the cap, respectively, are mediators of an RNP organization, which provides the context necessary for efficient translation to occur. The importance of this configuration has been demonstrated by several studies from which we learn that a cap and a poly(A) tail function cooperatively to promote the translation of an mRNA (Gallie, 1991, Tarun and Sachs, 1995). A key mediator of this arrangement is eIF4G which contains a conserved interaction sequence for the cap-binding factor eIF4E (Mader et al., 1995), as well as a binding site for the PABP (Tarun and Sachs, 1996), thus acting as a bridging factor that brings the two ends of the mRNA in proximity. Indeed, in a reconstitution study employing only a capped, polyadenylated mRNA and purified eIF4E, eIF4G and PABP proteins, it was possible to visualize the predicted circular RNA-protein complex (Wells et al., 1998). Furthermore, during translation, the eIF4E interaction with the PABP-bound eIF4G greatly stabilizes the physical association of eIF4E to the cap (von Der Haar et al., 2000, Kahvejian et al., 2005).

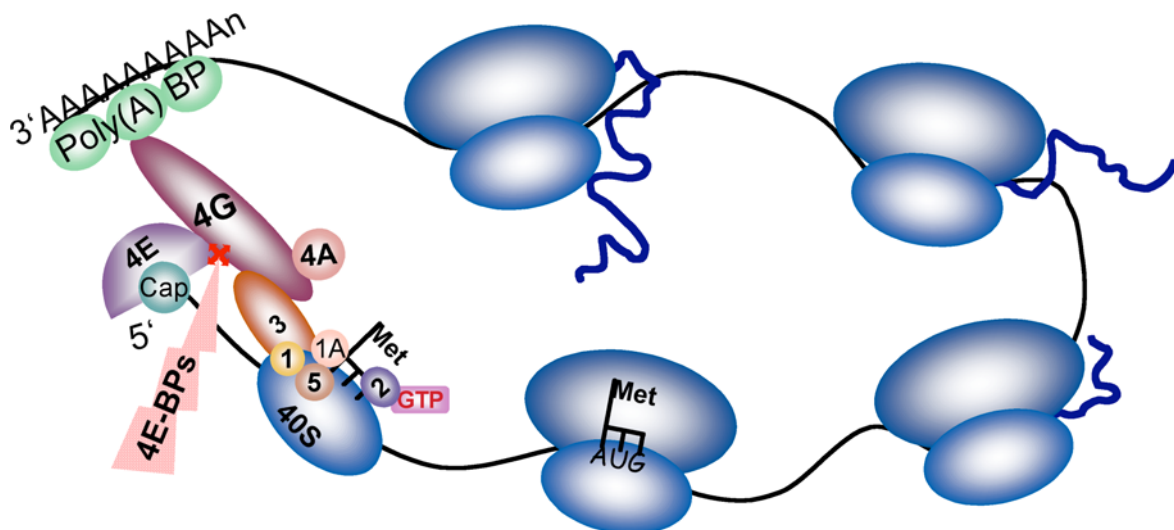


Figure 2.3. The closed loop model of cap-dependent translation. Translation initiation factors are depicted as coloured shapes, encoded by numbers as described in the text. The cap represents the m⁷G residue, at the 5' end of the mRNA (black line), whereas PABP stands for the Poly (A)-binding protein molecules attached to the adenosine residues situated in the 3' end of the mRNA. The red block arrow marks conserved interaction sites between eIF4E and its binding partners (4E-BPs), here, eIF4G. Due to the simultaneous interaction of eIF4G with PABP and eIF4E, circularization of the mRNA is induced.

During degradation of the mRNA, the cap and the poly (A) tail play important roles, too (Wilusz et al., 2001). Due to the dual role of the m⁷G cap in promoting assembly of a translation initiation apparatus and providing protection to the mRNA body against 5' to 3' exonuclease activity, a strict control of decapping is necessary as it represents a crucial switching point that inactivates and irreversibly targets the transcript for degradation. At the 3' end, PABP acts as an inhibitor of decapping by maintaining the mRNA in a stable translational loop through the interaction with eIF4G (Coller and Parker, 2004). Also, the translating mRNP is protected against removal of the m⁷G, in part by the tight association of the eIF4F initiation complex with the cap. Consistently, upon co-overexpression of eIF4E and of the eIF4G interacting domain resulted in an increased mRNA stability. In turn, mutations in the translation initiation factors negatively affect translation and result in an increase of decapping rates (Schwartz and Parker, 1999). In yeast, it was shown that following deadenylation, the mRNA coimmunoprecipitates with Pat1p, the LSm complex and the decapping enzyme subunits Dcp1/2p (Tharun and Parker, 2001). What has yet to be clarified is the critical transition at the 5' end of the mRNA that includes dislocation of the initiation complex eIF4F and accessing of the cap by the decapping complex (Schwartz and Parker, 2000, Vilela et al., 2000). Apart from removal of the poly(A) tail, which destabilizes the transcript, inhibitors of translation that directly interact with the cap-binding protein eIF4E may be involved. The general effect of their binding to eIF4E is mediated by sequestration of the cap binding protein, which results in repression of the translation of the bulk mRNA, as is the case with the eIF4E- Binding Protein (Haghighat et al., 1995) (Fig. 2.4).

In several regulatory systems discriminate binding to eIF4E can take place in order to control translation of specific transcripts. For example, an eIF4E- inhibitory protein also interacts with a particular RNA- binding protein that is anchored to its target response element, located on a particular transcript.

An intensively studied scheme in *Xenopus* oocytes comprises the eIF4E interacting protein Maskin, which also contacts CPEB, the Cytoplasmic Polyadenylation Element (CPE) Binding protein. In turn, CPEB interacts with the CPE region found in the 3' UTR of mRNAs with short poly(A) tails, which cannot be translated in this conformation (figure 6.1). Upon phosphorylation of CPEB, Maskin releases eIF4E and extension of the poly(A) tail is performed, creating a favorable mRNA substrate on which an active translational complex can assemble (Stebbins-Boaz et al., 1999,

Mendez et al., 2000). Moreover, human CPEB-1 was shown to be enriched in cytoplasmic foci containing Dcp1 and GW182 (Wilczynska et al., 2005).

Similarly to Maskin, Neuroguidin contains the eIF4E binding consensus motif and inhibits translation in a CPE-dependent fashion, by interacting with CPEB, too. Neuroguidin is widely expressed in the mammalian nervous system and was detected as puncta that resemble RNP granules, in both axons and dendrites (Jung et al., 2006).

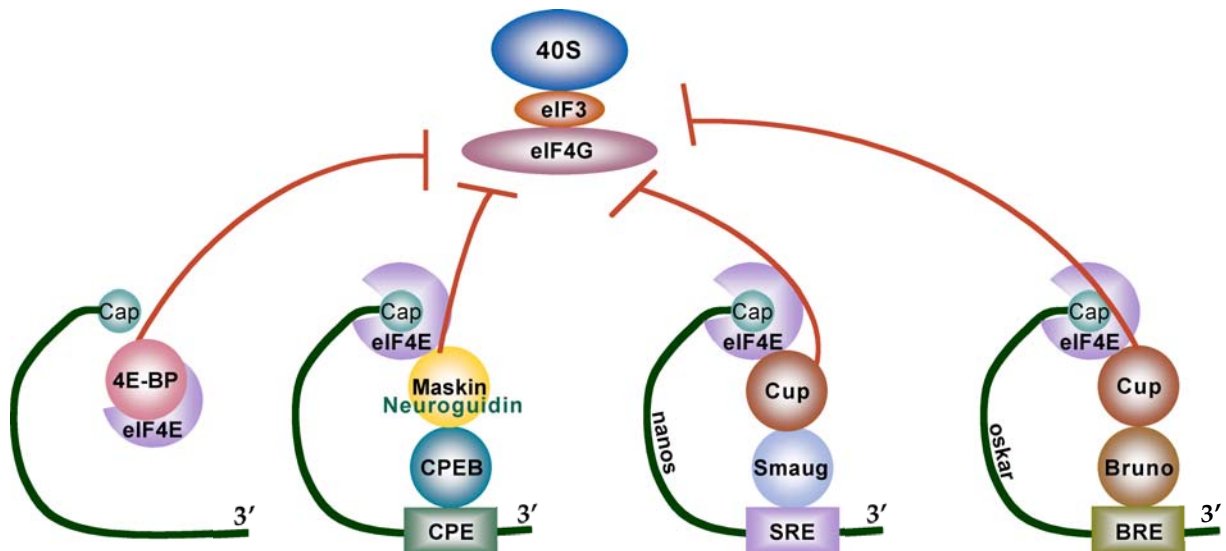


Figure 2.4. Translational repression mediated by eIF4E binding proteins. 4E-BP prevents formation of eIF4F initiation complexes by sequestering the free eIF4E. This inhibits translation of mRNAs, which require that high levels of eIF4E be available. Maskin and Cup can displace eIF4G from eIF4E when the latter is bound to cap structures of mRNAs containing specific 3' UTR sequences (cytoplasmic polyadenylation element CPE, Smaug Response Elements, SRE, and Bruno Response Element, BRE respectively). A protein binding this cis element (CPEB, Smaug and Bruno, respectively) also interacts with the eIF4E repressor protein (here Maskin or Neuroguidin and Cup), inhibiting translation. This mode of inhibition is thus achieved by tethering the eIF4E binding protein to specific mRNAs. Modified from Richter and Sonenberg, 2005.

In a different example from *Drosophila*, *oskar* mRNA, is known to contain in its 3' UTR a Bruno Response Element that mediates its translational repression upon binding of Bruno. Subsequently, Bruno interacts with the eIF4E-binding, repressor protein Cup. It thus acts as an adaptor protein connecting regulatory sequences in the 3' UTR to the 5' transcript end to yield a translationally compromised mRNA. This is required in *Drosophila* eggs during transport of maternal *oskar* mRNA from the nurse cells to the oocyte and until it is properly localized to the posterior pole (Wilhelm et al., 2003, Nakamura et al., 2004). Moreover, Me31B (P body component and homolog of rck/p54 in *Drosophila*) was found to specifically associate to

complexes containing Bruno, Cup and the repressed oskar mRNA (Chekulaeva et al., 2006).

In a functionally equivalent complex, translational repression of unlocalized nanos mRNA is mediated by two *cis* Smaug Response Elements, located in its 3' UTR (Dahanukar and Wharton, 1996). These stem-loop structures are bound by Smaug, which additionally interacts with Cup that in turn blocks assembly of a competent translation initiation complex at the eIF4E- bound cap structure (Nelson et al., 2004). Furthermore, it was recently reported that Smaug recruits the CCR4-NOT deadenylase complex to the nanos mRNA, supporting activation of its deadenylation and subsequent decay of the nanos transcript in the bulk cytoplasm of the early *Drosophila* embryo (Zaessinger et al., 2006). In contrast, stabilization and translation of nanos mRNA appear to be mediated by Oskar, which is thought to hinder Smaug binding to the SRE, and thus prevents recruitment of the deadenylase complex. Immunostaining experiments also pointed to the presence of Smaug, CCR4 and CAF1 (deadenylase subunit) in cytoplasmic foci containing Dcp1 and Pacman (the homolog of Xrn1 exoribonuclease in *Drosophila*) (Zaessinger et al., 2006).

2.3.3 Regulation of mRNA stability

Individual mRNAs were shown to have individual turnover rates. The rate of mRNA decay can be set by *cis*-acting elements within the mRNA, which are recognized by *trans*-acting factors that act by means of poorly understood mechanisms. The *cis*-acting sequences appear to have common motifs that are located in the 3' untranslated regions (UTR) of the transcripts and represent a docking site for regulatory proteins of the degradation machinery.

For example in mammals, several short-lived mRNAs encoding oncoproteins, cytokines and transcription or growth factors contain A-U-rich elements (AREs) in their 3' UTR. Generally, AREs promote rapid deadenylation and subsequently trigger degradation of the transcript by the exosome, in a 3' to 5' manner (Chen et al., 2001). Recent findings have shown that ARE containing mRNAs can also undergo degradation via the 5' to 3' deadenylation dependent decapping decay pathway (Stoecklin et al., 2006). Several ARE binding proteins (AUBPs) are involved in the regulation of the ARE-mediated decay processes. One example is HuR, which was

shown to selectively stabilize ARE-containing mRNAs against degradation (Fan and Steitz, 1998, Peng et al., 1998). In contrast, tristetraprolin (TTP), another AUBP, binds to AREs of TNF α and of other cytokine transcripts, promoting their degradation by recruitment and activation of the decay machinery (Lai et al., 1999, Lykke-Andersen and Wagner, 2005). Also, TTP was shown to collaborate with a miRNA to affect the decay rate of some mRNAs (Jing et al., 2005).

A stabilizing sequence element was described on the α -globin mRNA, which contains a cytosine-rich element in its 3'UTR. This is a nucleation site for a stabilizing α -complex that protects the α -globin against deadenylation-dependent decay, as well as from an endoribonucleolytic cleavage (Wang and Kiledjian, 2000).

3. Rationale

While several factors involved in mRNA degradation are known to be present in P bodies, many unanswered questions concerning the assembly and function of these foci remain and investigations of this thesis aimed at clarifying the following issues. For example, what are the factor requirements for the assembly of P bodies and how are degradation factors targeted to these sites? Are they imported independently of each other or as part of protein or mRNP complexes? And finally, what targets a translating mRNA to these structures and which factors are required to initiate the transition from translation to degradation within P bodies?

The transition of an mRNA from active translation to being committed for degradation has been proposed to involve one or more mRNP remodeling events (Tharun and Parker, 2001). Deadenylation is clearly a crucial determinant for initiating mRNA degradation, and thus factors involved in 3' end trimming may play an important role. In addition, factors interacting at the 5' end of the mRNA could also be involved. For example, a block in translation initiation could potentially trigger the degradation process and thus, translation initiation factors and proteins that repress their activity might also play a decisive role. However, whether translation factors are present in P bodies, and more importantly, whether they are required for P body formation were unknown facts and we addressed these in the present study.

The structure of the rearranged mRNP that is ultimately targeted to P bodies is also presently not known. To learn more factors comprising this mRNP we tried to purify complexes enriched in P body components and analyzed them by mass spectrometry. We analyze the connections established among several P body components in order to elucidate individual steps of the rearrangement of translating mRNP particle, towards its targeting to these sites. A knockdown screening of various factors using RNA interference was undertaken, through which the role of individual components in the P body assembly and stability is assessed. Mutagenesis of P body proteins coupled with fluorescence microscopy has been used in the quest for a putative P body-targeting signal. Altogether, these studies would further substantiate the understanding of the way these structures take on shape.

4. Materials and Methods

4.1 Materials

4.1.1 Equipment

„head-over-tail“-Rotor, Cole-Parmer, USA

Agarose gel electrophoresis chamber, Bio-Rad, München

Autoclave, Varioklav Steam sterilizer Tecnomara, Schweiz/H+P Labortechnik

Automated thermal cycler, Hybaid, USA

Cell Counter system CASY, TT Schärfe System, Reutlingen

Cooling Microcentrifuge Biofuge fresco, Heraeus

Heating block Eppendorf, Hamburg

Incubator BBD 6220 and BK-600, Kendro, USA

Magnetic stirrer RCT basic, Janke & Kunkel, Staufen i. Br.

Microscope: Inverted Zeiss LSM 510 META Zeiss, Jena Laser Scanning Microscope

Objectives: Plan NEOFLUAR 10x/0.3

Plan NEOFLUAR 20x/0.50

Plan NEOFLUAR 40x/1.3 oil

Plan APOCHROMAT 63x/1.4 oil

Milli-Q Ultrapure Water Purification System, Millipore, Schwalbach

NanoDrop® ND-1000 Spectrophotometer, NanoDrop Technologies

Opticon qRT- PCR cycler, MJ Research, USA

PAGE in-house made chambers

pH-Meter, Mettler Toledo, Schweiz

Power supply Power Pac 3000, Bio-Rad

Powersupply EPS 2A 2000, Hoefer Pharmacia Biotech, USA

Powersupply EPS 3501/XL, Amersham Pharmacia, Freiburg

Shaking incubator for microorganisms, Multitron Infors, Schweiz

Sorvall Centrifuge RC 5B/Evolution, Kendro, USA

Sorvall SLA-1500, Kendro, USA

Sorvall SS-34 Rotor, Kendro, USA

Spectrophotometer Ultraspec 3000 pro, Amersham PB, Freiburg

SpeedVac Lyophilizer Concentrator 5301, Eppendorf, Hamburg

Sterile hood Hera Safe, Class 2 Type H, Kendro, USA

Table Centrifuge Megafuge 1.0R, Heraeus

UV Gel documentation system: GelDoc system, Bio-Rad, München

Vortex, Janke & Kunkel, Staufen i. Br.

Water bath Type 1012, Gesellschaft für Labortechnik, Burgwedel

Waterbath HBR4 digital, Janke & Kunkel, Staufen i. Br.

4.1.2 Chemicals and consumables

Chemicals

2-Mercaptoethanol	Roth, Karlsruhe
Rotiphorese Gel 30 (30 % Acrylamide, 0.8 % Bis-Acrylamide)	Roth, Karlsruhe
Agarose (low melting point)	Invitrogen, The Netherlands
Agarose (NuSieve GTG)	BioWhittaker, USA
Ammoniumperoxodisulphate (APS)	Merck, Darmstadt
Ampicillin	Sigma, Deisenhofen
Bacto-Agar	Difco Laboratories, USA
Bovine serum albumin (BSA)	Sigma, Taufkirchen
Bradford-Dye	Bio-Rad, München
Bromphenolblue	Merck, Darmstadt
CASYton (isotonic solution)	Schärfe System, Reutlingen
Complete EDTA-free Protease Inhibitor Cocktail Tablets	Roche, Mannheim
Coomassie Brilliant Blue G250 (Protein determination)	Serva, Heidelberg
R250 (Staining of SDS-Gels)	Serva, Heidelberg
Cycloheximide	Sigma-Aldrich, Steinheim
Dithiothreitol (DTT)	Roth, Karlsruhe
DMSO (Dimethylsulfoxide)	Roth, Karlsruhe
Dulbecco's Modified Eagle Medium (DMEM)	Invitrogen, The Netherlands
EDTA (Dinatriumsalt Dihydrate)	Roth, Karlsruhe
Ethidiumbromide solution (10mg / ml)	Boehringer, Mannheim
Fetal Calf Serum (FCS)	GibcoBRL, Karlsruhe
Fugene 6	Roche, Mannheim
Glycerol	Merck, Darmstadt
Hepes (N-2-Hydroxyethylpiperazin-N-2-ethansulfonsäure)	Calbiochem, USA
Kaliumchloride	Roth, Karlsruhe
Kaliumphosphate	Sigma, Deisenhofen
Kanamycin	Roche, Mannheim
LB-Agar BIO 101 medium	Q-Biogene ,USA
LB-Liquid medium BIO 101	Q-Biogene ,USA
Mowiol 4-88	Calbiochem, USA
Natriumchloride	Roth, Karlsruhe
Natriumcitrate	Roth, Karlsruhe
Oligofectamine	Invitrogen, Karlsruhe
OptiMEM 1	Invitrogen, The Netherlands

Paraformaldehyde	Merck, Darmstadt
Penicillin/Streptomycin	Biochrom, Berlin
PMSF (Phenylmethylsulfonylfluoride)	Roche, Mannheim
Ponceau S	Serva, Heidelberg
Protein G Sepharose	Amersham Pharmacia, Freiburg
Puromycin (10mg/ml)	Sigma Aldrich
SDS (Natriumdodecylsulphate)	Serva, Heidelberg
Silver nitrate	Merck, Darmstadt
TEMED (N,N,N',N'-Tetramethylenethylenediamine)	Sigma, Taufkirchen
Tris-(hydroxymethyl)aminomethane (Tris)	Roth, Karlsruhe
Triton X-100	Sigma, Taufkirchen
Trypsin-EDTA	GibcoBRL, Karlsruhe
Xylene cyanol	FF Fluka, Schweiz

4.1.3. Buffers and solutions

6X DNA loading dye:	10X TBE:	10X PBS:
0.25% bromphenol blue	0,89 M Tris	0,2 M K ₂ HPO ₄
0.25% xylene cyanol	0,89 M Boric Acid	1,3 M NaCl
30% glycerol in water	25 mM EDTA pH 8	pH 7,4 or 8,0

Roeder A (hypotonic buffer):

10 or 20 mM HEPES/KOH pH 7.9 (or Tris/HCl pH 7.9/8.0)
 1.5 mM MgCl₂
 10 mM KCl
 0.5 mM DTE or DTT
 0.5 mM PMSF (of 0.1M isopropanol stock)
 protease inhibitor cocktail tablet EDTA free 1 tablet to 50 ml buffer

10 X Roeder B buffer (cytoplasmic extract buffer):

300 mM HEPES/KOH pH 7.9
 7.9
 1.4 M NaCl
 protease inhibitor cocktail tablet EDTA free

IPP150:

20 mM Tris/ HCl pH
 150 mM NaCl
 (0.1% Triton X 100)

10X Elution buffer (immunoprecipitation):

0.2 M HEPES/KOH pH 7.9
 1.5 M NaCl
 0.5 % Triton X 100
 5 mM DTT

4.1.4 Growth media

Luria-Bertani broth (LB medium):

1% (w/v) tryptone
 0.5% (w/v) yeast extract
 0.5% (w/v) sodium chloride

LB agar (plates): LB medium Bacto-agar (Gibco-BRL) 15 g added before autoclaving to 1L purified water. After autoclaving and cooling, ampicillin (50 µg/mL) or kanamycin (100 µg/mL) was added to the media.

Eukaryotic cell culture medium:

Dulbecco's Modified Eagle Medium (DMEM)
10% (v/v) Fetal Calf Serum (FCS)
100 U/ml Penicillin/100 µg/ml Streptomycin

Freezing medium:

DMEM
20% (v/v) FCS
10% (v/v) DMSO

4.1.5 Enzymes, antibodies and reaction kits

Calf intestinal phosphatase (CIP), restriction enzymes and corresponding digestion buffers were purchased from New England Biolabs (NEB, Schwalbach).

DNase I	Roche, Mannheim
Pfu Ultra DNA Polymerase	Stratagene, Heidelberg
SuperScript™ III One-Step RT-PCR System with Platinum® <i>Taq</i> High Fidelity	Invitrogen, Karlsruhe
Rapid DNA ligation kit	Roche, Mannheim
RNeasy Mini Kit	Qiagen GmbH, Hilden
QuantiTect SYBR Green RT-PCR Kit	Qiagen GmbH, Hilden
QuickChange® Site-Directed Mutagenesis Kit	Stratagene, Heidelberg
QIAquick PCR purification Kit	Qiagen GmbH, Hilden
QIAex Gel Extraction Kit	Qiagen GmbH, Hilden
QIAprep Plasmid mini/ midi prep kit	Qiagen (Hilden)
<i>In situ</i> Cell Death detection Kit	Roche, Mannheim
FLAG® Tagged Protein Immunoprecipitation Kit	Sigma, Deisenhofen
Anti-HA Affinity Matrix	Roche, Mannheim

1 kb or 100 bp DNA ladder from NEB, Schwalbach

Protein Standard (All Blue) marker from BioRad, Munchen

The following primary antibodies were used in this study in immunofluorescence (IF) or immunoprecipitation (IP):

affinity-purified anti-LSm1 polyclonal peptide antibodies (1:500 dilution, see (Ingelfinger et al., 2002) IF

rabbit anti-Xp54 (Ladomery and Sommerville, 1997, 1:200) IF

rabbit anti-Ccr4 (E.Wahle, 1:100) IF

rabbit anti-eIF4E and eIF4G serum (Naegele and Morley, 2004) IF

goat anti-eIF4G (1:400) , mouse anti-eIF4E (P-2, 1:800), and goat anti-eIF4E-T (E-18, 1:400) (purchased from Santa Cruz Biotechnology, Heidelberg) IF

Anti-FLAG-tag: mouse monoclonal antibody clone M2 from Sigma, Deisenhofen, IP

Anti-HA Rat monoclonal antibody (clone 3F10) from Roche, Mannheim, IP

The following secondary antibodies were purchased from Molecular Probes

Alexa Fluor 488 goat anti-mouse IgG (H+L)

Alexa Fluor 488 goat anti-rabbit IgG (H+L)

Alexa Fluor 647 chicken anti-rabbit IgG

Alexa Fluor 647 chicken anti-mouse IgG (H+L)

Alexa Fluor 647 donkey anti-goat IgG (H+L)

4.1.6 dsRNA synthetic oligonucleotides

The siRNA oligos have been designed by Markus Hossbach (Department Cellular Biochemistry, Max-Planck-Institute for Biophysical Chemistry, Göttingen) and synthesized in-house or at Ambion (USA). The chosen target sequences were aligned using BLAST (*Basic Local Alignment Search Tool*), against the human genome sequence (NCBI UniGene Database, <http://www.ncbi.nlm.nih.gov/BLAST/>), to lower the possibility of off-target reactivity. For use in RNA interference experiments, two complementary strands have to be annealed to generate the double stranded silencing effectors of RNAi. For this, equimolar concentrations of the single strands were mixed together with annealing buffer, incubated to denature at 90°C for 1 minute, then hybridized for 1 hour at 37°C (Elbashir *et al.* 2002). Successful annealing was evidenced by running the double-strands on a 4% NuSieve GTG agarose gel. The siRNA duplex should be stored frozen at -20°C and can be freeze-thawed many times without any further heat-shock treatment. To reduce the rate of hydrolysis, the solution containing the siRNA should be kept on ice during use.

2X Annealing-Buffer

200 mM KOAc

4 mM MgOAc

60 mM Hepes/KOH pH 7.4

double distilled H₂O

siRNA-Duplex mix

20 μM sense Oligonucleotide

20 μM antisense Oligonucleotide

2X Annealing-Buffer

4.1.7 DNA primers

DNA primers for use in PCR amplification have been synthesized at MWG Biotech (Martinsried).

4.1.8 DNA vectors

The following commercially available plasmids were used in this study:

pEYFP: This vector belongs to the Living color™ series of vectors from BD Biosciences (Clontech), which allow for the expression of enhanced green fluorescence protein (EGFP)-fusion proteins in mammalian cells. The C1-type vectors were used in which the protein of interest has a fused EGFP to the amino-terminus. The vector contains a kanamycin resistance gene for selection during amplification in *E. coli*.

pCMV Tag 2A: This vector purchased from Stratgene fuses the FLAG tag (amino acid residues DYKDDDK) to the protein of interest, to its amino-terminus. This vector allows for constitutive expression of the fusion protein in eukaryotic cells, owing to its cytomegalovirus promoter. The vector contains a kanamycin resistance gene for selection during amplification in *E. coli*.

Another vector we used, pcDNA-HA is a construct modified by T. Achsel, to express the protein of interest in eukaryotic cells, fused to the *Influenza* hemagglutinin (HA) tag sequence, at its amino-terminus. The vector contains an ampicillin resistance gene for selection during amplification in *E. coli*.

4.1.9 Software and World Wide Web resources

Adobe 6.0 Professional Adobe Systems, San Jose, CA, USA

Adobe Photoshop 7.0.1 Adobe Systems

DNAStar Lasergene v6 and Vector NTI: for DNA and protein sequence analysis
BLAST (Basic local alignment search tool) on NCBI Homepage NCBI
www.ncbi.nlm.nih.gov/BLAST/

ExPASy Proteomics Server (Expert Protein Analysis System) Swiss Institute of Bioinformatics (SIB) www.expasy.org

Microsoft Office Applications Microsoft, Unterschleißheim

NCBI Homepage database for DNA, proteins, literature, etc: www.ncbi.nlm.nih.gov

Zeiss LSM 510 software for database and image handling

Matlab/DIP image: Matlab and the Matlab toolbox DIPImage from Delft University (available at <http://www.ph.tn.tudelft.nl/DIPlib>)

4.2 Methods

4.2.1 Microbiological methods

Culturing of bacteria

E.coli HB101 from Stratagene, Heidelberg was used for amplification of plasmid DNA and grown in Luria Bertani broth for this purpose.

Preparation of chemically competent bacterial cells and transformation

We used heat shock transformation as standard transformation procedure for bacteria. To obtain chemically competent *E. coli*, 50 ml LB medium were inoculated from a fresh culture on an agar plate and incubated at 37° C, 250 rpm until the OD600 reached 0,4. Cells were harvested in sterile centrifuge tube for 10 min at 4000 rpm and 4°C. The cell pellet was resuspended in 10 ml sterile ice-cold 0.1 M calcium chloride solution and incubated on ice for at least 15 minutes. After harvesting the cells again by centrifugation the pellet was resuspended in 2 ml 0.1 M calcium chloride solution. Glycerol was added to a final concentration of 10% and 80 µl aliquots were either used immediately for heat shock transformation or shock frozen in liquid nitrogen and stored at -80° C.

For transformation, bacteria aliquots were thawed at room temperature and placed immediately on ice. Up to 200 ng plasmid DNA or ligation reaction were added to 100 µl cell suspension and gently mixed. After 30 minutes of incubation on ice cells were heat shocked at 44°C for exactly 30 seconds and taken back on ice for another 5 minutes. For plasmids containing an antibiotic resistance gene for bactericidal antibiotics, such as kanamycin, 400 µl pre-warmed LB medium was added to cells that were transferred to a heating block and incubated at 37° C /300rpm for at least 30 min to allow for resistance gene expression, before plating on selective agar medium. For bacteriostatic antibiotics, such as ampicillin, bacteria were plated directly after 5 min of incubation on ice on selective, pre-warmed LB agar plates.

4.2.2 Molecular biology methods

Isolation of plasmid DNA from bacteria

DNA was isolated from bacterial pellets by the alkaline lysis method using the Qiagen mini or midiprep kits, according to the manufacturer protocol.

Isolation of total RNA from eukaryotic cells in culture

HeLa cells were grown in culture and used to obtain total RNA extracts, using the RNeasy kit from Qiagen, according to the manufacturer protocol.

Determination of nucleic acid concentration is performed in water solutions by measuring the extinction coefficients at 260 nm and is calculated as follows:

1 OD₂₆₀ = 50 µg/ml double stranded DNA

1 OD₂₆₀ = 33 µg/ml single stranded DNA

1 OD₂₆₀ = 40 µg/ml single stranded RNA

PCR and RT-PCR amplification

PCR was used for amplification of DNA fragments and ORFs with simultaneous addition of restriction sites, or for PCR site-directed mutagenesis.

When a DNA template was not available Reverse Transcription PCR was employed to amplify ORFs starting from RNA templates.

For the polymerase chain reaction, to avoid insertion of untoward mutation during amplification of long DNA sequences, Pfu Ultra, a high-fidelity proofreading DNA polymerase was used in a 50 µl reaction with the following components:

0,4 µl dNTPs (of 25nM each)
100 ng 5'-primer
100 ng 3'-primer
40 ng template (plasmid)
5 µl 10X Pfu Ultra reaction buffer
1 µl Pfu Ultra
water to 50 µl

The amplification was carried out in a Hybaid thermocycler according to a three-step protocol, as shown in the following example:

1x	96° C	2 minutes, initial denaturation of the vector	
95° C	30 sec	denaturation	} extension, 22 cycles
50° C	30 sec	annealing of primers	
72° C	60 sec	/ 1 Kbp DNA elongation	
1x	72° C	5 minutes	final elongation

For amplification of genes for which no DNA template was at hand, one-step RT-PCR was performed. This implies synthesis of the cDNA strand from an RNA template and synthesis of the complementary strand from one reaction mix, which contains both the reverse transcriptase and the DNA polymerase. This allows for

easier handling and helps minimize contamination problems. Also, sensitivity of the reaction is increased by amplification of the entire cDNA sample. Particularly, the SuperScript™ III RT system enabled the amplification of long targets and provided greater primer specificity. This made possible the amplification of the demanding sequence of the Argonaute 2 gene. A general RT-PCR reaction is described bellow:

Reaction components:

2X reaction buffer
total RNA 300 ng
forward/reverse primer 10μM
Reverse Transcriptase and DNA polymerase mix
water to 50 μl

Reaction steps:

cDNA synthesis: 1 cycle at 45°C for 15 minutes
1 cycle at 55°C for 20 minutes
denaturation of the template 1 cycle at 94°C for 2 minutes

PCR amplification: extension of the amplicon:

94°C 15 sec denaturation	} extension, 22 cycles
54°C 30 sec annealing of primers	
68°C 60 sec / 1 Kbp DNA elongation	

1x 68° C 5 minutes final elongation

The following human ORFs have been amplified by RT-PCR from HeLa total RNA and subcloned into mammalian expression vectors, using the primers listed in table 4.1:

eIF4E ORF (GenBank Acc. number NM_001968)

rck/p54 ORF (GenBank Acc. number NM_004397)

PCBP1 ORF (GenBank Acc. number NM_006196)

Ago2 ORF (GenBank Acc. number BC007633)

The eIF4E-T ORF was PCR amplified from the cDNA clone MGC-32981 purchased from ATCC.

Gene product	Sequence (5' --> 3')	Restriction site	Vector
eIF4E	F: TAAGAATTCTATGGCGACTGTCTGAACCGGAAAC R: CGGGATCCTTAAACAACAAACCTATTTTAGTGG	EcoRI BamHI	pEY(C)FP-C1
eIF4E HP	F: GCGGAAGCTTCGATGAACAACAAGTTCGACGC R: TAGGTACCTCATGGCACATTCAACCGCGGCTT	HindIII KpnI	pEYFP-C1
eIF4E-T	F: TCAGAAGCTTACATGGATAGGAGAAGTATGGGTG	HindIII	pEY(C)FP-C1

continued

	R: TCGGTACCTCACTGTCGGTATTCCAATTCATC	KpnI	
eIF4E-T	F: TAGGATCCAATGGATAGGAGAAGTATGGGTGAAAC	BamHI	pCMV-FLAG
	R: GGAAGCTTTCACTGTCGGTATTCCAATTCATC	HindIII	
eIF4E-T	F: TAGGATCCCAATGGATAGGAGAAGTATGGGTG	BamHI	pcDNA-HA
	R: AAAATTTAAAGCGGCCGCTCACTGTCGGTATTCCAATTC	NotI	
Argonaute 2	F: TGAATTCCACCATGTACTCGGGAGC	EcoRI	pcDNA-HA
	R: AAATTTAAAGCGGCCGCTCAAGCAAAGTACATGGTGCGCAG	NotI	
rck/p54	F: TCAGAAGCTTACATGGGTCTGTCCAGTCAAAATGG	HindIII	pEY(C)FP-C1
	R: TCGGTACCTTAAGGTTTCTCATCTTCTACAGG	KpnI	
eIF4E BP1	F: TAAGCTTGGAGGAATGTCCGGGGGAGCAGCTGCAGC	HindIII	pEYFP-C1
	R: CGGGATCCTTAAATGTCCATCTCAAAGT	EcoRI	
PCBP1	F: TCAGAAGCTTACATGGATGCCGGTGTGACTGAAAGTG	HindIII	pECFP-C1
	R: TTCGGTACCCTAGCTGCACCCCATGCCCTTCTC	KpnI	

Table 4.1. Primers used to amplify the ORF of several P body resident proteins. F and R indicate the forward and reverse direction of synthesis.

The following **eIF4E-T** deletion constructs have been generated with the purpose of expression in mammalian cells:

Gene product	Sequence (5' --> 3')	Restriction site	Vector
eIF4E-T			
1-194	F: TCAGAAGCTTACATGGATAGGAGAAGTATGGGTG	HindIII	pEYFP-C1
	R: GGGGTACCTTAGAAACGCTTGTCTTGAAGTCCCTC	KpnI	
1-321	R: AGGTACCTCAAGCCAAGCATGGCACCTTATC	KpnI	pEYFP-C1
1-447	R: AGGTACCCTAAACCTTCAAGCCCTTCAGACC	KpnI	
212-447	F: CCAAGCTTATATGGATTCTTACACAGAAGAAGAACCAGAGTG	HindIII	pEYFP-C1
212-447	F: GAGGATCCTAATGGATTCTTACACAGAAGAAGAACCAG	BamHI	pcDNA-HA
212-447	R: AAGCGGCCGCCTAAACCTTCAAGCCCTTCAGACCTGC	NotI	
212-447	F: TAGGATCCAATGGATTCTTACACAGAAGAAGAACC	BamHI	pCMV-FLAG
212-447	R: CAGAATTCCTAAACCTTCAAGCCCTTCAGAC	EcoRI	
430-503	F: CAAGCTTCTATGGGGGTGTGCTTTCAGTGGAGG	HindIII	pEYFP-C1
505-985	F: CAAGCTTCTATGAACCTTGAAGCCATTTGATGTC	HindIII	pEYFP-C1
	R: TCGGTACCTCACTGTCGGTATTCGAATTCATC	KpnI	
642-801	F: GAAGATCTATGAACCTTACCAGCCTGGTTTTGGC	BglII	pEYFP-C1
	R: AACTGCAGTTAAGGAAGTGGGGATGCCAAGG	PstI	
770-985	F: GAAGATCTATGCCACTGTCCCAGGCCAACCG	BglII	pEYFP-C1

Table 4.2. Primers used to amplify eIF4E-T deletion constructs with the full-length eIF4E-T protein serving as template. Numbers in the gene product column indicate the aminoacid residue in the full-length protein

Site-directed mutagenesis

In the site directed mutagenesis experiments, the following primers have been employed for introducing point mutations in the gene product ORF of eIF4E and eIF4E-T in the vectors listed in table 4.3:

Gene product	Sequence (5' --> 3')	Vector
eIF4E ^{W73A}	F: GTTTGATACTGTTGAAGACTTTGCGGCTCTGTACAACCATATCCAG R: CTGGATATGGTTGTACAGAGCCGCAAAGTCTTCAACAGTATCAAAC	pEYFP-C1
eIF4E ^{WE102103AA}	F: GGATGGTATTGAGCCTATGGCGGCAGATGAGAAAAACAAACGGGGA GG R: CCTCCCCGTTTGTTTTCTCATCTGCCGCCATAGGCTCAATACCATCC	pEYFP-C1
eIF4E-T ^{LL3536GG}	F: CCAAATGCCCCCATCGCTATACAAAAGAAGAAGGCGGGGATATAAAA GAATCCCCCATTC R: GGAATGGGGGAGTTCTTTTATATCCCCGCCTTCTTCTTTTGTATAGCGA TGGGGGCATTGG	pEYFP-C1
eIF4E-T ^{Y30A}	F: GCCTCCAAATGCCCCCATCGCTATACAAAAGAAGAACTCTTG R: CAAGAGTTCTTCTTTTGTAGCGCGATGGGGGCATTGGAGGC	pEYFP-C1

Table 4.3. Primers used to insert point mutations in the ORF of eIF4E and eIF4E-T

Mutations were introduced by PCR amplification of the vectors containing the desired target ORF, by use of the mutagenic primers, according to the protocol in the QuickChange® Site-Directed Mutagenesis Kit from Stratagene.

Molecular cloning

Preparation of the vector for cloning by linearization is the most important step in cloning. To prevent self re-ligation of the vector digestion was allowed to proceed between 4 hours to overnight and dephosphorylation was performed by incubating the digestion mix for 1 hour with CIP at 37°C (for 5'overhanging sticky ends) or at 50°C (for 3' overhanging or blunt end).

Digestion reaction:

Plasmid vector 5 µg
10X enzyme buffer 5 µl
Enzyme 20 U (never add >10%v/v of enzyme)
Water up to 50 µl

Dephosphorylation reaction:

Plasmid digestion reaction 50 µl
CIP 0,5 µl

When performing digestion with two enzymes, firstly cut with the enzyme that requires less salt and then add salt or buffer to increase the salt concentration for the second enzyme.

Agarose gel electrophoresis was used to separate DNA fragments after restriction enzyme digestion of vectors. 1% agarose gels were prepared in 1X TBE buffer and ethidium bromide 0,5 µg/ml was added. Samples were supplemented with 6 x loading dye. Gels were run at 100 V for approximately 45 minutes in 1X TBE buffer.

Gels were documented on the BioRad GelDoc station. Bands were excised from the gel and the DNA was recovered using the gel extraction kit from Qiagen.

Alternatively, digestion reactions of PCR generated inserts were purified with the PCR purification kit from Qiagen. In either case, the DNA was eluted with water and the extinction was measured at 260 nm.

Following insert and vector digestion, the two fragments were ligated by the T4 DNA ligase, from the Rapid Ligation Kit that was purchased from Roche. A typical ligation mix contains the following:

Linearized plasmid vector	25-100 ng	} mix well
Insert	in molar excess to the vector, at least 3:1	
DNA dilution Buffer 2	up to 10 μ l	

Add ligation mix:	2X T4 DNA ligation buffer 1	10 μ l
	T4 DNA ligase	1 μ l

The reaction was allowed to proceed for 5 minutes and then stopped by transferring the tube on ice.

The ligation reaction is next transformed into bacteria, plated onto agar plates and incubated at 37°C for 14-16 hours. Several colonies are picked and grown in 4 ml of LB medium, overnight at 37°C as cultures for minipreparative plasmid DNA extraction.

Sequencing of plasmid DNA

Sequencing was performed to verify generated plasmid constructs. We used the sequencing facility of the Sequencing Laboratories GmbH (Göttingen). For this purpose 700 ng of purified plasmid DNA were mixed with sequencing primers dissolved in water, in a final volume of 7 μ l and sent for analysis. Sequencing results were aligned with the target sequence using the “Align two sequences” application (bl2seq) on the NCBI Blast homepage (<http://www.ncbi.nlm.nih.gov/blast/bl2seq/wblast2.cgi>).

RNA Interference and validation of siRNA knockdown efficiencies.

LSm1, eIF4E-T, rck/p54, and Ccr4 siRNA duplexes were designed and synthesized in-house with 3'dTdT overhangs as described previously (Elbashir et al., 2002). The Dcp2 siRNA duplex was purchased from Ambion (USA). A BLAST search against

the human genome sequence (NCBI UniGene database) was used to confirm that only the gene of interest would be targeted. The sense-strand sequences used to target each gene were as follows (table 4.4). The indicated accession numbers are from GenBank.

mRNA target	siRNA Sequence (5'--> 3')	Target region
LSm1 (NM_014462)	AAGTGACATCCTGGCCACCTCAC	3' UTR
eIF4E-T (NM_019843)	CAGTCGAGTGGAGTGACATTGT	3' UTR
rck/p54 (NM_004397)	AAAAGGCTCGTTTGGATCTGTGA	3' UTR
Ccr4 (NM_015455)	AATGTGTGAACAGCGTATTCTC	3' UTR
Dcp2 (NM_152624)	GTGGCATGTAATGGACATTGC	ORF
Xrn1 (NM_019001)	GTCATGGCAAGGAGTTAC	3' UTR
Firefly luciferase (X65324)	CACGUACGCGGAUACUUCGAAA	ORF

Table 4.4. siRNA oligonucleotides (forward strand) used for knockdowns in HeLa cells

Ccr4, LSm1, eIF4E-T, rck/p54 and Dcp2 knockdowns were determined by the relative quantification based on the relative amount of target mRNA in knockdown cells versus target mRNA in control cells with real-time qRT-PCR. For normalization of the target genes glyceraldehyde-3-phosphate dehydrogenase (GAPDH) was used as an endogenous standard. Relative expressions of the RNA in experimental samples with respect to control samples were obtained using duplicate samples and at least two independent RT-qPCR experiments.

Total RNA was isolated from HeLa SS6 cells treated with a GL2 control siRNA or Ccr4, hLSm1, eIF4E-T, rck/p54 and Dcp2 siRNAs (RNeasy Mini Kit, Qiagen) and treated with RQ1 DNase. RNA integrity was electrophoretically verified by ethidium bromide staining and by an OD260/OD280 nm absorption ratio >1.95.

Specificity of qRT-PCR products was documented with high-resolution gel electrophoresis, and resulted in a single product with the desired length. In addition, the OPTICON melting curve analysis was performed, which resulted in single product specific melting curves. Investigated transcripts showed real-time PCR efficiency rates (E) ranging from 1.8 to 2.1 (Pfaffl, 2001) in the investigated range from 6.25 to 100 ng total RNA input with high linearity (Pearson correlation coefficient $r > 0.98$). Relative quantification of knockdown versus control mRNA levels was accomplished according to the Pfaffl-method (Pfaffl, 2001).

To verify the knockdown efficiency the following exon/exon-spanning PCR primers were used in qRT-PCR reactions employing total RNA extracts from HeLa cells where RNAi was performed:

Gene target	Sequence (5' --> 3')
hXrn1 (XM_033181)	F: GAAAGTGTCTTTATGGCTGTAGAT R: AATCTGGCCTCTGTAGGAAGAGTTT
hDcp2 (NM_152624)	F: GAACTTGCCCATTGGTTTTACTTGG R: TATATTCCTTCCATTCATCCAAAAC
rck / p54 (NM_004397)	F: GACACAGCAACAGATGAACCAGCTG R: GAGGTCACATCCGAAGTTTGTATTC
eIF4E-T (NM_019843)	F: ACAAGTCAGTCTGAAACCATCGAAC R: CTCATCCTCTTCGCCACTCCTCC
Ccr4 (NM_015455)	F: TCACAATCTGGTGTATTGGACCTG R: TAAGGGGATTTCCTTTCAGGCCTAA
hLSm1 (NM_014462)	F: CTATATGCCTGGCACCGCCAGCCTC R: CCTCGAGGAATATCACCGTATTTTTTGC

Table 4.5. Primers used in qRT-PCR to verify efficiency of mRNA reduction upon treatment of HeLa cells with the respective siRNAs

4.2.3 Cell biological methods

Cultivation of cell lines

HeLa is a human cervix carcinoma cell line that we preferred because of its robustness.

HeLa cells were cultured in incubators at 37°C, 5% carbon dioxide, and 95% humidity. Media were purchased from GibcoBRL (Eggenstein). In general, we used DMEM containing glutamax, sodium pyruvate, pyridoxine, and glucose, supplemented with 10% fetal calf serum, and antibiotics (100 units/ml Penicillin, 100 µg/ml Streptomycin). Cells were propagated in adherent conditions and passaged at 75% confluence. For this purpose, the medium was removed and cells were washed with 1X PBS pH 7,4 then trypsin/EDTA solution was added and the dishes were put back in the incubator, for 5 minutes. The trypsin was quenched by addition of a double volume of DMEM containing 10% FCS. Detached cells were resuspended by pipetting the medium in and out, against the bottom of the dish. To maintain the cells in an exponential growth phase, they were diluted before plating onto a new dish.

Long-term storage of cell lines

At regular intervals stocks from our cell lines were prepared in freezing medium and stored in liquid nitrogen. For freezing, at 80% confluency, the cells were detached from a 14 cm culture dish as described above. Cells were pelleted by centrifugation at 800 rpm for 3 minutes, the supernatant was removed and cells were resuspended in 3 ml freezing medium. 1 ml aliquots were frozen at -80° C and transferred to liquid nitrogen one day after freezing.

Transfection of cell lines

For transfection of siRNA, cells were plated at 15000 cells/well of a 24 well plate, in medium without antibiotics, to prevent untoward effects on the cell metabolism and ensure efficient transfection. For immunofluorescence experiments, autoclaved glass coverslips (12 mm diameter, Menzel-Gläser, Marienfeld) were deposited on the bottom of the wells, prior to addition of the medium containing the cells. After 24 hours, transfection of the cells was performed using Oligofectamine, according to the manufacturers instructions and as described in Elbashir et al., 2002. Generally, 3µl Oligofectamine were diluted in 12 µl serum-free medium (OptiMEM), and incubated for 7 minutes. Meanwhile, 3µl of a 20 µM siRNA solution was diluted in 50 µl OptiMEM. Then, the latter solution was added to the Oligofectamine solution and incubated for an additional 20 minutes. Next, the Oligofectamine-siRNA complexes were evenly distributed by drop-wise pipetting onto the HeLa cells. Cells were returned to the incubators and grown for different times, as described in section 5.2.1.1. As a control, a siRNA duplex against the firefly luciferase was transfected into the cells. Since it has no target among the human genes this should allow differentiating between specific and unspecific effects of the knockdowns.

For transfection of cell lines with plasmid constructs we used the liposome based transfection reagent Fugene 6 from Roche, according to the manufacturer instructions. Cells have been plated 24 hours before the transfection experiment, to reach a density of minimum 60%. For each well, 300 ng of DNA were transfected. To 100 µl OptiMEM, 1.6 µl Fugene 6 were added, and the solution was mixed. Then, 300 ng DNA was pipetted in the reaction tube, and incubated for 15 minutes at room temperature, to allow for the DNA to be taken up into the liposomes. The

transfection mixture was evenly distributed by drop-wise pipetting onto the HeLa cells. Cells were assayed for protein expression between 14 and 30 hours after transfection.

TUNEL test for apoptosis detection

Apoptosis indicating DNA fragmentation can be monitored by a TUNEL test. In this assay, free 3'OH ends of fragmented DNA are labeled with FITC-tagged deoxynucleotidephosphates by the enzyme Terminal deoxynucleotidyl Transferase (TdT) which is a component of the *In situ* Cell Death detection Kit (Roche). The protocol is basically according to the manufacturer handbook.

Cells grown on coverslips are fixed for 4 minutes with ice-cold methanol (-20° C) and then rinsed with 1X PBS. Next, they are permeabilized for 2 minutes on ice with permeabilization buffer:

sodium citrate	0.1% (w/v)
Triton X 100	0.1% (v/v)
in PBS pH 7.4	

Alternatively, just 0.2% Triton X 100 in PBS can be used. Coverslips are washed 3 times in PBS and excessive buffer is removed with filter paper. Then, 30 µl of staining mix containing TdT plus the labeled nucleotides per coverslip should be added and incubated for 1 hour at 37° C in a wet chamber in the dark. The staining mix is produced from 1 volume of TdT Enzyme solution and 9 volumes of Label solution, which should be mixed well.

As negative control, 30 µl of Label solution alone is added to a coverslip.

As a positive control, fixed and permeabilized cells were incubated for 10 minutes at room temperature with micrococcal nuclease or DNase I (30U/ml) to induce DNA strand breaks, prior to labeling.

Next, the coverslips were washed 4 times at least 5 min or 3 times for 10 min with PBS pH 7.4. Finally, the coverslips are mounted in antifade (Mowiol) on glass slides and examined under the fluorescent microscope.

4.2.4 Biophysical methods

Immunofluorescence

HeLa SS6 cells were grown on glass coverslips and were fixed for 20 minutes with PBS pH 7.4/4% w/v paraformaldehyde, washed with PBS pH 7.4 and permeabilized in PBS pH 7.4/0.2% Triton X-100 (Sigma) for 20 minutes. Cells were then rinsed with PBS, blocked in PBS pH 7.4/10% Fetal Calf Serum (FCS) for 30 minutes and incubated with the primary antibody diluted in PBS pH 7.4/10% FCS for 1 hour. Subsequently, cells were washed with PBS pH 7.4 (4x 15 min) and incubated with the secondary antibody diluted in PBS pH 7.4/10% FCS for 1 hour. The cells were again washed with PBS pH 7.4 (4x 15 min) and mounted in anti-fade (Mowiol, Calbiochem). All steps were performed at room temperature.

Confocal laser scanning microscopy

Samples were visualized using a Zeiss LSM 510 Meta inverted confocal laser scanning microscope. Fluorophores were excited using standard laser lines. Images were successively acquired in 0.5 to 0.7 μm optical sections. Images were processed and merged to allow for a whole-cell overview, using Adobe Photoshop (version 7.0).

Fluorescence recovery after photobleaching (FRAP)

In FRAP, a region of interest is shortly (<200 ms) bleached at a high laser power that will lead to photodestruction of the fluorescent molecules in that area. Recovery of the fluorescence in the bleached area of the living cell is then monitored at the lowest possible laser intensity to avoid monitoring photobleaching.

All data were obtained on a LSM 510 Meta scanning laser confocal microscope (Zeiss, Jena) using the 488 nm line of a 30 mW argon ion laser with a pinhole adjustment resulting in a 2 μm optical slice. A circular region of interest (ROI) with a diameter of 1.5 μm containing one P body was recorded five times for 5 seconds with a laser power 0.6 mW and maximum scan speed (pixel-time 1.28 μs). The ROI was then bleached with 40 scan iterations at 12 mW. Fluorescence recovery was measured every 20 seconds for 400 seconds. An additional ROI in the cytoplasm of another cell

was monitored in parallel to detect fluorescence fluctuations independent of bleaching. A third ROI was placed outside the cell to measure background fluorescence. Average fluorescence intensities within ROIs were measured under the same conditions for each data set and exported into Microsoft Excel. For each fusion protein this procedure was repeated five times in different cells and the mean intensity value for each time point was calculated. The half-time of fluorescence recovery ($t_{1/2}$) was determined by curve fitting of experimental data using nonlinear regression to a single-exponential curve (Marquart method, GraphPad Software).

Fluorescence resonance energy transfer (FRET)

All data were obtained on a LSM 510 Meta (Zeiss, Jena). Samples were fixed with 4% PFA for 20 min and images acquired with a C-APOCHROMAT 63×/1.4 oil Korr objective (Zeiss). Specific excitation and emission of the CFP-fusion proteins were effected by excitation at 458 nm with a 30 mW Argon/2 laser (AOTF transmission 15%) and collection of emitted light with a 480/20 nm bandpass filter. No emission from YFP fusion proteins was detected in this channel. CFP images were taken before and after photobleaching of the YFP signal by using exactly the same sensitivity settings. YFP signals were photobleached by full power excitation at 532 nm with a 50 mW solid-state laser. Images of the YFP-fusion protein expressing cells were obtained before and after photobleaching by excitation with a 30 mW Argon/2 laser (transmission 5%) at 514 nm excitation and the emission was collected from 531 to 606 nm (LSM 510 Meta Detector, Zeiss). No photobleaching of the CFP signal was observed under conditions of >90% photodestruction of the YFP signal. To enhance the reliability of the acquired data, two P-bodies and one square-shaped region in the cytoplasm were bleached per acquired sample region. The intensity of the remaining, unperturbed p-bodies served as internal control to correct for image-induced donor bleaching and fluctuations in laser intensity.

FRET efficiencies were calculated by Dr. R. Heintzmann using a MATLAB and DIPimage-based (Luengo Hendriks et al., 1999) script (available from the authors upon request). After cross-correlation based image alignment and brightness normalization estimated from intensity in the unperturbed p-bodies, the FRET efficiency was determined for each p-body separately: $E = \frac{F_{D1} - F_{D0}}{F_{D1}}$, with F_{D0} and F_{D1}

denoting the sum of the respective pre- and post-bleach donor intensity in a P body. P bodies were segmented using a fully automatic global thresholding based on the chord method (Zack et al., 1977).

4.2.5 Biochemical methods

Preparation of cytoplasmic extracts from eukaryotic cells in culture

In order to retrieve protein complexes enriched in P body components, HeLa cells grown in 14 cm dishes were transiently transfected with vectors containing HA and FLAG-tagged proteins described as residents of P bodies (see section 5.5). 24 hours after plating, at 60% cell confluency, 6 μ g of DNA were transfected to each plate: to 564 μ l OptiMEM, 36 μ l Fugene 6 were added, then the 6 μ g of DNA mix containing several plasmids in equal amounts. Protein expression was allowed to proceed for 32 hours and efficiency of transfection was verified by immunostaining of coverslips that were deposited onto the dishes, previous to plating of the cells.

An S30 cytoplasmic extract was prepared as follows:

Plates were washed twice with 10 ml ice-cold PBS pH 7,4 and then cells were harvested with a rubber policeman in 5 ml ice-cold PBS. The cells collected were pelleted by centrifugation at 4°C, 2000 rpm for 5 minutes, without brake. Supernatant was discarded and cells were resuspended in ~ 1ml of PBS, then transferred to a 2ml Eppendorf tube. This was centrifuged for 5 minutes at 4° C/2000 rpm, the supernatant was discarded and the Packed Cell Volume (PCV) was determined.

Cells were resuspend in 1 PCV of ice-cold Roeder A buffer and incubated for 15 minutes on ice to allow for swelling of the cells. Next, cells were lyzed by pushing them through a narrow (25g/8 G-16mm) needle and a 5 ml syringe, with 10 fast strokes. The nuclei and cell debris were collected by centrifugation for 60 seconds in a microfuge at 4° C, 13000 rpm. The supernatant (cytoplasmic extract) is collected into a new tube and 0,11X volumes of the 10 X Roeder B buffer is added.

To clear the cytoplasmic extract centrifugation at 30000 x g for 30 minutes at 4°C was performed using the Beckman S100-AT4 rotor (33000rpm) in 2 ml polycarbonate tubes. The supernatant was saved as S30 cytoplasmic extract, and the protein concentration was measured using the Bradford assay. The extract is then either frozen in liquid nitrogen (and stored at -80° C), or used immediately in immunoprecipitation.

Determination of total protein concentration in the extract

The Bradford assay (Bradford, 1976) was used as a standard method for protein quantification that is based on detecting an absorbance shift in Coomassie Brilliant Blue G250 when bound to arginine or to aromatic residues. The anionic, bound form has an absorbance maximum at 595 nm, whereas the unbound (cationic) form exhibits its absorbance maximum at 470 nm. Firstly, a standard curve using BSA was generated. The extract of unknown concentration was brought in a total volume of 800 μ l water and 200 μ l Bradford reagent was added. After 10 minutes of incubation at room temperature we measured the extinction at 595 nm and calculated the actual protein concentration by means of the BSA standard curve. All samples were determined in duplicates or triplicates.

HA- and Flag- Pull Down Assay

Before the immunoprecipitation, the cytoplasmic extract was pre-cleared on 60 μ l slurry ProteinG Sepharose by rotating it for 45 minutes “head over tail” at 4° C.

Since both HA- and FLAG- containing proteins will be immunoprecipitated, a mix of affinity matrixes with either specificity was employed.

200 μ l Sigma FLAG and 200 μ l HA matrix beads were washed with 2ml IPP 150 (without detergent), then incubated for 12 minutes with elution buffer (0.1M glycine pH 3.5) at room temperature. Beads were washed several times with IPP150 buffer to re-equilibrate. The FLAG and HA beads were then blocked with BSA 1mg/ml for 30 minutes and washed thoroughly with IPP 150 as previously.

Pre-cleared extracts (~2mg total protein) were incubated with the equilibrated anti-HA+FLAG affinity matrix mixture and rotated “head over tail” for 2 hours and 30 minutes at 4° C. Next, beads were spun down and washed 5 times with 1 ml IPP150 each.

For elution of complexes, to 200 μ l total volume of beads, 300 μ g HA peptide and 120 μ g FLAG peptide were added, in elution buffer. Beads were mixed “head over tail” for 2 hours at 4°C, then spun down and the eluate was collected.

Eluates were run onto SDS-PAGE and stained with either Coomassie and sent for microsequencing, or silver stained.

SDS polyacrylamide gel electrophoresis

Denaturing sodium dodecyl sulfate polyacrylamide gel electrophoresis (SDS PAGE) is a commonly used method to separate proteins on polyacrylamide gels according to their molecular weight (Laemmli, 1970). Sodium dodecyl sulfate (SDS) is an anionic detergent that denatures the secondary and non-covalently linked tertiary structures of proteins. In addition, it covers the protein with a negative charge. SDS binds to the protein in a ratio of approximately 1,4 :1, resulting in a relatively uniform mass:charge ratio for the majority of proteins. In order to denature secondary, and also disulfide-bridged tertiary and quaternary structures completely, the loading buffer is supplemented with reducing reagents, such as dithiothreitol (DTT) or 2-mercaptoethanol. The samples are additionally denatured by boiling. The uniform mass:charge ratio and the complete destruction of secondary and tertiary structures allows for migration of the protein in gel to be directly related to its size.

Silver staining of protein gels

Protein detection by silver staining is 100-fold more sensitive than Coomassie Brilliant Blue staining and we used a protocol based on the method described by Blum et al., 1987.

1. The gel was fixed with gently rocking in a solution of 50% methanol / 12% acetic acid overnight at room temperature.
2. The fixative was removed and the gel washed two times with 50% ethanol and one time with 30% ethanol, for 20 minutes each.
3. For sensitization, the gel was submersed 60 seconds in 0.8 mM $\text{Na}_2\text{S}_2\text{O}_3 \cdot 5\text{H}_2\text{O}$ and then washed three times for 20 seconds each, with H_2O .
4. The gel was soaked for 20 minutes in the impregnation solution, containing formaldehyde, for increased sensitivity.
5. The gel was washed three times with deionized water, 20 seconds each.
6. Developing solution was added to the gel, and then quickly exchanged with fresh developing solution. The tray was continuously rocked, until the bands developed.
7. When the desired degree of banding is attained the developing is stopped by addition of 50% methanol / 12% acetic acid
8. The gel can be stored in 5% acetic acid.

Fixation/ stop solution:

50% methanol
12% acetic acid

Washing solutions:

50% ethanol
30% ethanol
H₂O, ad 100%

Storage solution:

5% acetic acid

Sensitizing solution:

0.8 mM Na₂S₂O₃·5H₂O

Impregantion solution:

2g/L AgNO₃
0,026% formaldehyde (0,7ml/L of 37% formalin)

Developing solution:

60g/L Na₂CO₃
0,0185% formaldehyde (0,5ml/L of 37% formalin)
16 μM Na₂S₂O₃·5H₂O

5. Results

5.1.1 The cap-binding translation initiation factor eIF4E is present in P bodies.

In order to find out whether there is a connection between the translation machinery and the P bodies, the cellular localization of the translation initiation factor eIF4E was checked in HeLa cells by performing immunocytochemistry experiments. For this purpose, a mouse monoclonal anti-eIF4E antibody was employed and the fixed cells were counterstained with antibodies against LSm1, which is a known and specific marker for P bodies (Ingelfinger et al., 2002). Microscopy recordings revealed that eIF4E was distributed throughout the cytoplasm, but not the nucleoplasm of HeLa cells and appeared to be enriched in discrete cytoplasmic foci (Fig. 5.1 A-C).

A similar distribution of eIF4E in HeLa cells was also observed when using a previously characterized rabbit anti-eIF4E serum (data not shown, see materials and methods). The latter represent P bodies as evidenced by the co-localization of eIF4E with LSm1 in these foci (Fig. 5.1 C). To rule out antibody-dependent effects and independently confirm our findings, a plasmid encoding a YFP-eIF4E fusion protein was constructed and transiently delivered into HeLa cells.

Significantly, the distribution pattern of YFP-eIF4E in transfected cells (Fig. 5.1 D) was indistinguishable from that of the endogenous protein, as detected by immunofluorescence (compare Fig. 5.1 F with Fig. 5.1 C). The presence of eIF4E in P bodies suggested that other translation factors might also be present in these structures. Thus, we subsequently tested for the presence of the translation initiation factors eIF4G, eIF4A, and eIF4B in P bodies. As shown in Fig. 5.1 G-I, eIF4G did not co-localize with LSm1 in P-bodies. Similar results were obtained with antibodies against eIF4A and eIF4B, as well as with other components of the translation machinery, namely the eukaryotic elongation factor 2 (eEF2), the poly(A) binding protein (PABP), and proteins of the small and large ribosomal subunits: rpS6 and rpL28, respectively. None of these factors co-localized with P body markers (data not

shown) indicating that neither active translational complexes nor ribosomes are found in the P bodies and thus translation does not occur at these sites.

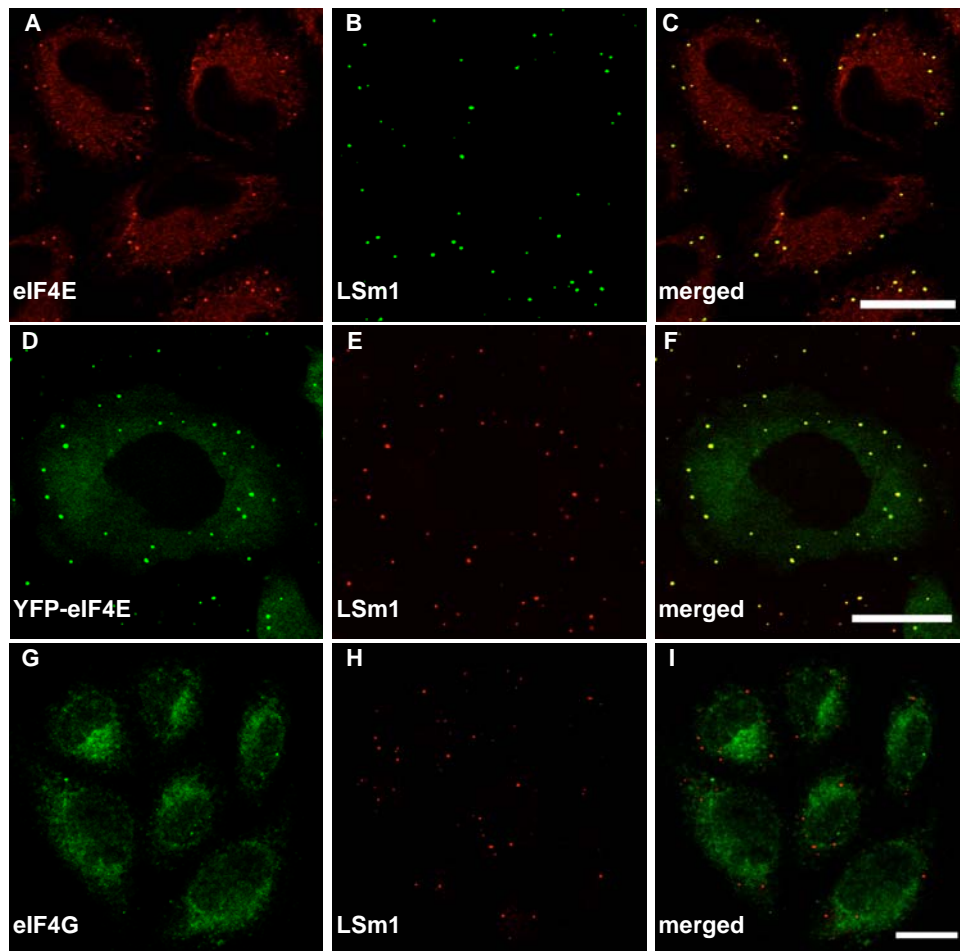


Figure 5.1. The translation initiation factor eIF4E localizes to the cytoplasm of HeLa cells and is enriched in foci containing LSm1. HeLa SS6 cells were grown on coverslips, fixed, and stained with antibodies specific for eIF4E (monoclonal anti-eIF4E, Santa Cruz Biotechnology), (red, **A**), LSm1 (**B**, **E**, **H**) and eIF4G (green, **G**). Alternatively, cells were transfected with a plasmid encoding YFP-eIF4E (**D**) and fixed after 16 hours. Panels **C**, **F**, **I** show the merged picture of the proceeding two panels, with overlaying signals appearing yellow. In these confocal microscopy pictures, scale bars indicate 10 μ m.

5.1.1.1 The eIF4E Homologous Protein is present in P bodies.

Apart from the canonical eIF4E protein, an isoform of it, which has 30% sequence identity and 60% sequence similarity named eIF4E Homologous Protein, is known to be expressed in human (Rom et al., 1998). Its sequence was amplified by RT-PCR from HeLa total RNA and then cloned into a YFP expression vector. Following transfection of the vector encoding for the YFP-eIF4E HP fusion protein,

counterstaining with the P body marker LSm1 (Fig. 5.2 C) revealed an expression pattern similar to that of the canonical eIF4E. The only notable difference was that the fusion protein was additionally dispersed in the nucleoplasm (A).

The novel finding that a second isoform of eIF4E has a similar distribution (at least with respect to the P bodies) is an indication of a redundant genetic trait. Functional aspects of eIF4E HP have been recently demonstrated in *Drosophila* where binding of eIF4E HP to the cap inhibits translation initiation (Cho et al., 2005).

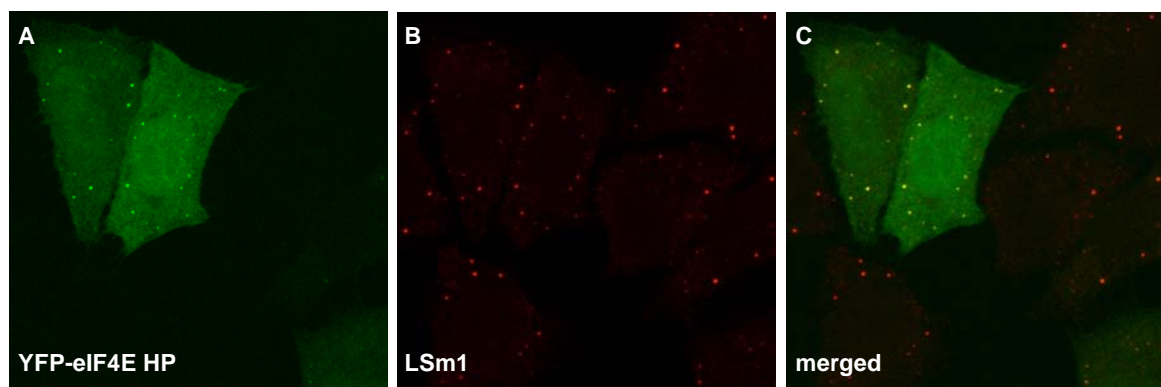


Figure 5.2. The eIF4E- Homologous Protein localizes to the cytoplasm of HeLa cells and is enriched in foci containing LSm1. Immunocytochemistry experiments using HeLa SS6 in which cells were transfected with a plasmid encoding a YFP-eIF4E HP fusion protein (green, A). After 16 hours, cells were fixed and counterstained with LSm1 (red, B). Panel C shows the merged picture of the proceeding two panels, with overlaying signals appearing yellow.

5.1.2 Comparison of two cytoplasmic compartments- the Stress Granules and P bodies

In higher eukaryotes, under certain non-physiological conditions such as thermal or chemical stress, mRNPs accumulate in cytoplasmic structures called stress granules (SG). They store inactive translation pre-initiation complexes that contain eIF4E and eIF4G, which means that both factors are part of the mRNP complexes in SGs (Kimball et al., 2003). The presence of eIF4E in distinct foci was reminiscent of, and thus suggested a possible relationship to SGs. To investigate similarities and/or differences between P bodies and SGs directly, HeLa cells were treated with arsenite to generate oxidative stress and hence the formation of stress granules. Then, the composition of both P bodies and SGs was compared by immunofluorescence microscopy using antibodies against LSm1 (as a marker of P bodies) and the translation initiation factors eIF4E and eIF4G. While eIF4G was observed to solely

accumulate in SGs and LSM1 solely in P bodies (Fig. 5.3 A-C), eIF4E localized to both structures (Fig. 5.3 D, F).

Hence, we could demarcate P bodies from stress granules as distinct cytoplasmic compartments that share at least one component (eIF4E) but which can perform distinct functions in mRNA regulation by means of their individual components. In our future experiments we will only focus on the typical round shape cytoplasmic foci- the P bodies whose earmark component is, as demonstrated already, LSM1.

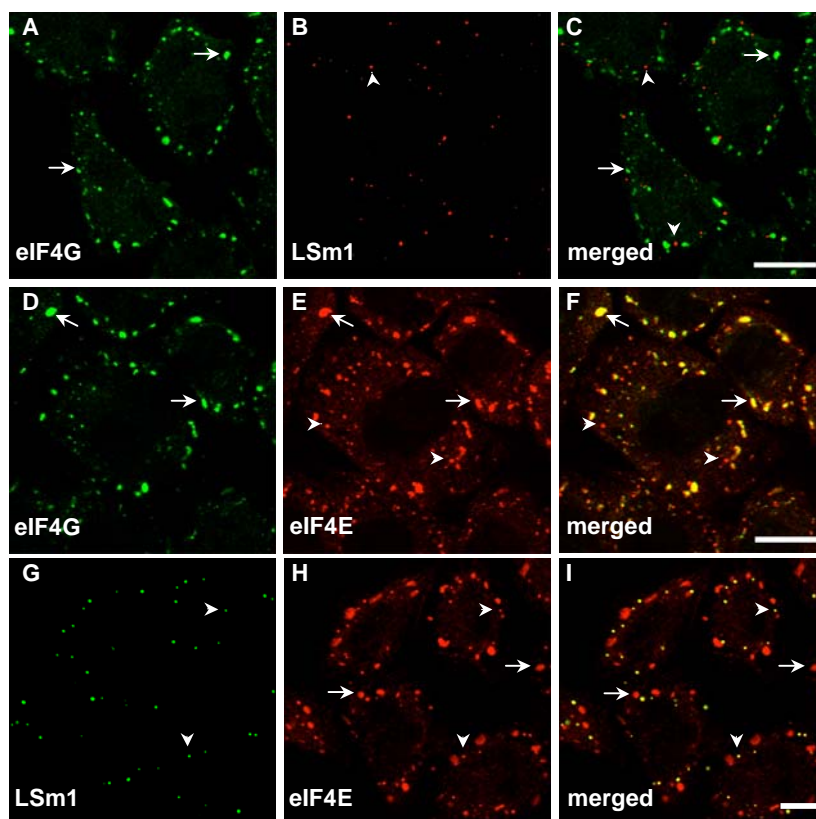


Figure 5.3. Stress granules are structures distinct from the Processing bodies. HeLa cells were treated with 100 μ M arsenite for 45 min at 37°C to induce stress granules formation (indicated by **arrows**). Cells were grown on coverslips, fixed, and stained with antibodies specific for eIF4E (monoclonal anti-eIF4E, Santa Cruz Biotechnology), (red, **E, H**), eIF4G (green, **A, D**). The P bodies (indicated by **arrowheads**) are labeled with anti-LSM1 antibody (**B, G**). Panels **C, F** and **I** show the merged picture of the proceeding two panels. Overlaying signal denoting co-localization of two factors inside the stress granules/ P bodies appears yellow in the merged picture (**F/ I**). In these confocal microscopy pictures, scale bars indicate 10 μ m.

5.1.3 The eIF4E-binding protein eIF4E-T is a component of P bodies

Since eIF4E, but not other translation factors are present in P bodies, we assumed that early acting translational repressors prevent the assembly of competent

translational mRNP complexes. It is known that association of eIF4E with the 5' cap is greatly stabilized by its binding to eIF4G (von Der Haar et al., 2000), and thus by hindering access of the decapping enzymes to the m⁷G, the transcript is stabilized against decay, too. The lack of eIF4G from P bodies suggested that disruption of the eIF4E/eIF4G contact could be a potential destabilizer of the active translation loop. Inhibitors of this interaction would then be responsible for making the mRNA vulnerable to the degradation apparatus. To understand the sequence of events leading to the inactivation of the mRNAs and their confinement within the P bodies, we tried to find out potential interaction partners of eIF4E capable of altering this connection. Several eIF4E-binding proteins were described to contain conserved interaction sites by which they compete with eIF4G for the same binding region on eIF4E and thus prevent the assembly of active translational complexes (reviewed in Richter and Sonenberg, 2005; Fig. 5.4).

eIF4GI	415	R	Y	D	R	E	F	L	L	G	423
eIF4E-BP1	52	I	Y	D	R	K	F	L	M	E	60
eIF4E-T	29	R	Y	T	K	E	E	L	L	D	37
consensus		Y	X	X	X	X	L	Φ			

Figure 5.4. Consensus sequence of eIF4E interacting proteins. The aminoacids in red represent conserved residues of the eIF4E interaction motif in three different eIF4E binding proteins- the canonical eIF4G, the eIF4E Binding Protein 1 and the eIF4E-Transporter protein. X represents any aminoacid residue, whereas Φ can be leucine, methionine or phenylalanine. *Modified from Dostie et al., 2000.*

In addition, studies in *Xenopus* oocytes suggest that Xp54 [the orthologue of yeast Dhh1, a decapping enzyme stimulator (Fisher and Weis, 2000)] may also bind eIF4E, but a direct interaction has not been conclusively demonstrated (Minshall and Standart, 2004).

We investigated by immunofluorescence microscopy whether one or more of these factors are residents of the P bodies in HeLa cells.

The first protein checked was the eIF4E Binding Protein 1 (eIF4E-BP1), which is known to repress translation globally, by sequestering eIF4E and thus preventing the formation of the eIF4F heterotrimeric complex (Haghigat et al., 1995). By using antibodies against eIF4E-BP1 in immunofluorescence experiments, as well as by constructing and expressing the plasmid encoding YFP-eIF4E-BP1 it was possible to see that eIF4E-BP1 does not accumulate in P bodies (data not shown).

In contrast, studies with antibodies raised against the *Xenopus* counterpart of human rck/p54 (designated Xp54), which recognize the human protein, and YFP-LSm6 as P body-marker, revealed that endogenous rck/p54 is present in P bodies in HeLa cells.

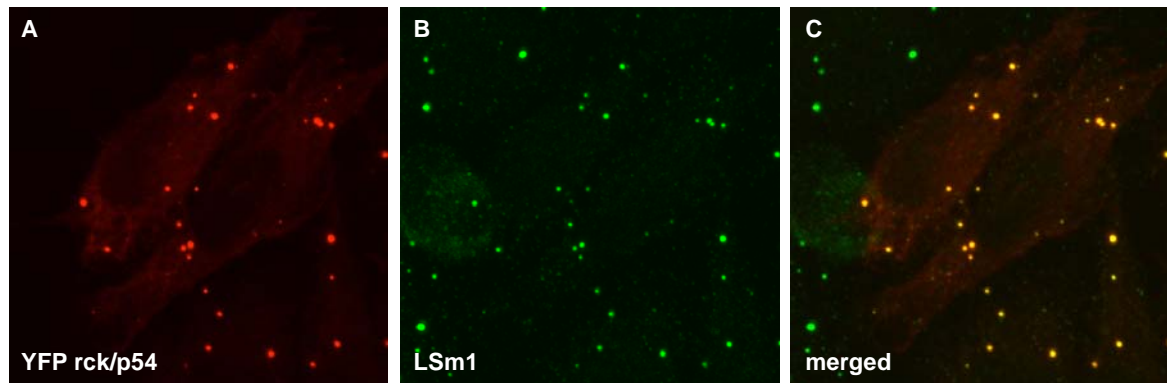


Figure 5.5. The rck/p54 protein is enriched in the cytoplasmic Processing bodies. HeLa SS6 cells were grown on coverslips, transfected with a plasmid encoding YFP-rck/p54 (A), fixed after 16 hours and stained with antibodies specific for LSm1 (B). Panel C shows the merged picture of the proceeding two panels, with overlaying signals appearing yellow. Pictures represent confocal microscopy sections.

To validate this finding, a YFP-rck/p54 fusion protein was expressed and colocalization with the P body marker LSm1 was verified (Fig. 5.5 C).

Another eIF4E-interacting protein we checked was the nucleocytoplasmic shuttling protein eIF4E-T, previously proposed to mediate the nuclear import of eIF4E (Dostie et al., 2000). The distribution of the endogenous eIF4E-T was tested by use of peptide antibodies against eIF4E-T in immunofluorescence experiments. The protein appeared to have a cytoplasmic localization and was concentrated in distinct foci (Fig. 5.6 A). Counterstaining with LSm1 demonstrated that eIF4E-T co-localizes with the P body marker protein (Fig. 5.6 C). Also, to exclude the possibility of unspecific antibody interactions, a vector encoding for YFP-eIF4E-T was constructed, and upon overexpression the fluorescent fusion protein exhibited a similar distribution (Fig. 5.6 D, F).

In order to get a hint for a possible new role of eIF4E-T, by comparison to that of the eIF4E translation binding partner, eIF4G, the cellular distribution of eIF4E-T was checked following induction of oxidative stress by incubation of HeLa cells with arsenite. Different from previous observations recorded with eIF4E or eIF4G (see unit 5.1), eIF4E-T was found to be enriched solely in P bodies and not in the stress granules that had formed (data not shown). This indicates that an eIF4E- eIF4E-T

interaction is only specific to the P bodies and speaks for a specific function of eIF4E-T within the frame of the cytoplasmic structures.

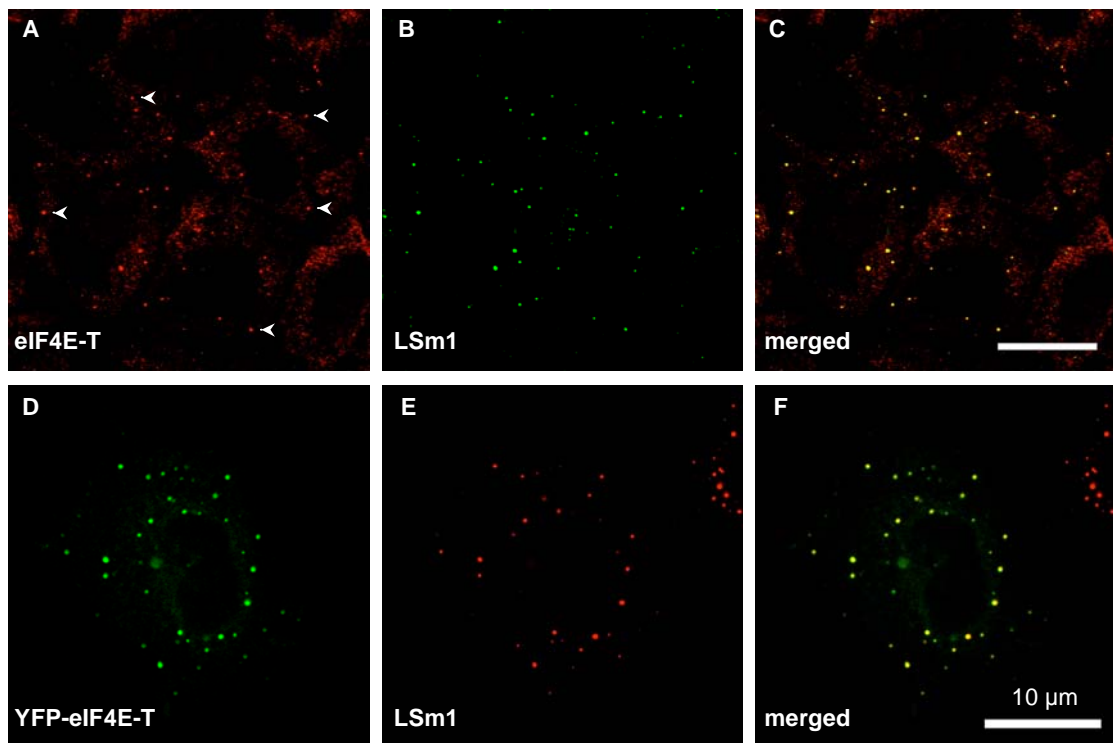


Figure 5.6. The eIF4E-Transporter protein is enriched in the cytoplasmic Processing bodies. HeLa SS6 cells were grown on coverslips, fixed, and stained with antibodies specific for eIF4E-T (goat anti-eIF4ET, Santa Cruz Biotechnology), (**A**, **arrowheads** indicate P bodies), LSM1 (**B**, **E**). Alternatively, cells were transfected with a plasmid encoding YFP-eIF4E-T (**D**) and fixed after 16 hours. Panels **C** and **F** show the merged picture of the proceeding two panels, with overlaying signals appearing yellow. Pictures represent confocal microscopy sections.

5.1.4 eIF4E interacts with eIF4E-T and rck/p54 in P bodies.

Biochemically, it has been reported that eIF4E and eIF4E-T interact *in vivo* and *in vitro* (Dostie et al., 2000a). Therefore it was tempting to study if these proteins interact inside P bodies *in vivo*. To determine whether the presumed protein pair eIF4E/eIF4E-T indeed forms a molecular complex inside P bodies *in vivo*, we performed fluorescence resonance energy transfer (FRET) measurements. In our system, we used the fluorescent protein pairs of CFP and YFP which can serve as donor and acceptor, respectively, with a calculated Förster distance, R_0 , of 4.9 nm for unoriented molecules (Patterson et al., 2000). Hence, only protein molecules within approximately 7 nm ($1.5 \times R_0$) of each other can generate FRET. Owing to the presence of endogenous eIF4E and eIF4E-T proteins in the cells and the variable expression of

the FP-eIF4E/eIF4E-T constructs, it is difficult to demonstrate FRET unambiguously by using sensitized acceptor emission alone. However, the FRET efficiency can be measured by acceptor photobleaching. We used this method that makes use of the fact that FRET quenches the donor fluorescence as the excitation energy is transferred to the acceptor. After photobleaching of the acceptor, this quenching no longer occurs, and the donor fluorescence increases. Quantification of this increase is a reliable and robust measure of FRET (Bastiaens, 1997; Miyawaki and Tsien, 2000). In cells expressing FP-tagged eIF4E and eIF4E-T we measured an average FRET efficiency of 13%. In contrast, cells expressing only YFP and CFP (negative control) did not show any FRET (Fig. 5.7 A).

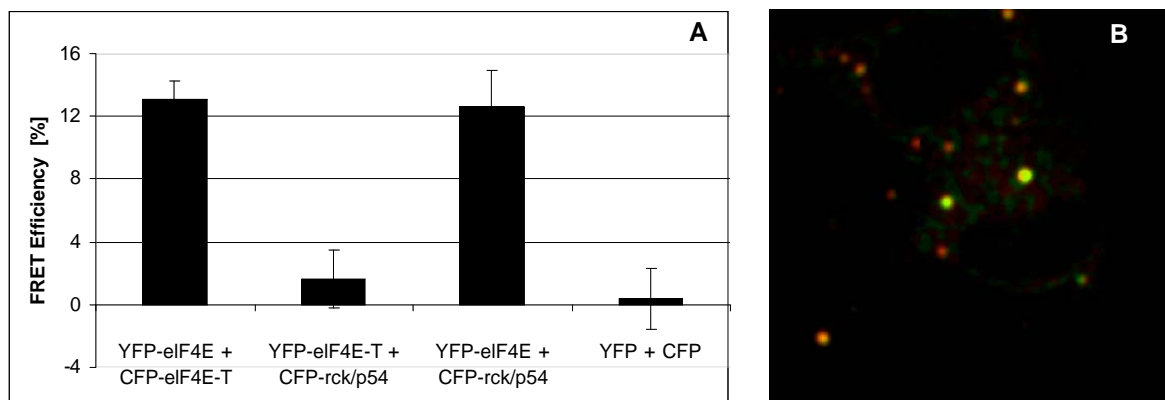


Figure 5.7. eIF4E and eIF4E-T proteins interact directly *in vivo* as demonstrated by FRET. (A) Bar chart represents the mean values of the apparent FRET efficiencies of three protein pairs from several P bodies in different cells. Error bars indicate the standard deviation from the mean values. (B). The protein pair CFP-eIF4E-T/YFP-eIF4E was co-expressed in HeLa SS6 cells. 16 hours after transfection cells were fixed and confocal images of both CFP and YFP channels were taken before and after photobleaching. The difference in post- and pre-bleach (of the YFP acceptor) intensity of the CFP-fluorescence was divided by the post-bleach CFP-fluorescence. The ratio was calculated pixel-by-pixel, and the result is shown color-coded. Green indicates a FRET efficiency of 15%, red indicates a FRET efficiency near 0 (no FRET). The image was contrast enhanced to display also the dim P bodies, in the pre-bleach donor image, which is the brightness channel of this image. The total size of this image corresponds to 56 μm in the sample.

Fig. 5.7 B shows a color-coded image of a cell co-expressing YFP-eIF4E and CFP-eIF4E-T. Green indicates a FRET efficiency of 15%, which is the case for the two bleached P bodies in this cell. The non-bleached P bodies did not exhibit FRET as indicated in red (~0% efficiency). In the same way, interactions between LSm proteins and Dcp1/Dcp2 were identified in P bodies, previously (Ingelfinger et al., 2002; Cougot et al., 2004). Therefore we decided to screen for interactions between other protein pairs. YFP-eIF4E-T/CFP-rck/p54 and YFP-eIF4E/CFP-rck/p54 fusion-protein pairs were co-expressed in HeLa SS6 cells. Cells expressing fluorescent

protein-tagged eIF4E and rck/p54 showed an average FRET efficiency of 12.6%, whereas cells expressing FP-tagged eIF4E-T and rck/p54 did not exhibit FRET (1.6% efficiency) (Fig. 5.7 A).

In conclusion, these studies indicate that the cap-binding translation initiation factor eIF4E is in molecular contact with eIF4E-T and rck/p54 in P bodies *in vivo*.

5.2. Factor requirements for the assembly of P bodies

At the beginning of this work, little was known about the factor requirements for the recruitment of P body components into these novel structures. mRNA degradation factors could be targeted independently to P bodies or, alternatively, together as part of a complex, or associated with their target mRNA. To understand their assembly mechanism we used RNA interference to deplete the cells of P body proteins or applied translation inhibitors to modulate the size of the mRNA pool available for processing within P bodies.

5.2.1 Interdependence of degradation factors for accumulation in P bodies determined in an RNA interference screen

To determine which are the proteins necessary for the concentration of degradation factors in P bodies, we took advantage of the newly established RNA interference technology and selectively depleted cells of a given P body factor and then assayed for the presence of LSM1, rck/p54, eIF4E, eIF4E-T, and Ccr4, as markers for P bodies. To check for the efficiency of the knockdowns, target mRNA levels were monitored by quantitative RT-PCR whereas protein levels were estimated in immunofluorescence microscopy observations.

5.2.1.1 Validation of knockdown efficiency by real-time RT-PCR

For RNAi, small-interfering RNA (siRNA) duplexes, 21 nucleotides long have been chemically synthesized targeting a perfect complementarity region in the coding sequence for the Dcp2 mRNA or regions in the 3'UTR of the mRNAs for Ccr4, LSM1, eIF4E-T and rck/p54. As siRNA control, a duplex representing a sequence

targeting the mRNA encoding for the luciferase enzyme of the firefly (*Photinus pyralis*) was used (GL2 siRNA), which has no homology with any human sequences.

In the quantitative, real-time reverse-transcription PCR (qRT-PCR) experiments, the primers used to check for siRNA targeted mRNAs were chosen to span exon- exon junctions in the genomic sequence as this is necessary to avoid unspecific amplification from genomic DNA (refer to Materials and Methods). GAPDH (Glyceraldehyde-3-phosphate dehydrogenase) has been regarded as a constitutive housekeeping gene and we used GAPDH gene primers in qRT-PCR amplification as a control to normalize changes in specific gene expression (Ullmannova and Haskovec, 2003). Quantification of the remaining mRNA by real time RT-PCR amplification following treatment of the cells with different siRNAs indicated an 82, 90, 79, 85 and 84% reduction in the mRNA levels of Ccr4, LSm1, eIF4E-T, rck/p54 and Dcp2, respectively, in the treated cells (Fig. 5.8). Thus, specific and almost complete removal of individual mRNAs could be obtained by delivering siRNA oligonucleotides to human cells in culture. However, different effects of the knockdowns on cell proliferation and cell survival were observed over time. For example, depletion of LSm1 had a pronounced negative effect on the viability of the knockdown cells as determined by counting the cell population at several time points (Ingelfinger, 2004).

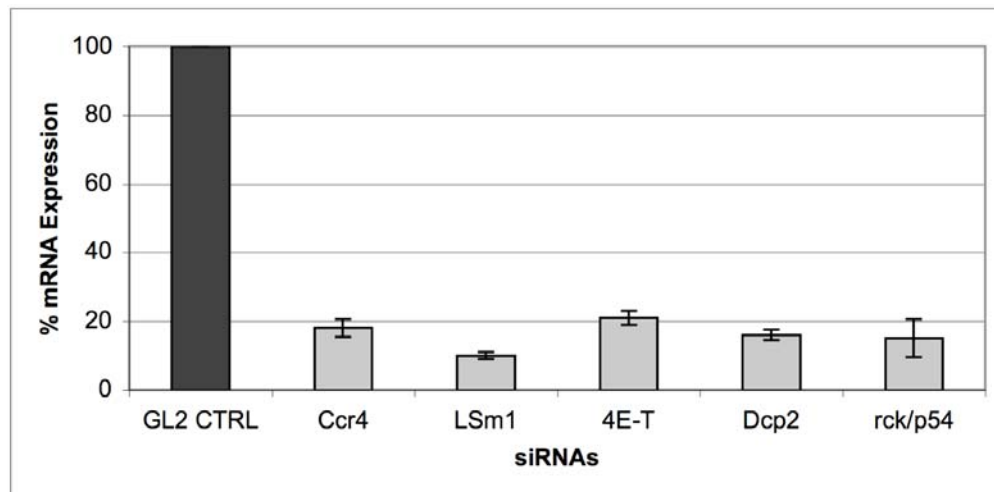


Figure 5.8. Efficient knockdown of Ccr4, LSm1, eIF4E-T, Dcp2 and rck/p54 mRNA levels is achieved by RNA interference as demonstrated by real-time RT-PCR. At different time points after transfection of the specific siRNAs (see text) cells were harvested and total RNA was extracted and incubated with RQ1 DNase. 50 ng of total RNA was used in one-step RT-PCR. The graph shows the reduction in target mRNA expression levels calculated from the real-time RT-PCR data compared to mRNA levels from cells transfected with GL2 control siRNA. Error bars indicate the standard deviation from several independent experiments.

Additionally, it led to the activation of the apoptotic cascade, which could be monitored by the TUNEL assay (data not shown). These observations were taken into account and integrated in the optimization of the knockdown protocol, for all proteins to be depleted. This was designed such that cell-biological recordings were made in a chosen time frame wherein efficient depletion of the protein is achieved and before apoptotic events are initiated, as to avoid untoward secondary events susceptible of generating artefactual results. Therefore, cells were assayed 32 h (Ccr4 knockdown), 50 h (LSm1 knockdown) and 60 h (eIF4E-T, rck/p54, and Dcp2 knockdowns) after transfection. At these time points the mRNA levels were clearly reduced but no apoptosis was observed by the TUNEL assay.

In an attempt to establish a possible role for the translation initiation factor eIF4E in the organization of the P bodies, several siRNAs have been designed and transfected in different combinations in order to deplete the protein from HeLa cells. These efforts have nevertheless failed and eIF4E protein or mRNA levels could not be satisfactorily reduced. This is most likely due to the fact that at least two eIF4E isoforms are being expressed simultaneously in human HeLa cells. Also, since they are both enriched in the P bodies, it can be assumed that they have a redundant function so that one isoform could take over the function of the other one missing.

5.2.1.2 Impact of the depletion of P body protein factors on their organization

Next, HeLa cells were depleted of single components and immunofluorescence labeling was used to determine the knockdown efficiency and monitor the role of individual components in P body stability. Following RNA interference, the presence of LSm1, rck/p54, eIF4E, eIF4E-T, and Ccr4 in P bodies was microscopically assayed. Efficient knockdown of eIF4E-T, LSm1 and rck/p54 proteins was visualized by the reduction of their own immunofluorescence signal (Fig. 5.9 panels I, K, Q). The distribution of the tested proteins was indistinguishable from that observed with untreated cells when the control siRNA (GL2) directed against the firefly luciferase mRNA was delivered to the cells (Fig. 5.9, panels A-E). Opposed to that, RNAi-mediated knockdown of eIF4E-T resulted in a dramatic reduction of rck/p54, eIF4E, and Ccr4 in P bodies as well as of that of the LSm1 marker (Fig. 5.9, panels F-J), which now appeared evenly distributed in the cytoplasm and no longer accumulated in the cytoplasmic foci. Similar results were

obtained when cells were depleted of LSm1 (Fig. 5.9 panels K-O) or rck/p54 (Fig. 5.9 panels P-T) when the P bodies could no longer be evidenced by any of the known markers tested. Hence, these components depend on each other for their accumulation in P bodies, suggesting that they are targeted to these structures together, as a complex.

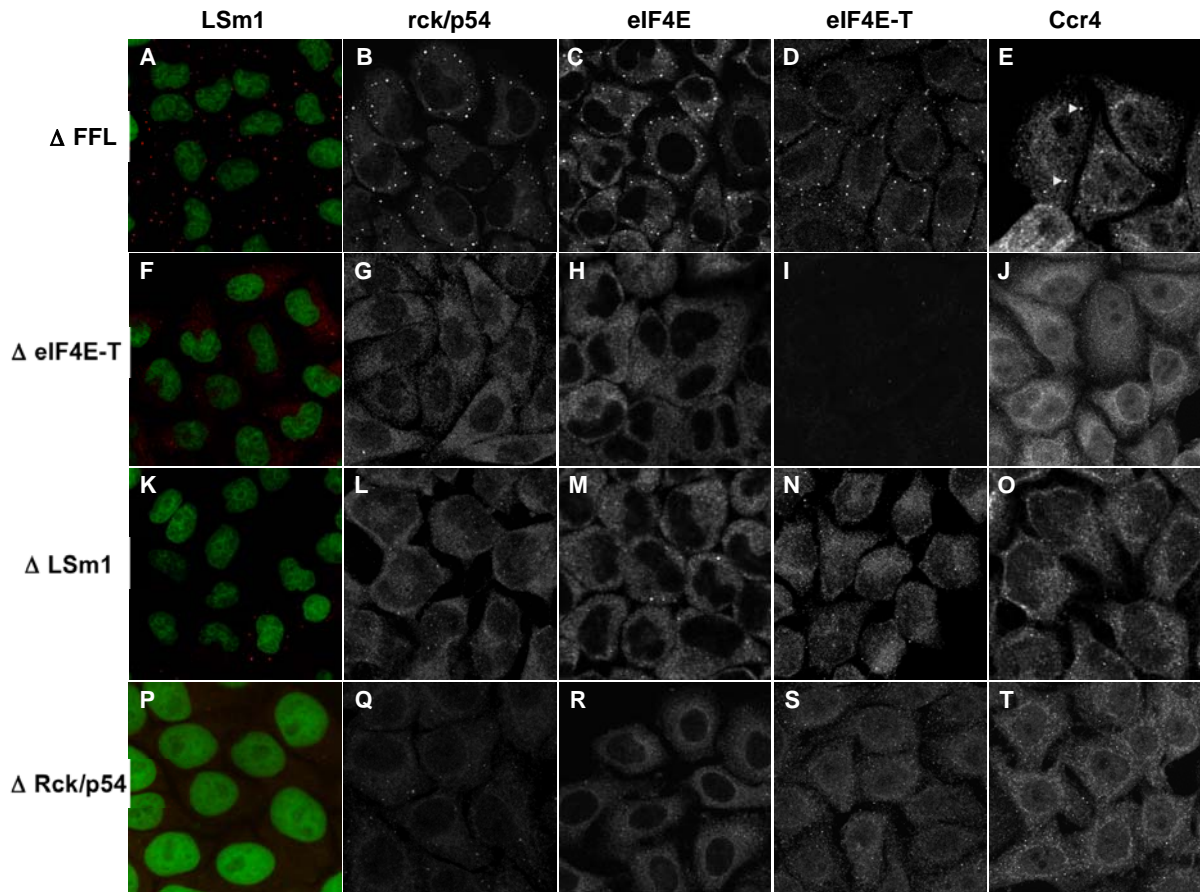


Figure 5.9. eIF4E-T, LSm1, rck/p54, are required for the accumulation of each other and of eIF4E and Ccr4 in P bodies. HeLa cells were transfected with GL2 luciferase control (Δ FFL, A-E), eIF4E-T (F-J), LSm1 (K-O) or rck/p54 (P-T) siRNA duplexes. Cells were immunostained with antibodies against LSm1 (A, F, K, P), rck/p54 (B, G, L, Q), eIF4E (C, H, M, R), eIF4E-T (D, I, N, S), and Ccr4 (E, J, O, T). Cells immunostained for LSm1 were counterstained with CybrGold highlighting cell nuclei (green). The panels show two-dimensional projections of a series of confocal fluorescence images in order to obtain sharp pictures displaying all P bodies in every cell. To highlight the significant structures, different magnifications were used for the various panels.

With regard to the enzymes carrying out the actual 5'→3' degradation of the mRNA (Ccr4, Dcp1/Dcp2 and Xrn1), it was important to determine how does their depletion affect the distribution of the P body factors. Upon successful depletion of the Ccr4 component of the cytoplasmic deadenylase, the P bodies have been again abolished from the cytoplasm, as demonstrated by immunostainings of several P body components tested (Fig. 5.10 panels A-E). This observation indicates that

abscission of the mRNAs' poly(A) tail is a prerequisite for the assembly of the P bodies.

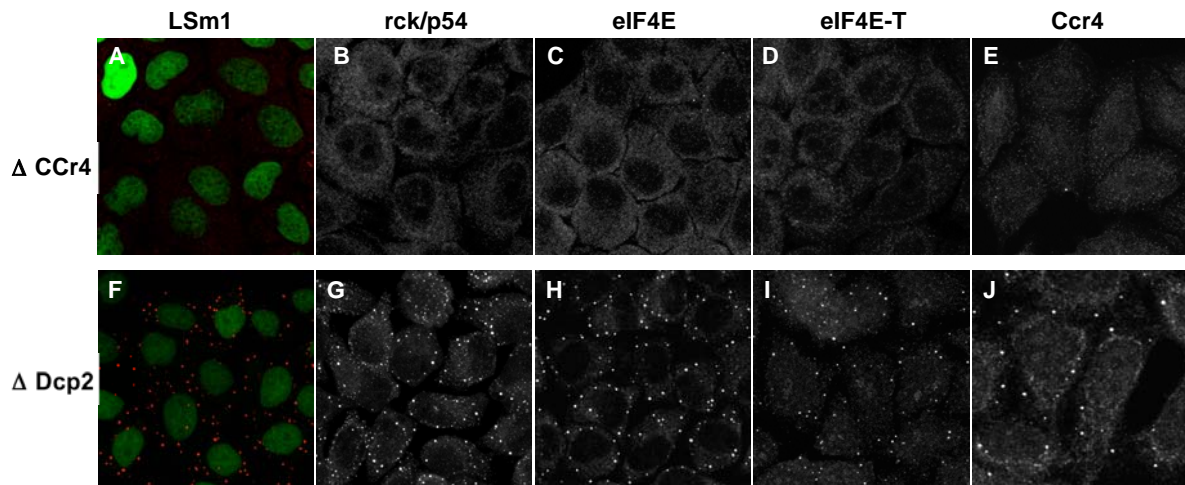


Figure 5.10. Ccr4, but not Dcp2, is required for the accumulation of P body components. HeLa cells were transfected with Ccr4 (A-E), and Dcp2 (F-J) siRNA duplexes. Cells were immunostained with antibodies against LSM1 (A, F), rck/p54 (B, G), eIF4E (C, H), eIF4E-T (D, I), and Ccr4 (E, J). In order to visualize individual cells in the depletion experiments, cells immunostained for LSM1 were counterstained with CybrGold labeling cell nuclei (green).

In striking contrast, RNAi-mediated knockdown of the decapping enzyme Dcp2, which initiates the actual 5'→3' degradation, did not have an inhibitory effect, but instead stimulated the accumulation of LSM1, rck/p54, eIF4E, eIF4E-T and Ccr4 in P bodies (i.e. an increase in the number of P bodies was observed (Fig. 5.10 panels F-J compare with Fig. 5.9, panels A-F). A similar effect was observed following the knockdown of the 5'→3' exoribonuclease Xrn1, whereby the P body number considerably increased as compared to the wild type cells [data not shown; see also (Cougot et al., 2004)]. Hence, the decapping and the mRNA body decay enzymes are dispensable for the targeting of other P body components to these sites.

5.2.2 mRNA flux is required for the maintenance of P bodies

The loss of accumulation of multiple factors in P bodies upon RNAi-mediated depletion of eIF4E-T, LSM1, rck/p54, or Ccr4, prompted us to believe that these proteins may be targeted to the foci together, either as part of one or more heteromeric protein complexes or a larger mRNP complex. To inspect whether mRNA is required for the accumulation of all tested P body factors, we varied the size of the free mRNA pool by applying different drugs to HeLa cells. Subsequently

we checked by immunofluorescence whether the accumulation of various factors in P bodies was affected.

First, we treated HeLa cells with cycloheximide, which sequesters the mRNAs during translation elongation.

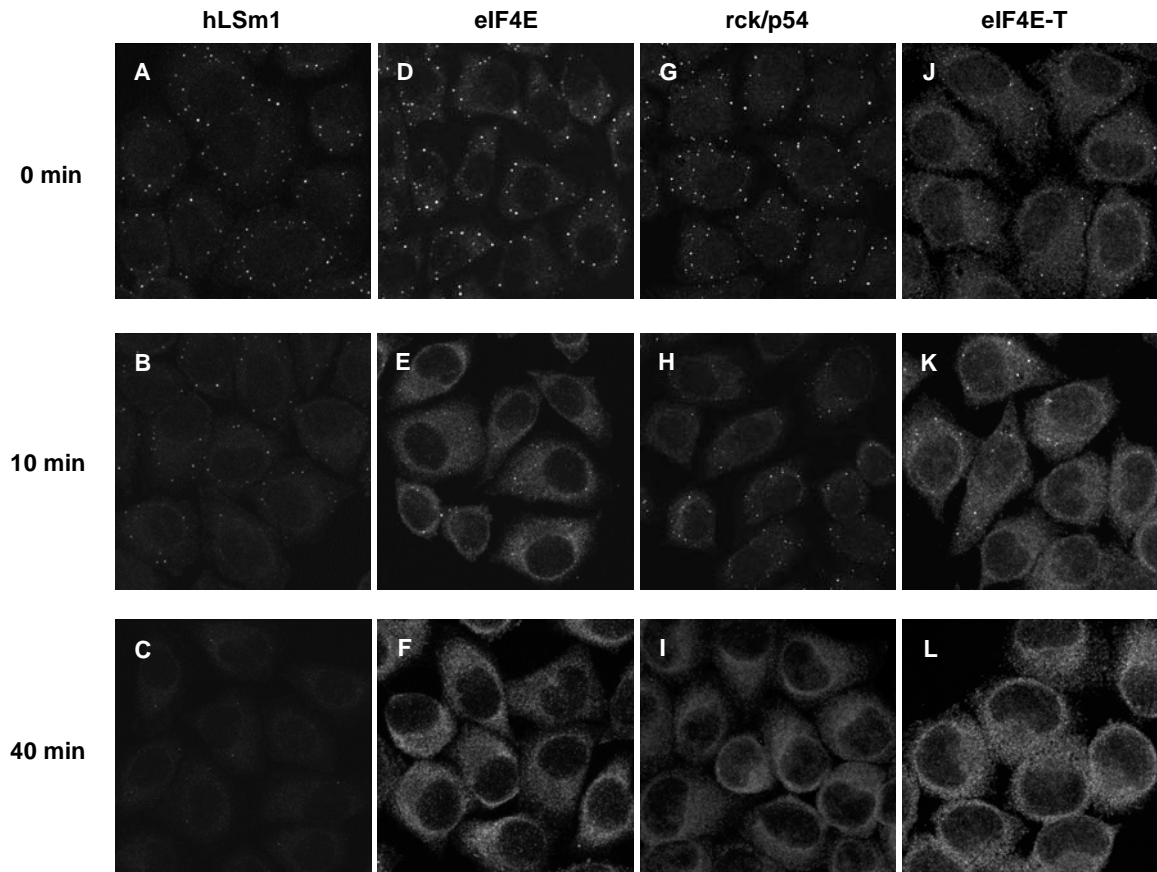


Figure 5.11. Effect of cycloheximide on the accumulation of LSm1, eIF4E, rck/p54, and eIF4E-T in P bodies. Cells grown on cover-slips were incubated with cycloheximide (20 $\mu\text{g}/\text{ml}$) and fixed at 0 min, 10 min, and 40 min after addition of inhibitor. Cells were immunostained with antibodies against LSm1 (A-C), eIF4E (D-F), rck/p54 (G-I), and eIF4E-T (J-L). The panels represent two-dimensional projections (Zeiss Software) of a series of confocal fluorescence images.

The drug stalls the mRNAs onto polysomes and prevents them from becoming available as substrates for decay (reviewed in Jacobson and Peltz 1996), (Ross, 1995). In fact, as shown in Fig. 5.11, treatment of cells with cycloheximide resulted in a rapid loss of LSm1 (A-C), eIF4E (D-F), rck/p54 (G-I) and eIF4E-T (J-L) from P bodies. Time-lapse imaging with cells expressing an YFP-eIF4E-T fusion revealed that 50% of the P bodies disappeared within 17 min of cycloheximide incubation (data not shown). Incubation with the solvent (DMSO) had no effect on P body formation. Therefore, cycloheximide not only acts as a translational inhibitor, but blocks degradation of the mRNA, too. The observation of the hasty disassembly of the P

bodies comes in support of a model in which P body residents are targeted to these foci together with mRNA as mRNP complexes.

In a complementary experiment, we inhibited translation by applying the drug puromycin onto HeLa cells in culture. This antibiotic has a similar structure to that of aminoacyl-tRNA and thus becomes incorporated into the nascent polypeptide. As opposed to cycloheximide, puromycin causes premature translation termination and release of mRNAs from polysomes.

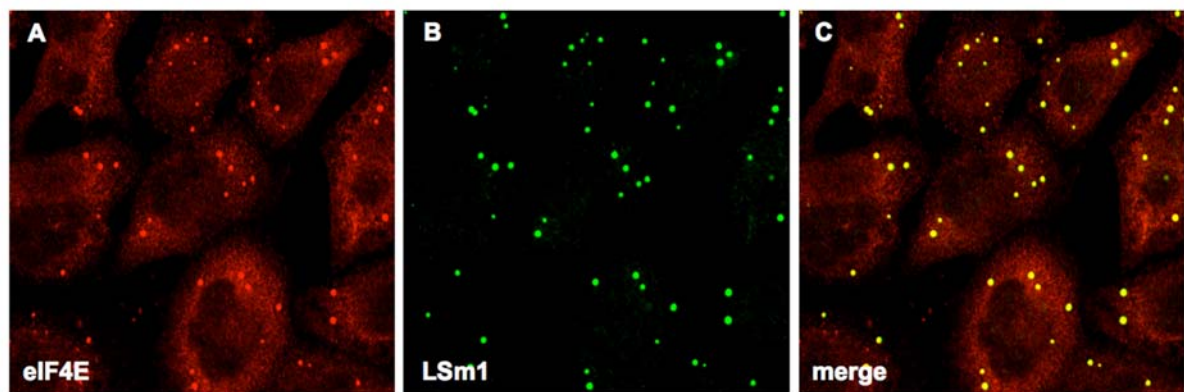


Figure 5.12. Effect of puromycin on the accumulation of eIF4E and LSM1, in P bodies. Cells were incubated with puromycin (50 $\mu\text{g}/\text{ml}$) and fixed 2 hours after addition of the inhibitor. Cells were immunostained with antibodies against eIF4E (A) and LSM1 (B). Overlapping signal of the P bodies in panel C appears yellow.

By this, the pool of naked, free mRNA is enlarged and hence, also that of the putative decay substrates. This is in agreement with the finding that upon puromycin treatment an enlargement of the P bodies is manifest, as shown (Fig. 5.12), suggesting that, the more mRNA is readily available in the cytoplasm, the more decay factors are prone to accumulate in the P body compartment to allow for increased efficiency and processivity.

5.3 FRAP reveals a rapid exchange of P body components.

The rapid loss of LSM1, eIF4E and eIF4E-T from P bodies upon cycloheximide treatment (see unit 5.2.2) suggested that factors exchange rapidly in these structures that seem to be very dynamic in nature. To learn more about the turnover of factors involved in P body formation, we performed fluorescence recovery after photobleaching (FRAP) experiments using YFP-LSM6, YFP-eIF4E, and YFP-eIF4E-T fusion proteins. The data were acquired 20 hours after transfection, when the P bodies were readily visible. Individual P bodies were bleached and fluorescence

recovery inside the bodies was measured in a time series up to 400 sec. The fluorescence of YFP-LSm6 and YFP-eIF4E-T recovered to a maximum level of $73 \pm 5\%$ ($t_{1/2} = 25 \pm 5$ sec) and $89 \pm 3\%$ ($t_{1/2} = 60 \pm 7$ sec), respectively, of the pre-bleaching intensity within the acquisition time. YFP-eIF4E recovered to $45 \pm 2\%$ with a calculated $t_{1/2}$ of 46 ± 8 sec (Fig. 5.13, graph).

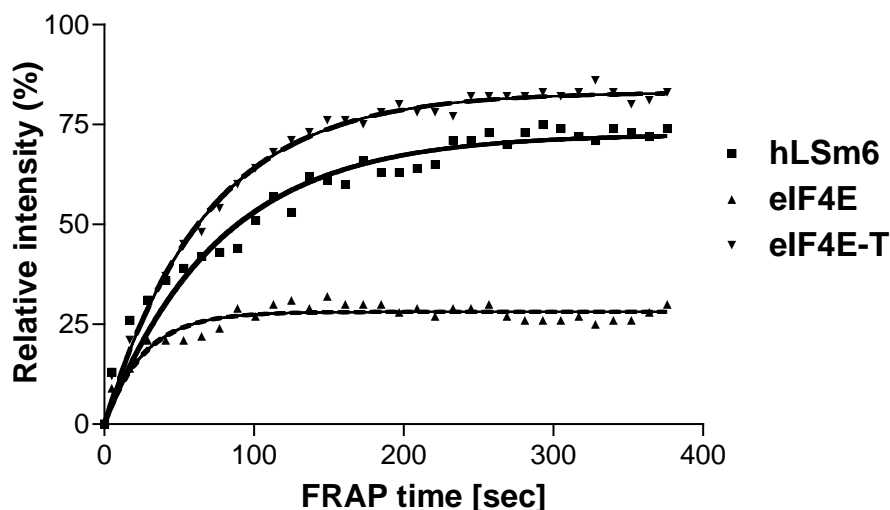


Figure 5.13. Fluorescence recovery after photobleaching indicates that P bodies have a highly dynamic nature. HeLa cells were transfected with plasmids encoding YFP-LSm6, YFP-eIF4E, or YFP-eIF4E-T. Individual P bodies were selected and recorded before bleaching. After the laser photobleaching was performed, images were collected every 20 sec during the course of fluorescence recovery. For each time point fluorescence intensity within the region of interest was measured and plotted in the graph shown relative to the intensity before bleaching. From each data set, fluorescence recovery curves were calculated using non-linear regression. Fitting was carried out by Dr. D. Ingelfinger using the Marquardt method (GraphPad Software).

These results demonstrate that YFP-eIF4E-T, YFP-LSm6 and YFP-eIF4E exchange quickly, supporting the notion that P bodies are dynamic structures rather than static aggregates.

5.4 Intrinsic signals responsible for P body targeting and assembly

In our work so far, we had identified several factors that are potentially involved in the transition of the mRNA from active translation to degradation and are essential for the accumulation of each other into P bodies. However, it was still not clear which are the individual, intrinsic structural features that would support their

assembly in these bodies and our next aim was to find out whether particular signals exist that may be responsible for the targeting/ accumulation into P bodies.

5.4.1 Mutagenesis analyses of eIF4E

It was particularly interesting to find out the modality by which eIF4E becomes associated to the P bodies, whether its interaction with the mRNA alone, or its binding to other proteins mediate eIF4E targeting to the foci. To address this question, we took advantage of the fact that previous investigations had identified the critical residues responsible for the interactions of eIF4E with the m⁷G and eIF4E-T, and we analyzed the effects of specific mutations within the cap-binding protein on its incorporation to the P bodies. Thus, recombinant eIF4E containing vectors were engineered to express proteins bearing mutations in the m⁷G -5'cap or eIF4E-T binding sites. The plasmids encoding mutated eIF4E proteins were transfected into HeLa cells and their ability to be integrated into P bodies was analyzed.

First, the cap-binding domain was modified whereby residues Tryptophan 103 and Glutamic acid 104 have been replaced by two Alanines (YFP-eIF4E^{WE 102,103 AA}), as this was shown to abolish cap interaction (Morino et al, 1996).

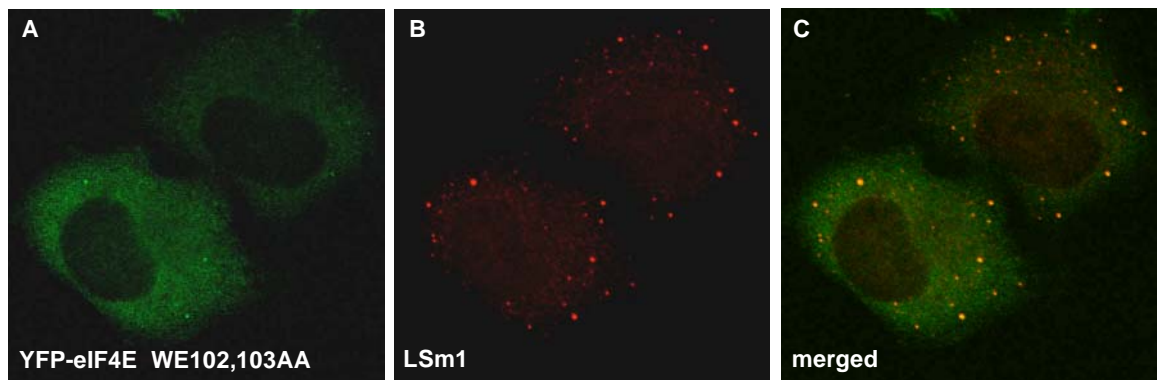


Figure 5.14. Accumulation of eIF4E in P bodies is negatively affected upon loss of cap binding. HeLa SS6 cells were grown on coverslips for 24 hours, then transfected with a plasmid encoding a mutant YFP-eIF4E (A). After 16 hours, cells were fixed and stained with antibodies specific for LSm1 (red, B). Panel C shows the merged picture of the proceeding two panels, with overlaying signals appearing yellow

Following overexpression of this YFP-tagged mutant protein and counterstaining with the P body marker LSm1, it became apparent that the mutants' capability to concentrate into the P bodies is substantially impaired, indicating that binding of

eIF4E to the mRNA is necessary for its enrichment in P bodies (Fig. 5.14 A, C compare to Fig. 5.1 D, F).

Second, the binding domain of eIF4E with eIF4E-T was modified in order to find out whether this interaction is also necessary for eIF4E to be directed to the P bodies. A mutated form of eIF4E fused to YFP was constructed in which the eIF4E-T interacting site is inactivated (Marcotrigiano et al, 1999), wherein the residue Tryptophan 73 was replaced by Alanine (YFP-eIF4E^{W73A}). In contrast to the wild type protein, eIF4E^{W73A} no longer localized to P bodies (Fig. 5.15 C) and was redistributed evenly between the cytoplasm and the nucleus in HeLa cells (Fig. 5.15 A compare to Fig. 5.1 D). These results indicate that an interaction between eIF4E and eIF4E-T is required for the targeting of eIF4E to P bodies, as well as for its exclusion from the nucleus.

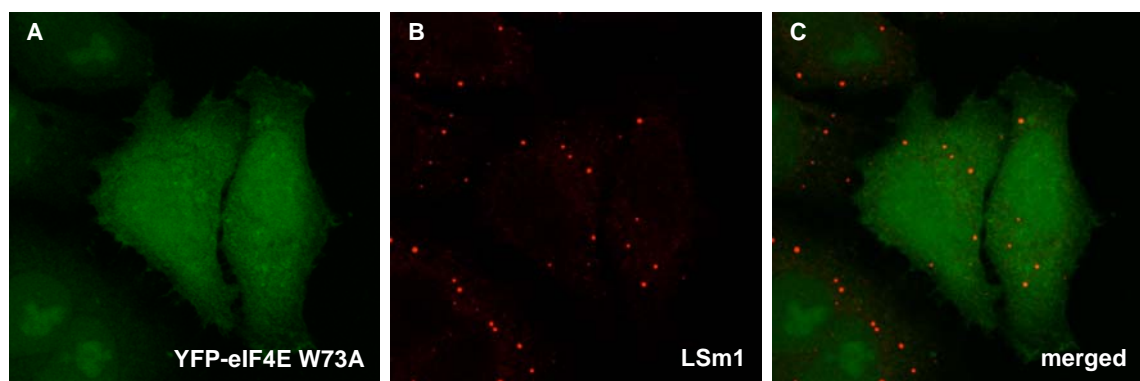


Figure 5.15. Accumulation of eIF4E in P bodies does not occur following removal of the eIF4E-T binding site. HeLa SS6 cells were grown on coverslips for 24 hours, then transfected with a plasmid encoding a mutant YFP-eIF4E (A). After 16 hours, cells were fixed and stained with antibodies specific for LSml (red, B). Panel C shows the merged picture of the proceeding two panels.

5.4.2 Mutagenesis analyses of eIF4E-T

The finding that eIF4E-T appears responsible for the localization of eIF4E into P bodies prompted us to further investigate the role of this critical P body component on the assembly and stability of these structures, by performing a mutagenesis screen.

5.4.2.1 Implications of eIF4E-T interaction site mutagenesis on P body formation

Taking into account the consequences of blocking the eIF4E interaction capabilities, a reciprocal approach was undertaken and an eIF4E-T mutant was generated that contained an inactivated eIF4E-binding site. This was achieved by

replacing the two conserved Leucine residues (Fig. 5.4) by two Glycines (YFP-eIF4E-T^{LL 35,36 GG}), within the previously biochemically characterized eIF4E binding site (Dostie et al., 2000). From Fig. 5.16 (A, D) it can be observed that the mutant protein also appeared concentrated in distinct foci. Immunofluorescence with antibodies against eIF4E (B) and the P body marker LSm1 (E) shows that the mutant eIF4E-T co-localized with the two proteins, in P bodies (C, F). This comes as an indication that accumulation of eIF4E-T inside the bodies occurs independent of the interaction with the translation initiation factor 4E.

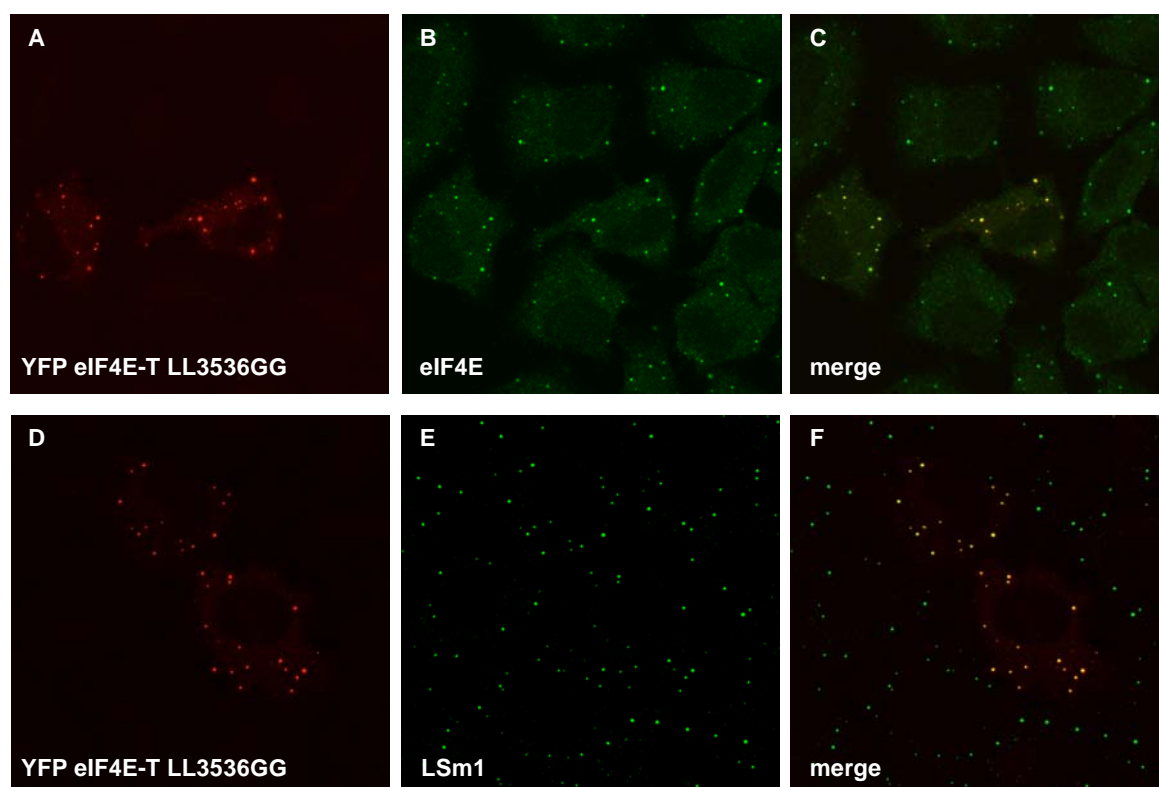


Figure 5.16. Accumulation of a mutant eIF4E-T protein in P bodies is not affected upon loss of eIF4E binding. HeLa SS6 cells were grown on coverslips for 24 hours, then transfected with a plasmid encoding a mutant YFP-eIF4E-T (A, D). After 16 hours, cells were fixed and stained with antibodies specific for eIF4E (B) or LSm1 (E). Panels C and F show the merged picture of the proceeding two panels, with overlaying signals appearing yellow.

To rule out the possibility of the endogenous eIF4E-T interfering with the localization of the mutant to the P bodies and that of mediating the transport of eIF4E to these sites, a knockdown-and-rescue approach was designed. This was used as an assay to further our understanding of the role of the interaction of the two proteins in P body formation. For this purpose, depletion of endogenous eIF4E-T by means of RNA interference was firstly accomplished. To allow for later restoration experiments

using exogenous recombinant protein, this was achieved by using a siRNA targeting a sequence in the 3' untranslated region (UTR) of the eIF4E-T gene. Readily, a clearance of the P bodies was observed as shown in Fig. 5.9 by immunostainings using antibodies against eIF4E (H) as compared to the control firefly luciferase siRNA (C). In the step following eIF4E-T knockdown a vector containing YFP-eIF4E-T was supplied to the depleted cells and the expression was monitored. As shown in Fig. 5.17 by counterstaining with eIF4E antibodies (B), the cells expressing the

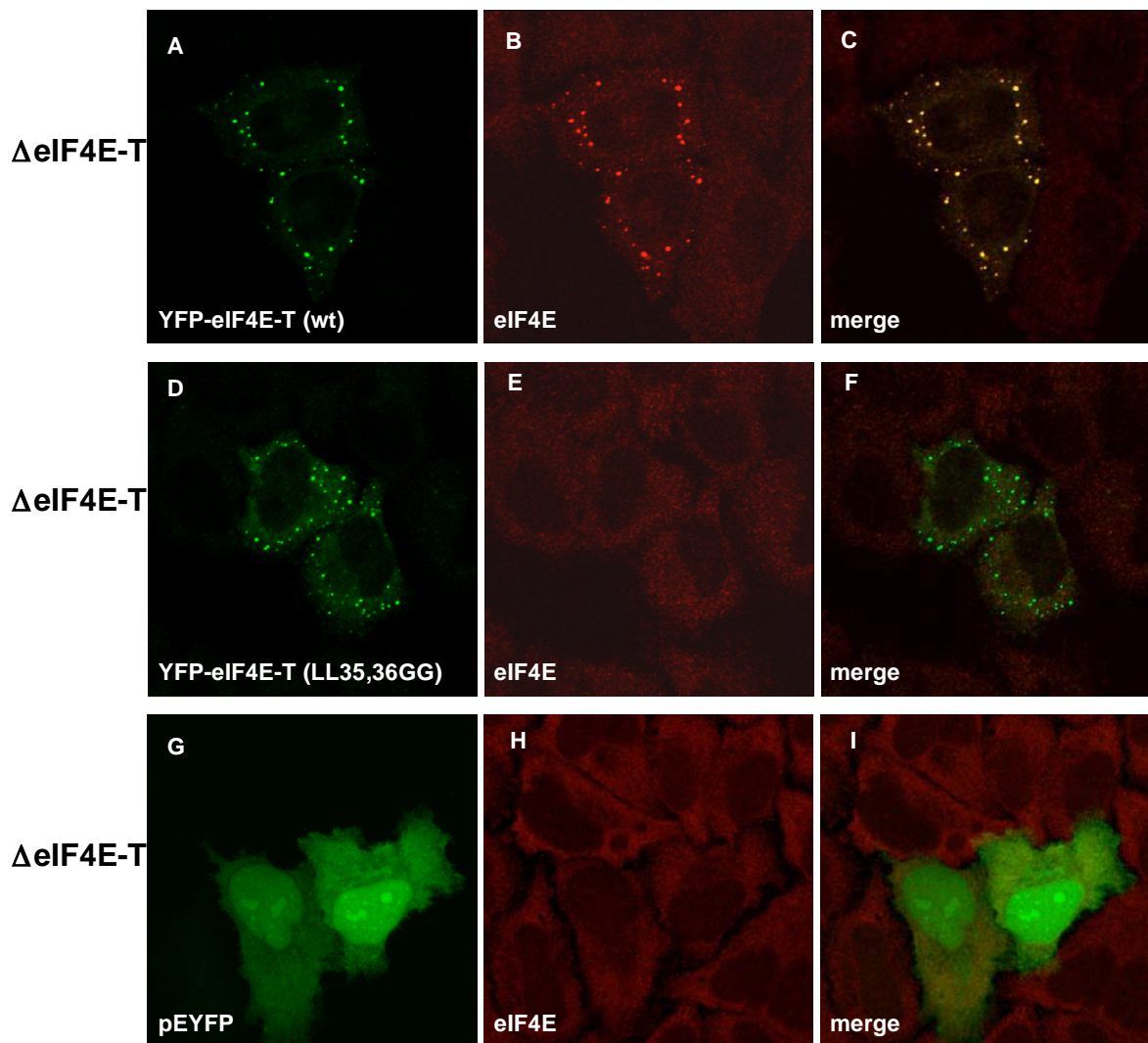


Figure 5.17. On a cellular substrate depleted of endogenous eIF4ET, only the wild-type, externally provided eIF4ET is able to restore de novo formation of P bodies. HeLa cells were plated on coverslips and after 24 hours siRNA duplexes targeting the 3'UTR of eIF4E-T has been delivered to the cells. 44 hours later, wild-type YFP-eIF4E-T (A) or a mutant YFP-eIF4E-T^{LL35,36 GG} (D) has been introduced in the cells by transient transfection. As a control, the empty pEYFP vector was delivered to the cells previously depleted of eIF4E-T (G). After 16 hours, cells were fixed and immunostained for eIF4E (red, B, E, H). Panels C, F and I show the merged picture of the proceeding two panels; the overlapping signal appears yellow.

wild-type eIF4ET-YFP fusion had recovered from the knock-down and reassembled P bodies (C) meaning that the exogenous protein is, as expected, capable of restoring the function of the missing, endogenous eIF4E-T.

In a similar experiment, following knockdown of endogenous eIF4ET, the YFP-eIF4E-T^{LL35,36GG} construct was introduced to the cells. However, in contrast to the wild type protein, when looking at the eIF4E localization (E), the mutant did no longer sustain eIF4E incorporation confirming that disruption of this interaction is incompatible with restoration of eIF4E inside newly formed P bodies.

As a control, the vector encoding the Yellow Fluorescent Protein was transfected and as shown in panel H, YFP alone was not able to promote the accumulation of eIF4E into P bodies, either. Altogether, these data demonstrate that eIF4E is dispensable for the formation of P bodies, and it is the interaction with eIF4E-T that promotes the targeting of eIF4E to these structures.

5.4.2.2 Functional mapping of eIF4E-T domains

From our work until now, it became manifest that eIF4E-T is a crucial component of the P bodies. Nevertheless, little was known about the structural features of eIF4E-Transporter and which are their functional implications. Apart from the eIF4E binding site, the two functional leucine-rich nuclear export signals and the functional nuclear localization signal no other particular elements could be resolved within the 985-aminoacid stretch of eIF4E-T (Fig. 5.18).

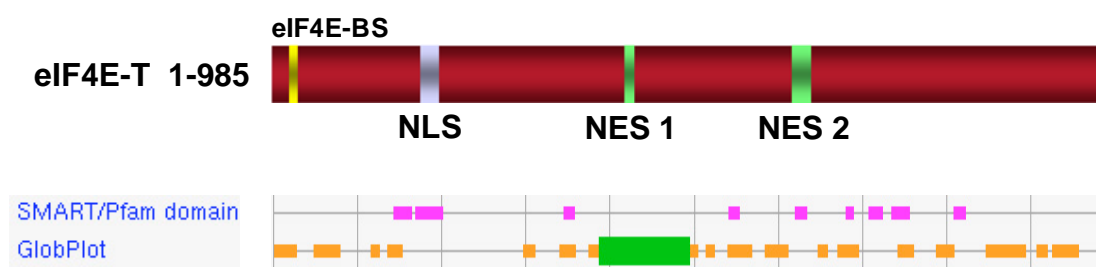


Figure 5.18. Structural and functional features of the eIF4E-T molecule. Aminoacids 29-36 contain the eIF4E binding site (yellow), aminoacids 194-211 encode a functional bipartite Nuclear Localization Signal (blue); aminoacids 438-447 and 613-638 encode the two functional Nuclear Export Signals (green, Dostie et al, 2000). One globular domain (aminoacids 386-493, green in lower schematic) is predicted to form, whereas the rest of the protein structure is disordered (orange). Purple blocks represent low complexity regions, as predicted by the *Eukaryotic Linear Motif* server.

Our finding that the mutant YFP-eIF4E-T^{LL35,36GG} could still become enriched in the cytoplasmic foci could be explained by at least two possible scenarios. In the first one, eIF4E-T would be capable of accumulating independently from mRNPs, possibly due to an intrinsic signal, which waits to be exposed. The second assumption would involve the requirement for additional interactions with proteins other than eIF4E, and for this also, the search for putative binding sites needs to be carried out. We anticipated that more interesting phenotypes would arise from a systematic analysis of the eIF4E-T sequence and this would help to elucidate the functional implications of this novel protein.

With the aim of defining the specific domain(s) capable of targeting the protein to the P bodies, a series of deletion mutants was generated (Fig. 5.19) and their cellular distribution was subsequently analyzed by fluorescence microscopy.

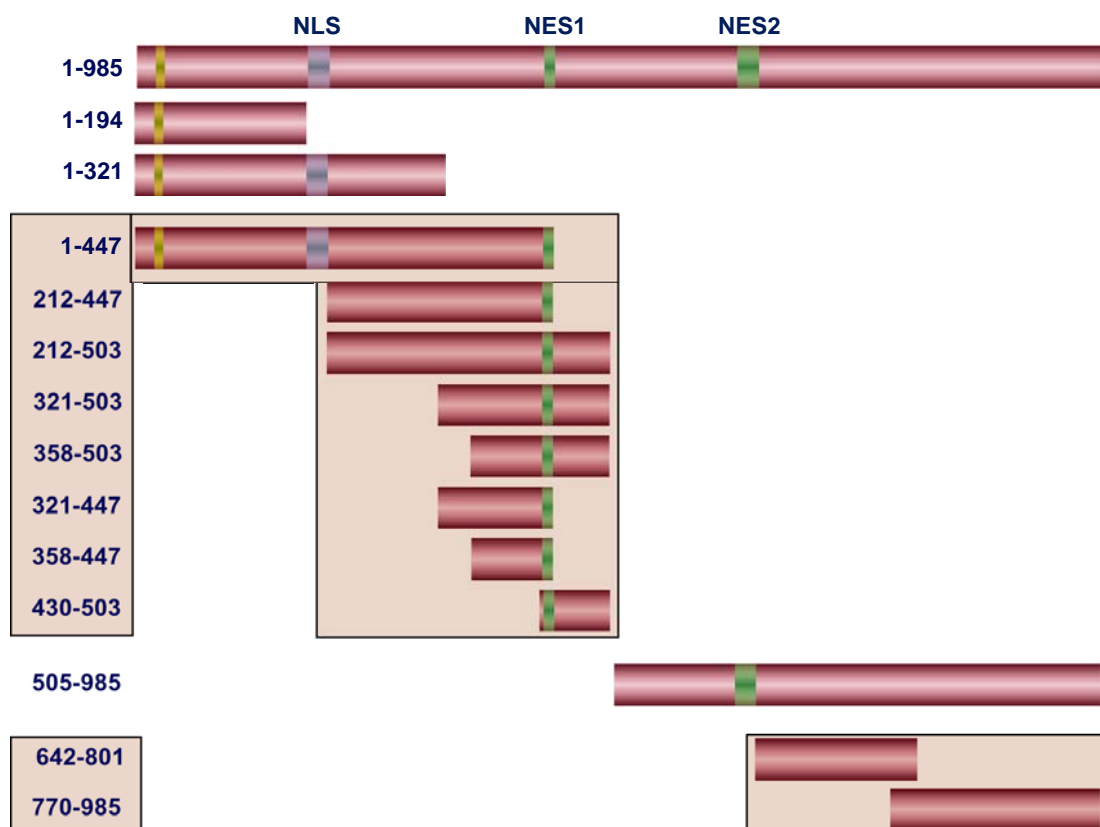


Figure 5.19. Schematic representation of the eIF4E-T molecule and several of its deletion constructs generated in order to define a P body localization signal. Numbers represent aminoacid residues of the subcloned fragments and originate from the full-length sequence (1-985) depicted at the top of the figure. Boxed in brown are truncated proteins that act as dominant negative molecules, i.e. whose expression in HeLa cells leads to dissolution of P bodies. Yellow bar represents the eIF4E-binding site, NLS stands for nuclear localization signal, NES stands for nuclear export signal.

Firstly, the N- terminal region of eIF4E-T was in focus, and for that, two C-terminus deletion constructs with or without the putative NLS/ NES1 were generated as fusions of YFP and their expression pattern is presented in Fig. 5.20.

The first fragment, YFP-eIF4E-T 1-194, which has the stop codon immediately before the NLS, has a diffuse presence in the cytoplasm of HeLa cells and is also localized to the nucleoplasm (**A**). This is presumably due to its low molecular weight, which can allow for free diffusion through the nuclear pore. The lack of a NES, however, might explain why the protein is not readily transported back into the cytoplasm. From the overlaid picture (**C**) it becomes clear that the cytoplasmic fraction of the recombinant protein is not being enriched into P bodies that are labeled by LSm1 (**B**).

A second N-terminal fusion protein YFP-eIF4E-T 1-321 that contains the full NLS but none of the NESs is, as expected, exclusively localized to the nucleus (**D**) and is not present in the P bodies (**E**), suggesting that the missing C- terminal domain is essential for the P body accumulation.

A third N-terminal fragment of eIF4E-T of the first 447 aminoacids contains both the NLS and the NES 1. The protein is uniformly distributed throughout the cytoplasm and is, again, excluded from the nucleoplasm confirming the fact that the two signal domains are functional (Fig. 5.20 **G**). This protein does not become enriched in cytoplasmic foci, and furthermore, cells expressing eIF4E-T 1-447 do no longer contain P bodies as evidenced by the staining of the P body marker LSm1 (**H**). This becomes more clear in the overlaid picture in which cells expressing the YFP-eIF4E-T truncated protein appear devoid of P bodies, as compared to the neighbouring cells harbouring the normal phenotype (**I**).

Taken together, we learn from these data that irrespective of a preserved eIF4E-binding site (aminoacids 29-36), the C- terminal part of eIF4E-T appears to be required to support incorporation of the protein into P bodies.

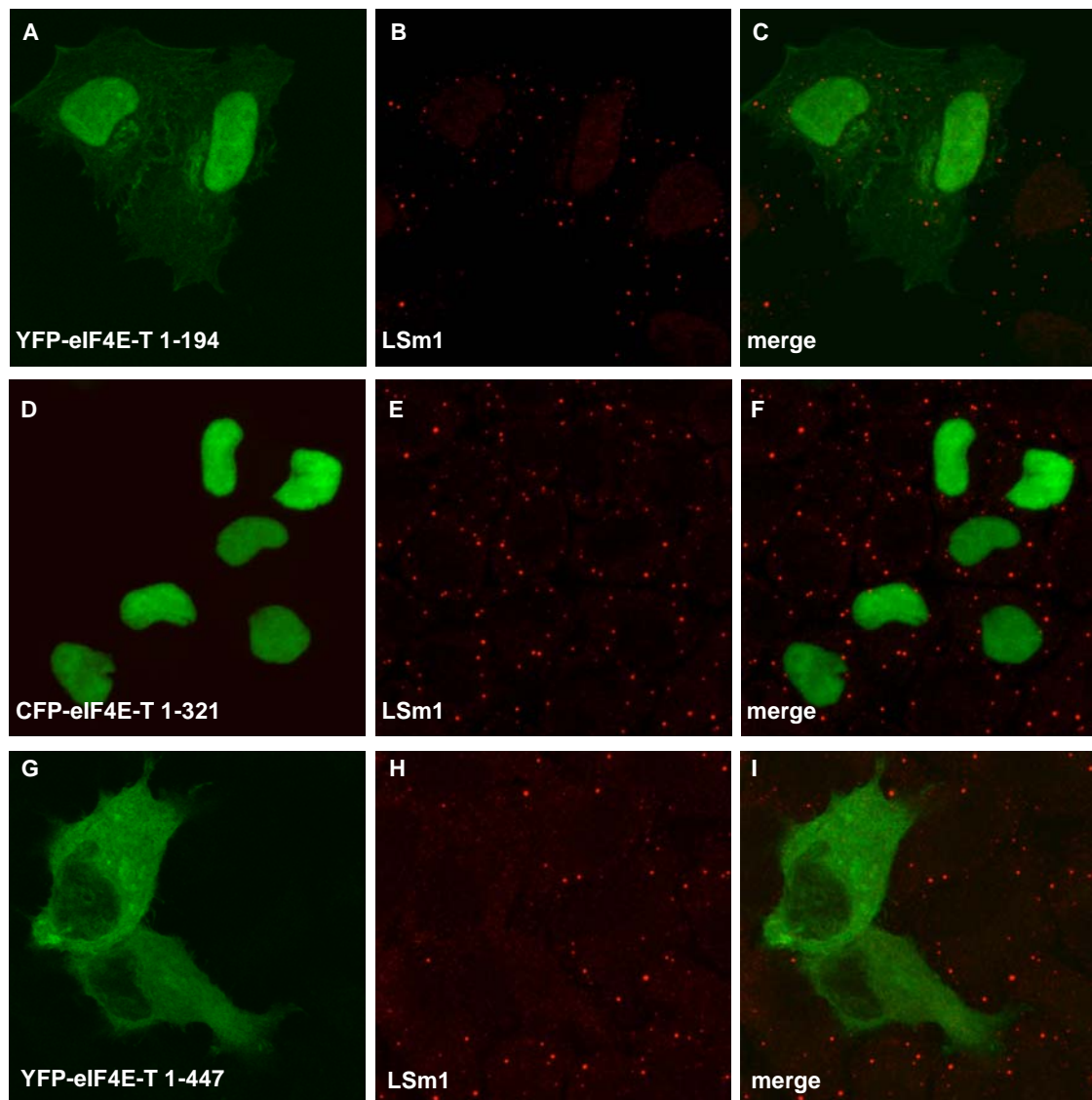


Figure 5.20. Cellular distribution of N- terminal fragments of the eIF4E-T molecule. HeLa S6 cells were grown on coverslips for 24 hours, then transfected with plasmids encoding truncated Y(C)FP-eIF4E-T proteins (aminoacids 1-194 Δ NLS Δ NES, **A**; aminoacids 1-321 Δ NES1, **D**; aminoacids 1-447, **G**). After 16 hours, cells were fixed and stained with antibodies specific for LSml (red, **B**, **E**, **H**). Panels **C**, **F** and **I** show the merged picture of the proceeding two panels.

In order to try to understand the basis for the striking phenotype whereby the expression of a truncated protein led to the loss of the P bodies as marked by LSml, we continued mapping the internal region of the eIF4E-T molecule. Several deletion constructs spanning the central domain of eIF4E-T have been designed by taking in consideration the primary protein sequence as well as the NES12 located between aminoacids 438-447. Due to the similarity of their phenotypes, only two examples will be discussed below.

The expression pattern of the fusion protein starting after the NLS and incorporating the NES1: YFP-eIF4E-T 212-447 is presented in Fig. 5.21, panel **A**. The protein exhibits a diffuse cytoplasmic distribution whereas it is not being concentrated in specific foci. Additionally, when looking at the counterstaining image of LSm1 (**B**), its signal appears to be lost in the cells expressing the deletion eIF4E-T construct. This is indicative of the fact that this recombinant protein may function as a dominant negative protein for the P bodies, i.e. its overexpression leads to a disequilibrium in the cell, whereby dismantling of the P bodies is triggered. In an attempt to narrow down the smallest possible region responsible for this effect several constructs have been generated as depicted in Fig. 5.19 upper brown box. All constructs schematized there featured the same visual aspect and had a similar impact as YFP-eIF4E-T 212-447, resulting in the loss of P bodies (data not shown).

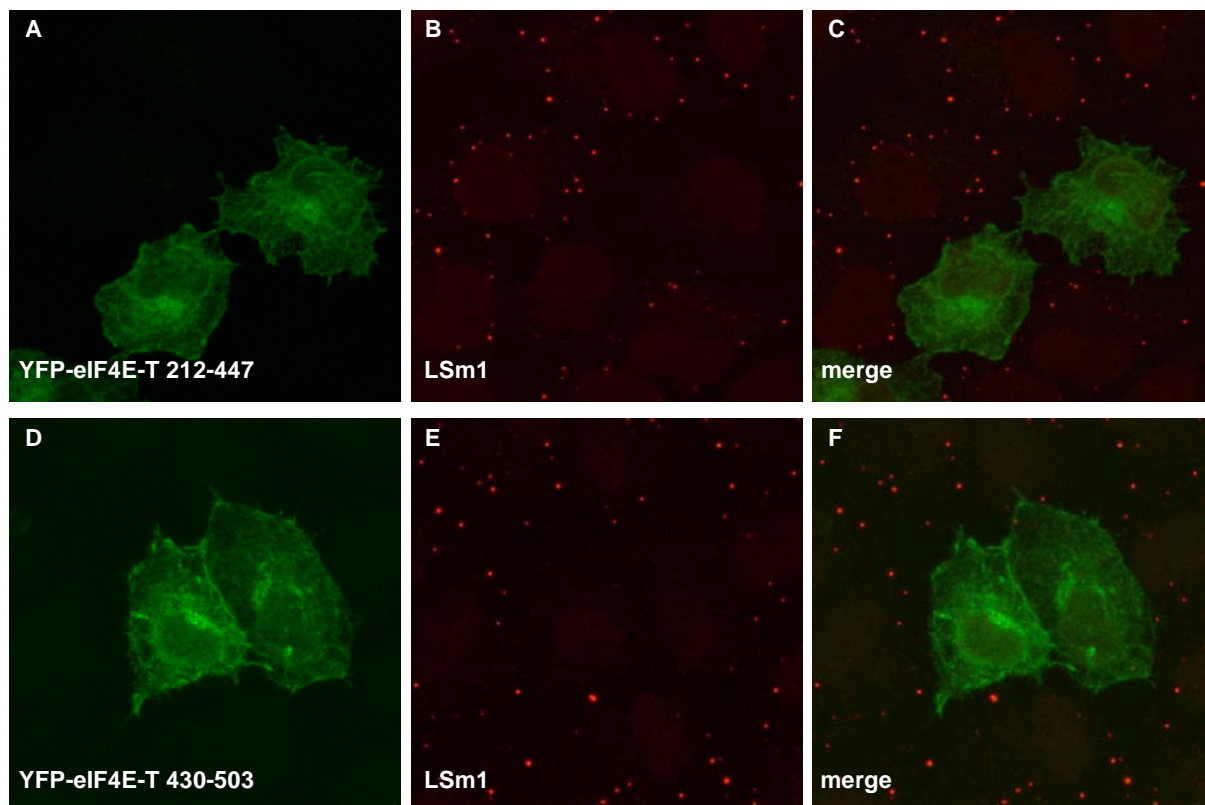


Figure 5.21. Cellular distribution of constructs expressing central domains of the eIF4E-T molecule. HeLa SS6 cells were grown on coverslips for 24 hours, then transfected with plasmids encoding truncated YFP-eIF4E-T proteins (aminoacids 212-447 Δ NLS, **A**; aminoacids 430-503 Δ NLS, **D**). After 16 hours, cells were fixed and stained with antibodies specific for LSm1 (red, **B**, **E**). Panels **C** and **F** show the merged picture of the proceeding two panels.

Shown in Fig. 5.21, panel **D**, is the shortest recombinant protein, YFP-eIF4E-T 430-503, that was generated and preserved the lack of self accumulation in the P bodies

as well as exerted the dominant negative effect on their stability, by de-localizing the marker protein LSm1 (**E**).

We next wanted to see if indeed, the C-terminal region of eIF4E-T contains the determinant(s) responsible for the accumulation of eIF4E-T into P bodies. A series of N-terminal deletion mutants was constructed taking into account the aminoacid sequence as well as the putative NES2 spanning between the aminoacids 613-638.

The largest C-terminal fusion-protein was designed to stretch from the site adjacent to the dominant negative domain, to the stop codon of the full-length eIF4E-T. As shown in Fig. 5.22, panel **A**, the YFP-eIF4E-T 505-985 protein is distributed throughout the cell, and despite its large size and the presence of the NES 2, it is well represented in the nucleoplasm, too, suggesting that NES2 is non-functional.

P bodies could be visualized by staining of the LSm1 marker (**B**), but from the overlaid picture (**C**) we learn that the C-terminal protein could not be incorporated into P bodies. Further fragmentation of the C-terminal domain did not result in proteins that could localize to the P bodies, either. This is the case with a central C-terminal construct, YFP-eIF4E-T 642-801, which is to a large extent enriched in the nucleoplasm and is not concentrated in any cytoplasmic structures (Fig. 5.22, **D**). Checking for the counterstaining with LSm1 (**E**), we observed a phenotype identical to that of the cells expressing the central eIF4E-T fragments that were lacking the P bodies (**F**). A similar phenomenon occurred when expressing YFP-eIF4E-T 770-985, which was also enriched in the nucleoplasm (**G**) but had a strong impact in the cytoplasm, where it resulted in a loss of P bodies, as shown by the LSm1 labeling (**H**), and in the superimposed pictures (**I**).

In summary, mapping of eIF4E-T did not result in the identification of a sequence targeting the protein to the P bodies, but rather of domains which act as powerful dominant negative effectors, probably by titrating out not yet determined factors (RNA or proteins).

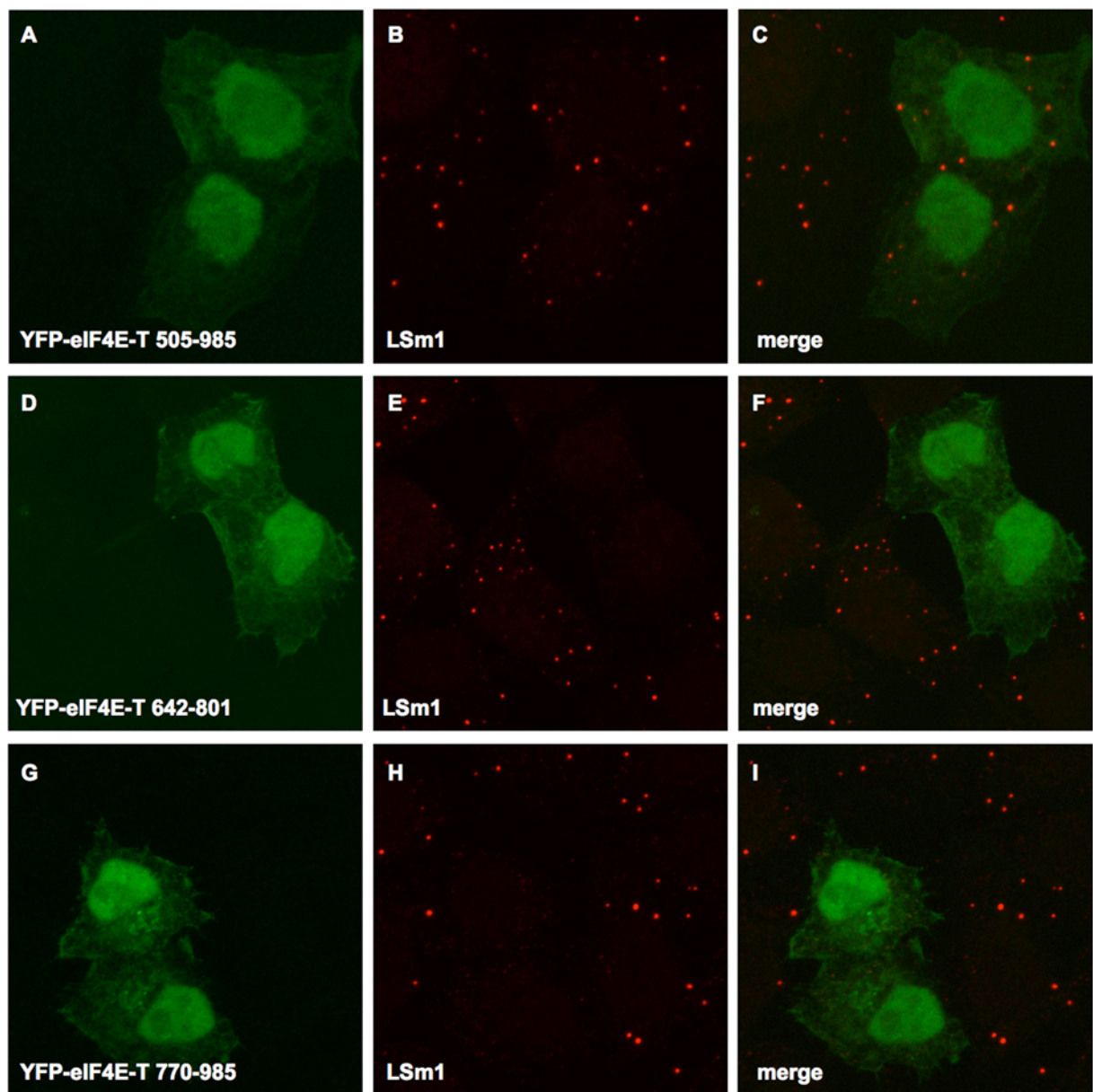


Figure 5.22. Cellular distribution of C- terminal fragments of the eIF4E-T molecule. HeLa SS6 cells were grown on coverslips for 24 hours, then transfected with plasmids encoding truncated YFP-eIF4E-T proteins (aminoacids 505-985 Δ NLS, **A**; aminoacids 642-801 Δ NLS, Δ NES, **D**, aminoacids 770-985 Δ NLS, Δ NES, **G**). After 16 hours, cells were fixed and stained with antibodies specific for LSM1 (red, **B**, **E**, **H**). Panels **C**, **F** and **I** show the merged picture of the proceeding two panels.

5.5 Biochemical investigations towards the elucidation of the P body composition

In order to understand more about the possible processes in which the P bodies are involved it was important to gain more insight of the composition of these domains. The dramatic effect that several eIF4E-T domains have on the P body stability underscores the major role that eIF4E-T plays in P body assembly. Hence, it appeared as a suitable approach to employ these dominant negative constructs in biochemical analyses aimed at identifying novel interaction partners that would allow for a better characterization of complexes residing in the foci.

A dual affinity purification procedure was initiated to try and identify specific interaction partners of P body components. For this, HeLa cells were co-transfected with vectors encoding for HA- and Flag-tagged P body- proteins, namely eIF4E-T, LSM1, Argonaute 2. Also, it seemed possible that a strong interaction, which destabilizes the P bodies, lies behind the dominant negative effect of the eIF4E-T 212-447 fragment. To expose this putative binding partner, HA and Flag constructs coding for the truncated eIF4E-T fragment were also employed in these purification experiments.

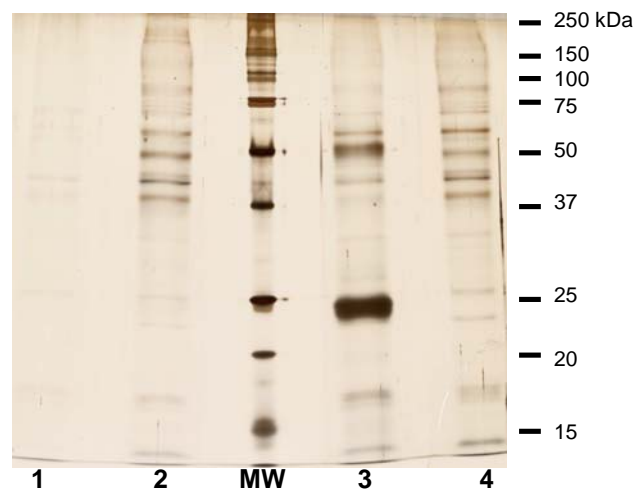


Figure 5.23. Dual affinity purification of P body components. HA and Flag-tagged proteins have been overexpressed in three different sets of HeLa cells. 32 hours after transfection of the expression vectors cells were harvested and cytoplasmic extracts were prepared. Extracts were incubated with a mixture of beads to which HA and Flag antibodies were covalently bound. After 5 hours, bound proteins were eluted with a mixture of HA and Flag peptides. Eluted proteins were separated electrophoretically on a polyacrylamide gel and visualized by silver staining as follows: eluate from an HA- and Flag-tagged eIF4E-T extract (lane 2), eluate from an HA- and Flag-tagged eIF4E-T 212-447 fragment extract (lane 3), eluate from an HA-LSM1, HA-Ago2 and Flag eIF4E-T extract (lane 4). Eluate of a cytoplasmic extract made from wild type HeLa cells was loaded onto lane 1.

32 hours after the vectors have been delivered to the cells, cytoplasmic extracts have been prepared and then incubated with a mixture containing HA and Flag affinity matrices, which would allow for more efficient recovery of complexes. Following binding to the matrix beads, proteins were eluted using a mix of HA and Flag peptides. Part of the eluate samples was visually inspected on an SDS denaturing polyacrylamide gel (Fig. 5.23). The rest of the immunoprecipitates were separated on an SDS-PAGE and following the in-gel trypsin digestion protocol, they were subjected to microsequencing by the Liquid Chromatograph-Mass Spectrometer. In the mass spectrometry analyses a number of proteins previously not related to the P bodies was retrieved.

Particularly interesting was to search among these, proteins with RNA binding properties. This is because, although the P bodies are considered to be sites of mRNA decay, only the LSm1-7 heteromeric complex, eIF4E and the GW182 protein are known as RNA interactors located to the foci. The discovery of new RNA binding proteins present in the P bodies could help explain how the mRNAs are targeted to the foci and also point out to specific *cis* features that make them a target for processing. Thus from several candidates the Polycytosine binding protein 1 (PCBP 1) was chosen, amplified by RT-PCR from HeLa total RNA and cloned into a CFP expression vector. Following transfection of the vector encoding the CFP-PCBP 1 fusion protein, the expression pattern was visualized by confocal microscopy (Fig. 5.24). As can be observed in panel A, PCBP1 has an extended localization, throughout the cytoplasm and the nucleoplasm of HeLa cells. Interestingly, tiny foci where the protein is enriched appear visible in the cytoplasm and they co-localize in the counterstaining with the P body marker LSm1 (C).

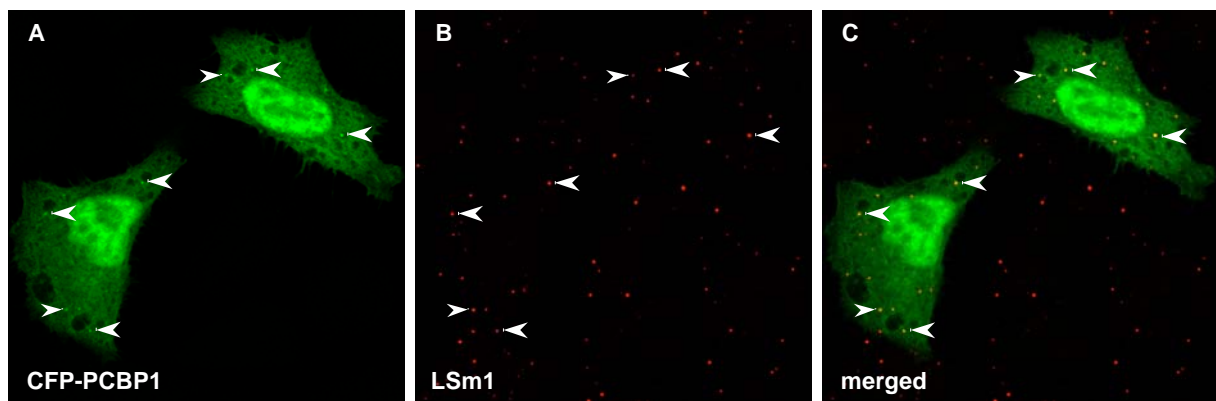


Figure 5.24. Expression pattern of the Polycytosine binding protein 1. HeLa SS6 cells were grown on coverslips for 24 hours, then transfected with a plasmid encoding for CFP-Poly Cytosine Binding Protein 1 protein (A). After 16 hours, cells were fixed and stained with antibodies specific for LSm1 (red, B). Panel C and shows the merged picture of the proceeding two panels where the overlapping signal appears yellow (arrowheads indicate P bodies).

The presence inside the P bodies of an RNA binding protein with sequence specificity is an indication for the mode of targeting of transcripts to the P bodies. Further analyses of its binding substrates could expand our knowledge on the expression regulation of particular mRNAs.

6. Discussion

In this study we address the sequence of events which results in silencing of a transcript that is actively translated, by its targeting to the Processing bodies as well as the requirements for the assembly of the P bodies. We demonstrate that the translation initiation factor eIF4E and two of its interaction partners are localized inside the P bodies and they may play a role in the remodeling of the translating mRNP particle to one in which the mRNA is repressed and made available for degradation. We established that the mRNA and several proteins are essential for the assembly of the P bodies. Our data support a model in which mRNPs undergo several successive steps of remodeling and/or 3' trimming until their composition or structural organization promotes their accumulation in P bodies. Additional proteins identified in this work as P body factors point out to a transcript-specific mode of targeting of mRNAs to these sites.

6.1.1 The translation initiation factor eIF4E and the translation inhibitor eIF4E-T are P body residents

A poorly understood process in the gene expression regulation field concerns the sequence of events that leads to targeting of an actively translating mRNA for degradation, within the P bodies. It appeared evident that a dramatic change in the mRNP composition has to take place in order for degradation factors to replace the translation machinery. Apart from previous extensive investigations at the 3' end of an mRNA, involving deadenylation, we considered that also factors interacting at the 5' end of the mRNA could be involved in such, that a block in translation initiation could potentially trigger the degradation process.

To get a first indication whether translation related factors play a role in this transition, we initiated an immunofluorescence localization screening in HeLa cells. By this, we found that eIF4E but not the translation scaffold protein eIF4G is present in the bodies (Fig. 5.1). This means that translationally active complexes are not

residing in the P bodies whereas the presence of the cap binding protein is indicative of capped mRNAs localization in the foci. In search of a factor responsible for destabilizing the eIF4E-eIF4G interaction we focused on a group of proteins, generically listed under the name of eIF4E inhibitory proteins. eIF4E-BP is an extensively studied regulator of overall translation levels in cells (Teleman et al., 2005). However data regarding its cellular localization was not available when we initiated this study. By performing immunolabeling experiments, or overexpressing fluorescently tagged eIF4E-BP in HeLa cells, we observed that the protein is diffusely spread throughout the cytoplasm and does not co-localize with markers for P bodies. In mammalian cells, a protein named eIF4E-Transporter was reported to bind to eIF4E through the consensus binding motif and to the same site as the other eIF4E binding proteins (Dostie et al., 2000). Although this novel factor was proposed to be a nucleocytoplasmic shuttling protein that functions in the nuclear import of eIF4E (Dostie et al., 2000), we checked its cellular distribution and found that it actually co-localized with eIF4E and LSM1 inside the P bodies (Fig. 5.6). This data speaks for an additional role of eIF4E-T in the cytoplasm, where it appears to be involved in translational repression and the transition to degradation of the mRNA. Interestingly, eIF4E-T possesses a short segment with a high degree of similarity to a region found in the *Drosophila* Cup protein (Zappavigna et al., 2004). Moreover, a recent report on *Drosophila* P bodies showed that they also contain Cup (Barbee et al., 2006).

The presence of eIF4E in mammalian P bodies is a first indication that, in addition to its involvement in translation initiation, eIF4E may also play a key role in mRNP remodeling events that target an mRNA for degradation in P bodies. As it appears, eIF4E-T likewise plays a special role in this process as it potentially inhibits the interaction of eIF4E with eIF4G, which would disrupt the communication between the 5' end of the mRNA and the poly(A) tail. This would in turn facilitate the inactivation of translation mRNP complexes and rendering them available for degradation inside the P bodies. Whether translational inactivation of the mRNA by eIF4E-T is also mediated by adaptor proteins (Fig. 6.1 A) such as CPEB, Bruno or Smaug, by analogy to the model discussed in section 2.3.2 (Fig. 2.4) and whether eIF4E-T targets the mRNA bulk or specific transcripts, requires further investigations.

Interestingly, there is no obvious counterpart for eIF4E-T in yeast cells, suggesting that not all aspects of mRNA regulation pathways are conserved between higher and lower eukaryotes. Moreover, although eIF4E was not found to be associated with yeast P bodies, retention of eIF4E in mammalian P bodies suggests that some mRNPs, while translationally repressed, may not immediately undergo 5'→3' degradation in these structures due to protection of the 5' cap against removal by the decapping enzyme Dcp1/2. This would be desirable in order to fit in a common yeast-human model of P body function, since it was shown in *Saccharomyces cerevisiae* that under specific experimental conditions, reporter mRNAs can exit the P bodies and resume translation (Brenques et al, 2005). Thus, mRNAs could be stored in P bodies in the form of an inactive mRNP before their fate is determined in a subsequent remodeling step. The presence of oligoadenylated mRNA in human P bodies comes in support of the model in which the mRNA could be reversibly stored as readily available substrate for new rounds of translation. This is because the structural elements needed to reinitiate translation are still present on the mRNA, namely the m⁷G cap and an oligo(A) tail which can be re-extended to produce a translationally competent mRNA. To establish whether P bodies, in addition to functioning as degradation sites, also represent mRNP storage sites or the place where the ultimate decision regarding the fate of an mRNA is made, requires additional studies.

6.1.2 The translational repressor rck/p54 is a P body resident

Data presented here and elsewhere demonstrate that the DEAD-box RNA helicase rck/p54 is also a component of P bodies (Fig. 5.8 B; also Cougot et al., 2004) and in other RNP granules of various organisms, involved in translation regulation and mRNA stability (reviewed in Weston and Somerville, 2006). The yeast counterpart, Dhh1, was shown to be a translational repressor that facilitates P body formation and activates decapping (Coller and Parker, 2005). It has recently been shown that rck/p54 is present together with eIF4E in RNP complexes in *Xenopus* oocytes and there it can repress translation (Minshall and Standart, 2004). Alike, our FRET studies indicate an interaction of rck/p54 and eIF4E in P bodies in vivo (Fig. 5.7). Thus, rck/p54 could also play an early role in the transition from translation to mRNA degradation in mammalian cells and modulate the interaction of eIF4E with components of the translation machinery. It is known that during translation eIF4G

interacts with the initiation factor 4E that is bound to the mRNA's 5' cap. Simultaneously, eIF4G interacts with the poly(A)-binding protein (PABP) that is bound to the 3' end of the mRNA. Thus, a closed loop, which has been shown to be necessary for optimal mRNA translation, may form between the 5' and 3' ends of the mRNA [for a review see Sachs and Varani (Sachs and Varani, 2000)]. However, based on the fact that P bodies also contain factors binding the 5' and the 3' end of the mRNA, one possible scenario is that there is also a molecular bridge formed between both ends of the mRNA. In this model, rck/p54 or eIF4E-T, which interact with eIF4E, might play a key, bridging role between components at the 5' and 3' end of the remodeled mRNA. This type of mRNA circularization could potentially replace the molecular bridge observed in active translation complexes, involving eIF4E, eIF4G and PABP, and by this, effect inhibition of translation.

6.1.3 The eIF4E Homologous Protein is a P body resident

An eIF4E related cap-binding protein was previously described in human, namely eIF4E Homologous Protein (Rom et al., 1998). We cloned and expressed it as a fluorescently-tagged fusion protein and could show that it co-localizes with P body markers. Since it does not bind to eIF4G (Rom et al., 1998, Hernandez et al., 2005), the function of eIF4E HP in translation remained elusive, until recent evidence from *Drosophila* came in support of a role for eIF4E HP in mediating cap-dependent translational control (Cho et al., 2005). There, eIF4E HP was shown to bind to the 5' cap of the caudal mRNA and simultaneously interact with Bicoid, whereas Bicoid also interacts with the Bicoid Binding Region present in the 3'UTR of caudal mRNA. This mechanism contrasts the Maskin, Neuroguidin or Cup mode of action, which involves translational repression by sequestration of eIF4E that can no longer form the initiation holoenzyme eIF4F (section 2.3.2). In turn, translation of the target mRNA, in this case caudal, can be repressed by sequestration of the cap itself from translation, by binding to the translational incompetent eIF4E HP. It is important to mention that Bicoid has no obvious vertebrate homolog, whereas eIF4E HP is widely present in somatic cells of higher eukaryotes. Thus, it will be interesting to explore the possibility of an adaptor protein mediating specific transcript repression via tethering of the 5' and 3' ends employing eIF4E HP, in mammals, too. Extrapolating this information, a model can be conceived in which mRNA sentenced for decay is

targeted via eIF4E HP to the P bodies where it is handed over to the degradation machinery (Fig. 6.1 B)

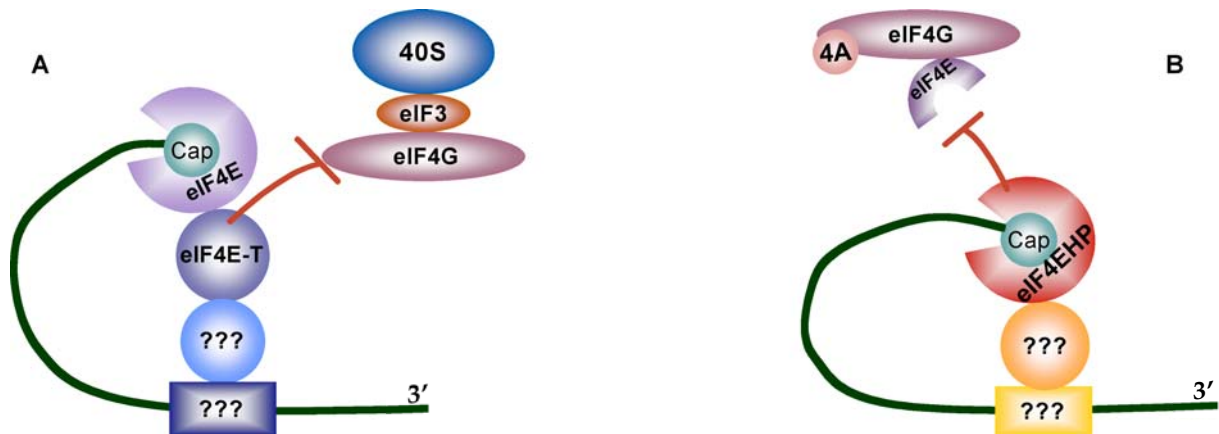


Figure 6.1. Proposed models for translational repression mediated by recruitment of the eIF4E-binding protein eIF4E-T or by sequestration of the m⁷G cap by eIF4E HP, in mammals.

(A) eIF4E-T binds to eIF4E and thus inhibits initiation of translation by blocking the assembly of the cap-binding complex, eIF4F, and recruitment of the 40S ribosomal subunit to the 5' end of the mRNA. Given its partial homology to the *Drosophila* Cup protein (see Fig. 2.4), an equivalent system can be envisioned, wherein eIF4E-T might have a still unknown binding partner that interacts with regulatory elements located on specific mRNAs, thereby controlling the fate of individual transcripts. (B) In *Drosophila*, translation of caudal mRNA is repressed upon sequestration of the 5' end cap structure by binding to eIF4E HP. eIF4E HP cannot bind to the translation scaffold protein eIF4G and thus, a translation initiation complex cannot form. To ensure for specificity of repression, Bicoid concomitantly interacts with eIF4E HP and docks onto its cognate binding site located in the 3'UTR of caudal mRNA. The discovery of the human homolog of eIF4E HP at a site of translational repression (the P body), suggests that it may also function in targetting of selected transcripts to these sites, in a manner mediated by an additional not yet identified adaptor proteins (similarly to Bicoid).

6.2.1 Depletion of P body proteins indicates a sequential assembly of the cytoplasmic structures and demonstrates the requirements for their assembly

A significant number of proteins with various functions have been so far identified as P body residents. Nevertheless, questions like how they are assembled into the foci, what is the sequence of events and precise coordination of the processes they take part in still wait for answers. Earlier work done in yeast employed deletion or conditional strains to establish the role of different factors with respect to mRNA stability (Hatfield et al., 1996, Schwartz and Parker, 1999, Tharun et al., 2000, 2005). To get more functional information concerning the role of individual P body components in human, we undertook a siRNA screen in which we depleted different factors and checked for subsequent intracellular modifications by immunostaining.

RNAi-mediated knockdown of eIF4E-T inhibited the accumulation of eIF4E, LSm1, rck/p54, and Ccr4 in P bodies, suggesting that repression of translation is an important remodeling event for the accumulation of mRNA and degradation factors in these structures. It is appealing to speculate that eIF4E-T could be involved in the earliest stages of the transition of an actively translating mRNA to one earmarked for degradation in P bodies. Not only does eIF4E-T depletion disrupt the P bodies, but also stability of a reporter mRNA was shown to have increased when eIF4E-T was missing from the cells (Ferraiuolo et al., 2005) meaning that eIF4E-T is a genuine player in the degradation pathway.

Also, RNAi-mediated knockdown of rck/p54 led to the loss of accumulation of P body factors in cytoplasmic foci. Previous studies indicated that in yeast, rck/p54 (Dhh1p) interacts with Dcp1 and may facilitate decapping (Coller et al., 2001). However, whereas knockdown of Dcp2 in HeLa cells revealed that it is not required for the accumulation of other RNA degradation factors in P bodies (Fig. 5.10), rck/p54 was required (Fig. 5.9). This suggests that rck/p54's function in higher eukaryotes is not limited to later stages of the degradation process, but rather that it plays a role in an early step. Data presented in a recent study revealed, also by depletion of rck/p54, a new role for this helicase, which additionally contacts Ago1 and Ago2, in the miRNA-induced and let-7-mediated translational repression (Cho and Rana, 2006). In the same study, depletion of the LSm1 protein, which also dispersed the P bodies, did not influence the inhibition of the let-7 miRNA target. Together, these observations point out to the intertwined pathways regulating the fate of the mRNA, which employ as a common site of action the P bodies and also suggest that at least one of the repression pathways, namely RNAi does not require the enrichment of its effectors in these structures for proper regulation of its targets.

Knockdown of two factors that bind the mRNA 3' end (e.g., Ccr4 and likely, also LSm1) prevented the accumulation of other degradation factors in P bodies (Fig. 5.10 and 5.9). This suggests that mRNAs must first be trimmed and then remodeled at their 3' end to convert the mRNP particle into a state that targets it to P bodies. Whether these events occur prior to remodeling steps at the 5' end of the mRNA is presently not clear. In yeast, Lsm1-7p play a role in deadenylation which leads to displacement of translation factors from mRNA (Tharun and Parker, 2001), suggesting they (together with Ccr4) might also play an early role in the transition from active translation to degradation. In contrast, knockdown of Dcp2 and Xrn1 did not inhibit the accumulation of eIF4E, LSm1, rck/p54, or Ccr4 in P bodies (Fig.

5.10 and Cougot et al, 2004). Thus we can infer that these enzymatic components, which catalyze decapping and subsequent 5'→3' degradation, do not appear to play a role in the targeting of mRNPs to the P bodies, but appear to act at a later stage i.e. after mRNPs accumulate in P bodies.

6.2.2 Variation of the mRNA flux to the P bodies has immediate repercussion on the organization of the cytoplasmic structures

In order to see how mRNA availability influences the formation of P bodies we treated HeLa cells with different drugs known to modulate the pool of free mRNA.

First, cycloheximide, which sequesters mRNAs onto polysomes, resulted into a fast dissolution of the P bodies, meaning that a constant flow of transcripts which exit translation are essential for assembly of the processing centers. In support of this idea, others have shown that by directly blocking RNA synthesis by the drug actinomycin D, which inhibits RNA Polymerase II, clearance of the bodies occurs, too (Cougot et al., 2004). Not only mRNA is synthesized by Pol II, but this enzyme was also described to transcribe miRNA genes (Lee et al., 2004). Thus its inhibition results in exhaustion of both RNA entities targeted to the P bodies, which has as a consequence dislodgement of the decay/silencing apparatus from the bodies, whose constitution becomes obsolete.

Next, we exposed the cells to the drug puromycin, which induces premature termination of translation and release of the mRNAs from polysomes. This resulted in a dramatic enlargement of the P bodies as visualized by immunostaining of several P body components. Therefore, an increase in freely available decay substrates can be correlated with an increase of the accumulation of degradation factors in P bodies, speaking for the necessity of a robust compartment that would allow for more efficient processing.

Taken together, data revealing the requirement for mRNA and demonstrating the interdependence of eIF4E-T, LSm1, rck/p54, and Ccr4 for the accumulation of each other and eIF4E in P bodies could be summarized in a model as follows. The mRNP reorganization towards P body integration could involve an allosteric cascade of interactions where the interaction of one factor is required for the subsequent recruitment of the next. Therein, do several factors sequentially interact with the

mRNA and only after the correct mRNP structure is formed, would these factors be transported together to P bodies as part of the mRNP.

6.2.3 P bodies are dynamic but stable structures

The fast onset of P body dissolution upon cycloheximide treatment indicated a fast turnover rate of its components. Indeed, fluorescence recovery after photobleaching measurements of several P body proteins demonstrated the quick exchange between the free cytoplasmic pool and that of the protein incorporated in the granules. The fact that the different proteins tested exhibit different exchange rates implies that they are a part of different (mRNP) complexes. Additional data coming from a time-lapse experiment where cells expressing fluorescently-tagged P body proteins have been monitored for several hours, demonstrated a remarkable stability of individual bodies over time. P bodies recorded largely maintained their position and did not dissociate in over three hours of the recording (data not shown).

6.3.1 Intact protein-protein interaction is vital for accurate targeting of the P body component eIF4E

For translation of a eukaryotic mRNA to take place, at the initiation step, eIF4E binds to the m⁷G cap at the 5' end. This is needed in order to stabilize the mRNA and facilitate binding of other translation factors that allow for further anchoring of the ribosomes in the translation process. We disrupted this interaction by mutating previously characterized residues (eIF4E^{WE102,103AA}). From the immunostaining experiment, it was manifest that this protein has a reduced potential to accumulate into P bodies, suggesting that binding of the mRNAs' cap by eIF4E is a prerequisite for its transfer to the P bodies. In other words, this is a strong indication that only capped mRNAs bound by eIF4E get to be recruited to the P bodies.

In a different mutagenesis experiment employing an eIF4E mutant (eIF4E^{W73A}, Fig. 5.15) the binding site to the P body component eIF4E-T was inactivated. The result was even more pregnant in that the cellular distribution of the recombinant eIF4E protein was totally altered. The protein distribution was diffuse and no cytoplasmic enrichments have formed; also an accumulation in the nuclear

compartment occurred. Although the observed redistribution of eIF4E most likely results from a loss of eIF4E-T binding, the eIF4E^{W73A} mutant could also fail to bind to other eIF4E interaction partners as well. This is because tryptophan 73 is the only one of eight conserved tryptophan residues of eIF4E that is exposed on the dorsal surface of the molecule as part of a hydrophobic region susceptible of interactions with proteins containing the common interaction motif Y-X-X-X-X-L-L (Marcotrigiano et al, 1999). Additionally, it was shown that the eIF4E^{W73A} mutant is also defective in binding the m⁷G cap and thus the effects of this mutation can be viewed as the result of the cooperative cap and eIF4E-T- binding inhibition.

The failure of an eIF4E mutant defective in eIF4E-T binding to locate inside the P bodies comes in support of the eIF4E-T depletion data where dissolution of the P bodies was recorded. From these observations we can infer that the interaction between eIF4E and eIF4E-T plays an important role in a remodeling event, which is necessary for the accumulation of mRNA and degradation factors in these structures.

In a knockdown and rescue assay, on a cellular substrate devoid of eIF4E-T and hence of P bodies (Fig. 5.9), exogenous wild type (Fig. 5.17 A) and mutant eIF4E-T^{LL35, 36GG} protein (Fig. 5.13 D), respectively, has been supplied to the cells. Whereas the wild type protein could fully restore de novo assembly of the P bodies, the recombinant protein containing an inactive eIF4E-binding site failed to regenerate the P body eIF4E pool (Fig. 5.17 C and F, respectively). Recent work done with a similar mutant eIF4E-T^{Y30A}, which also cannot interact with the cap-binding protein eIF4E (Ferraiuolo et al., 2005) shows that the protein is still capable of accumulating into cytoplasmic foci. We tested this mutant in our rescue assay and repeatedly observed that it is not able to restore the eIF4E P body pool. However, at least one component checked this far, LSm1 is detected to re-concentrate with the recombinant eIF4E-T^{Y30A} inside cytoplasmic foci (personal observation, data not shown). This means that a full-length mutated eIF4E-T protein is capable of forming structures that resemble P bodies, despite the lack of eIF4E indicating that eIF4E-T can assemble into foci *per se*. Future experiments are aimed to describe the nature of these structures in terms of organization and function, with respect to the canonical P bodies.

6.3.2 P body destabilizing domains within eIF4E-T

As shown in figure 5.18, eIF4E-T has a highly disorganized sequence and little was known about the eIF4E-T structure-function relationship. Having realized the crucial role of this protein in the organization of P bodies, we created a pool of deletion mutants, with the aim to find out whether there is a particular signal bearing responsibility for targeting of the protein to the P bodies. The constructs have been engineered to express the protein with different tags, enabling the microscopic visualization of the mutants. A common characteristic of all protein domains generated is that independently of the known functional features known so far that were included or not in the fragments (such as an intact eIF4E binding site), they were no longer competent to localize to the P bodies. This suggests that only the particular, unknown fold of the full-length protein may be capable of creating a favorable milieu, which allows the protein to assemble into the P bodies. Moreover, a series of dominant negative protein domains generated, have been observed to also dislocate other P body components, resulting in their complete dissolution. Further biochemical characterization of these dominant negative proteins is needed to explain the principle of their inhibition of the P body assembly, be it sequestration of other interacting proteins, or even, possibly of the mRNA substrate.

6.4 Identification of novel P body components using biochemical purification coupled to MS analyses

Much progress has been made in characterizing the P body composition and recent studies describe a number of translational repression systems driven by complex machineries, whose components are only partly known. Direct analysis of protein complexes by mass spectrometry has proven to be a powerful method for identification of novel interaction partners. Learning the identity and defining the roles of new P body components could help improve our present knowledge of their function. So, by analyzing the constitution of P body immunoprecipitates, it was possible to retrieve several factors novel to the cytoplasmic granules. RNA binding proteins are known to play crucial roles in RNA metabolism and determine their fate and stability (Dreyfuss et al., 2002). Even though P bodies are considered to be RNA processing sites, information about RNA-interacting factors is scarce and protein-complex analyses could bring insight about how selective targeting of specific

mRNAs to P bodies is achieved. We thus focused our attention on finding and selecting potential RNA-binding factors, and could originally show that the Poly(Cytosine) Binding Protein 1 (Leffers et al., 1995) is indeed enriched in P bodies. Initially, the protein was reported to participate in the formation of a sequence specific α -globin mRNP complex involved in the stability of the α -globin mRNA. This was mediated by the interaction with a cytosine rich domain, located in the 3' UTR of the globin mRNA (Kiledjian et al., 1995). More recent studies have indicated that PCBP1 alone, or in complex with hnRNP K RNA-binding protein, is able to silence translation of the LOX mRNA, again through interaction with the CU repeats, present in the 3' UTR of the mRNA (Ostareck et al., 1997, 2001). Other targets for translational inhibition by PCBP1, this time in association with hnRNP A2, were reported to be mRNAs containing A2 response elements (Kosturko et al., 2006). Moreover, from this latter study, which employed oligodendrocytes (non-neuronal cells that can perform synaptic transmission), it was possible to see that the two proteins co-localized with the target mRNA inside granules of unknown etiology.

One example where a P body-based regulatory mechanism is involved in sequence-specific mediated instability of particular mRNAs was described for the AU-rich elements (ARE) in the 3'UTR of the tumor necrosis factor- α (TNF α) transcript (Jing et al., 2005). There, the miR16 microRNA complementary to the ARE sequence was found to be required for ARE-RNA turnover, in a manner dependent on the ARE-binding protein tristetraprolin (TTP). TTP was shown to support targeting of the ARE-containing transcript by miR16 via its interaction with the RISC component AGO2. Future experiments will show whether stability of mRNAs containing C-rich sequences is regulated in a fashion similar to that described above, and whether PCBP acts as a TTP counterpart in a similar system.

7. References

- Achsel** T, Brahms H, Kastner B, Bachi A, Wilm M, Lührmann R. **1999**. A doughnut-shaped heteromer of human Sm-like proteins binds to the 3'-end of U6 snRNA, thereby facilitating U4/U6 duplex formation in vitro. *EMBO J* 18:5789–5802.
- Albert** TK, Lemaire M, van Berkum NL, Gentz R, Collart MA, Timmers HT. **2000**. Isolation and characterization of human orthologs of yeast CCR4-NOT complex subunits. *Nucleic Acids Res.* 28(3):809-17.
- Amrani** N, Sachs MS, Jacobson A. **2006**. Early nonsense: mRNA decay solves a translational problem. *Nature Rev. Mol. Cell Biol.* 7, 415–425.
- Andrei** MA, Ingelfinger D, Heintzmann R, Achsel T, Rivera-Pomar R and Lührmann R. **2005**. A role for eIF4E and eIF4Etransporter in targeting mRNPs to mammalian processing bodies. *RNA* 11, 717–727.
- Audhya** A, Hyndman F, McLeod IX, Maddox AS, Yates JR, Desai A, Oegema K. **2005**. A complex containing the Sm protein CAR-1 and the RNA helicase CGH-1 is required for embryonic cytokinesis in *Caenorhabditis elegans*. *J. Cell Biol.* 171, 267–278.
- Bagga** S, Bracht J, Hunter S, Massirer K, Holtz J, Eachus R, Pasquinelli AE. **2005**. Regulation by let-7 and lin-4 miRNAs results in target mRNA degradation. *Cell.* 122(4):553-63.
- Barbee** SA, Estes PS, Cziko AM, Hillebrand J, Luedeman RA, Collier JM, Johnson N, Howlett IC, Geng C, Ueda R, Brand AH, Newbury SF, Wilhelm JE, Levine RB, Nakamura A, Parker R, Ramaswami M. **2006**. Staufen- and FMRP-containing neuronal RNPs are structurally and functionally related to somatic P bodies. *Neuron* 52 997-1009
- Bartel** DP. **2004**. MicroRNAs: genomics, biogenesis, mechanism, and function. *Cell.* 116(2):281-97.
- Bashkirov** VI, Scherthan H, Solinger JA, Buerstedde JM, Heyer WD. **1997**. A mouse cytoplasmic exoribonuclease (mXRN1p) with preference for G4 tetraplex substrates. *J Cell Biol.* 136(4): 761-73.

Bastiaens PI. 1997. Fluorescence energy transfer microscopy (FRET). In JE, E. (ed.), Cell biology: A laboratory handbook. New York: Academic Press.

Behm-Ansmant I, Rehwinkel J, Doerks T, Stark A, Bork P, Izaurralde E. 2006. mRNA degradation by miRNAs and GW182 requires both CCR4:NOT deadenylase and DCP1:DCP2 decapping complexes. *Genes Dev.* 20(14):1885-98.

Benda C. 1891. Neue Mitteilungen über die Entwicklung der Genitaldrüsen und die Metamorphose der Samenzellen (Histogenese der Spermatozoen). Verhandlungen der Berliner Physiologischen Gesellschaft. *Archiv für Anatomie und Physiologie* 1891, 549–552.

Blum H , Beier H and GROSS HJ. 1987. Improved silver staining of plant proteins, RNA and DNA in polyacrylamide gels . *Electrophoresis* 8(2), 93-99.

Bouveret E, Rigaut G, Shevchenko A, Wilm M, Seraphin B. 2000. A Sm-like protein complex that participates in mRNA degradation. *EMBO J.* 19(7): 1661-71.

Bradford M M. 1976. A rapid and sensitive method for the quantitation of microgram quantities of protein utilizing the principle of protein-dye binding. *Anal Biochem* 72, 248-54.

Brengues M, Teixeira D, Parker R. 2005. Movement of eukaryotic mRNAs between polysomes and cytoplasmic processing bodies. *Science* 310(5747): 486-9.

Chang P, Torres J, Lewis RA, Mowry KL, Houlisto E and King ML. 2004. Localization of RNAs to the Mitochondrial Cloud in *Xenopus* Oocytes through Entrapment and Association with Endoplasmic Reticulum. *Mol Biol Cell*, 15, 4669-4681.

Chekulaeva M, Hentze MW, Ephrussi A. 2006. Bruno acts as a dual repressor of oskar translation, promoting mRNA oligomerization and formation of silencing particles. *Cell* 124(3):521-33.

Chen CY, Gherzi R, Ong SE, Chan EL, Raijmakers R, Pruijn GJ, Stoecklin G, Moroni C, Mann M, Karin M. 2001. AU binding proteins recruit the exosome to degrade ARE-containing mRNAs. *Cell.* 107(4): 451-64.

Chen J, Chiang YC, Denis CL. 2002. CCR4, a 3'-5' poly(A) RNA and ssDNA exonuclease, is the catalytic component of the cytoplasmic deadenylase. *EMBO J.* 21:1414-1426.

Cho P, Poulin F, Cho-Park YA, Cho-Park IB, Chicoine JD, Lasko P, Sonenberg, N. 2005. A new paradigm for translational control: inhibition via 5'-3' mRNA tethering by Bicoid and the eIF4E cognate 4EHP. *Cell* 121, 411–423.

Chu C Y and Rana T M. 2006. Translation repression in human cells by microRNA-induced gene silencing requires RCK/p54. *PLoS Biol.* 4, e210.

Coller JM, Tucker M, Sheth U, Valencia-Sanchez MA, Parker R. 2001. The DEAD box helicase, Dhh1p, functions in mRNA decapping and interacts with both the decapping and deadenylase complexes. *RNA* 7:1717-1727.

Coller J and Parker R. 2004. Eukaryotic mRNA decapping. *Annu. Rev. Biochem.* 73:861–890.

Coller J and Parker R. 2005. General Translational Repression by Activators of mRNA Decapping. *Cell* 122, 875–886.

Cougot N, Babajko S, Seraphin B. 2004. Cytoplasmic foci are sites of mRNA decay in human cells. *J. Cell Biol.* 165:31-40.

Czolowska R. 1969. Observations on the origin of the 'germinal cytoplasm' in *Xenopus laevis*. *J. Embryol. Exp. Morphol.* 22 229-251.

Dahanukar A, Wharton RP. 1996. The Nanos gradient in *Drosophila* embryos is generated by translational regulation. *Genes Dev.* 10(20):2610-20.

von Der Haar T, Ball PD, McCarthy JE 2000. Stabilization of eukaryotic initiation factor 4E binding to the mRNA 5'-Cap by domains of eIF4G. *J Biol Chem*, 275:30551-30555.

Ding L, Spencer A, Morita K, Han M. 2005. The developmental timing regulator AIN-1 interacts with miRISCs and may target the Argonaute protein ALG-1 to cytoplasmic P bodies in *C. elegans*. *Mol. Cell* 19, 437–447.

Dostie J, Ferraiuolo M, Pause A, Adam SA, Sonenberg N. 2000. A novel shuttling protein, 4E-T, mediates the nuclear import of the mRNA 5' cap-binding protein, eIF4E. *EMBO J.* 19:3142–3156.

Dreyfuss G, Kim VN, Kataoka N. 2002. Messenger-RNA-binding proteins and the messages they carry. *Nat Rev Mol Cell Biol.* 3(3):195-205.

Dunckley T, Parker R. 1999. The DCP2 protein is required for mRNA decapping in *Saccharomyces cerevisiae* and contains a functional MutT motif. *EMBO J.* 18(19):5411-22.

Elbashir SM, Lendeckel W, Tuschl T. 2001. RNA interference is mediated by 21- and 22-nucleotide RNAs. *Genes Dev.* Jan 15;15(2):188-200.

Elbashir SM, Harborth J, Weber K, Tuschl T. 2002. Analysis of gene function in somatic mammalian cells using small interfering RNAs. *Methods.* 26(2):199-213.

Eulalio A, Behm-Ansmant I and Izaurralde E. 2007. P bodies: at the crossroads of post-transcriptional pathways. *Nat. Rev. Mol. Cell Biol.* vol. 8 9-22.

Eystathioy T, Chan EKL, Tenenbaum S A, Keene JD, Griffith K, Fritzler MJ. 2002. A phosphorylated cytoplasmic autoantigen, GW182, associates with a unique population of human mRNAs within novel cytoplasmic speckles. *Molecular Biology of the Cell* 13, 1338–1351.

Eystathioy T, Jakymiw A, Chan EK, Seraphin B, Cougot N, Fritzler MJ. 2003. The GW182 protein colocalises with mRNA degradation associated proteins hDcp1 and hLSm4 in cytoplasmic GW bodies. *RNA* 9(10): 1 171-3.

Fan XC, Steitz JA. 1998. Overexpression of HuR, a nuclear-cytoplasmic shuttling protein, increases the in vivo stability of ARE-containing mRNAs. *EMBO J.* 17(12):3448-60.

Fasken MB, Corbett AH. 2005. Process or perish: quality control in mRNA biogenesis. *Nat Struct Mol Biol.* 12(6):482-8.

Ferraiuolo MA, Basak S, Dostie J, Murray EL, Schoenberg DR, Sonenberg N. 2005. A role for the eIF4E-binding protein 4E-T in P-body formation and mRNA decay. *J Cell Biol.* Sep 12;170(6):913-24. Erratum in: *J Cell Biol.* 2005 171(1):175.

Fischer N and Weis K. 2002. The DEAD box protein Dhh1 stimulates the decapping enzyme Dcp1. *EMBO J.* 21:2788–2797.

Frischmeyer PA, van Hoof A, O'Donnell K, Guerrierio AL, Parker R, Dietz HC. 2002. An mRNA surveillance mechanism that eliminates transcripts lacking termination codons. *Science.* 295(5563): 2258-61.

Gallie DR. 1991. The cap and poly(A) tail function synergistically to regulate mRNA

translational efficiency. *Genes Dev.*, 5, 2108–2116.

Gatfield D and Izaurrealde E. **2004**. Nonsense-mediated messenger RNA decay is initiated by endonucleolytic cleavage in *Drosophila*. *Nature* **429**, 575–578.

Gebauer F, Hentze MW. **2004**. Molecular mechanisms of translational control. *Nat Rev Mol Cell Biol.* 5(10):827-35.

Gingras A C, Raught B, Sonenberg N. **1999**. eIF4 initiation factors: effectors of mRNA recruitment to ribosomes and regulators of translation. *Annu. Rev. Biochem.* 68, 913–963.

Giraldez AJ, Mishima Y, Rihel J, Grocock RJ, Van Dongen S, Inoue K, Enright AJ, Schier AF. **2006**. Zebrafish MiR-430 promotes deadenylation and clearance of maternal mRNAs. *Science*. 312(5770):75-9.

Haghighat A, Mader S, Pause A and Sonenberg N. **1995**. Repression of cap-dependent translation by 4E-binding protein 1: competition with p220 for binding to eukaryotic initiation factor-4E. *EMBO J.* 14, 5701–5709.

Hatfield L, Beelman CA, Stevens A, Parker R. **1996**. Mutations in trans-acting factors affecting mRNA decapping in *Saccharomyces cerevisiae*. *Mol Cell Biol.* 16(10):5830-8.

Hernandez G, Altmann M, Sierra JM, Urlaub H, del Corral RD, Schwartz P, Rivera-Pomar R. **2005**. Functional analysis of seven genes encoding eight translation initiation factor 4E (eIF4E) isoforms in *Drosophila*. *Mech Dev.* 122(4):529-43.

Houseley J, LaCava J. and Tollervey D. **2006**. RNA-quality control by the exosome. *Nature Rev. Mol. Cell Biol.* 7, 529–539.

Hsu CL, Stevens A. **1993**. Yeast cells lacking 5'→3' exoribonuclease 1 contain mRNA species that are poly(A) deficient and partially lack the 5' cap structure. *Mol Cell Biol.* 13(8): 4826-35.

Humphreys DT, Westman BJ, Martin DI, Preiss T. **2005**. MicroRNAs control translation initiation by inhibiting eukaryotic initiation factor 4E/cap and poly(A) tail function. *Proc Natl Acad Sci U S A.* 102(47):16961-6.

Ingelfinger D, Arndt-Jovin DJ, Luhrmann R, Achsel T. **2002**. The human LSm1-7 proteins colocalise with the mRNA-degrading enzymes Dcp1/2 and Xrn1 in distinct cytoplasmic foci. *RNA.* 8(12): 1489-501.

Jing Q, Huang S, Guth S, Zarubin T, Motoyama A, Chen J, Di Padova F, Lin SC, Gram H, Han J. 2005. Involvement of microRNA in AU-rich element-mediated mRNA instability. *Cell*. 120(5):623-34.

Jung MY, Lorenz L, Richter JD. 2006. Translational control by neuroguidin, a eukaryotic initiation factor 4E and CPEB binding protein. *Mol Cell Biol*. 26(11):4277-87.

Kahvejian A, YV Svitkin, Sukarieh R, M'Boutchou MN, Sonenberg N. 2005. Mammalian poly(A)-binding protein is a eukaryotic translation initiation factor, which acts via multiple mechanisms. *Genes Dev*. 19:104–113.

Kedersha N, Anderson P. 2002. Stress granules: sites of mRNA triage that regulate mRNA stability and translatability. *Biochem Soc Trans*. 30(Pt 6): 963-9.

Kedersha N, Stoecklin G, Ayodele M, Yacono P, Lykke-Andersen J, Fitzler MJ, Scheuner D, Kaufman RJ, Golan DE, Anderson P. 2005. Stress granules and processing bodies are dynamically linked sites of mRNP remodeling. *J. Cell Biol*. 169:871–884.

Kiebler MA, Hemraj I, Verkade P, Kohrmann M, Fortes P, Marion RM, Ortin J, and Dotti CG. 1999. The mammalian stau protein localizes to the somatodendritic domain of cultured hippocampal neurons: implications for its involvement in mRNA transport. *J. Neurosci*. 19, 288–297.

Kiebler MA and Bassell GJ. 2006. Neuronal RNA granules: movers and makers. *Neuron* 51, 685-690.

Kimball SR, Horetsky RL, Ron D, Jefferson LS, Harding HP. 2003. Mammalian stress granules represent sites of accumulation of stalled translation initiation complexes. *Am. J. Physiol. Cell. Physiol*. 284: C273-84.

Kiledjian M, Wang X, Liebhaber SA. 1995. Identification of two KH domain proteins in the alpha-globin mRNP stability complex. *EMBO J*. 14 (17), 4357-4364.

Knowles RB, Sabry JH, Martone ME, Deerink TJ, Ellisman MH, Bassell GH, Kosik KS. 1996. Translocation of RNA granules in living neurons. *J. Neurosci*. 16, 7812-7820.

Kosturko LD, Maggipinto MJ, Korza G, Lee JW, Carson JH, Barbarese E. 2006. Heterogeneous nuclear ribonucleoprotein (hnRNP) E1 binds to hnRNP A2 and inhibits translation of A2 response element mRNAs. *Mol Biol Cell*. 17(8):3521-33.

Kotaja N, Bhattacharyya S N, Jaskiewicz L, Kimmins S, Parvinen M, Filipowicz W and Sassone-Corsi P. 2006. The chromatoid body of male germ cells: Similarity with processing bodies and presence of Dicer and microRNA pathway components PNAS 103 no. 8 2647–2652.

Krichevsky AM, Kosik KS. 2001. Neuronal RNA granules: a link between RNA localization and stimulation dependent translation. Neuron 32, 683–696.

Kshirsagar M and Parker R. 2004. Identification of Edc3p as an Enhancer of mRNA Decapping in *Saccharomyces cerevisiae* Genetics 166: 729–739.

Ladomery M, Wade E, Sommerville J. 1997. Xp54, the *Xenopus* homologue of human RNA helicase p54, is an integral component of stored mRNP particles in oocytes. Nucleic Acids Res. 25(5): 965–73.

Laemmli UK. 1970. Cleavage of structural proteins during the assembly of the head of bacteriophage T4. *Nature* 227, 680–5.

LaGrandeur TE, Parker R. 1998. Isolation and characterization of Dcp1p, the yeast mRNA decapping enzyme. EMBO J. 17(5):1487–96.

Lall S, Piano F, Davis RE. 2005. *Caenorhabditis elegans* Decapping Proteins: Localization and Functional Analysis of Dcp1, Dcp2, and DcpS during Embryogenesis. Molecular Biology of the Cell Vol. 16, 5880–5890.

Lai WS, Carballo E, Strum JR, Kennington EA, Phillips RS, Blackshear PJ. 1999. Evidence that tristetraprolin binds to AU-rich elements and promotes the deadenylation and destabilization of tumor necrosis factor alpha mRNA. Mol Cell Biol. 19(6):4311–23.

Lamphear B J, Kirchweger R, Skern T, Rhoads R E. 1995. Mapping of functional domains in eukaryotic protein synthesis initiation factor 4G (eIF4G) with picornaviral proteases. J. Biol. Chem. 270, 21975–21983.

Lasko P, Cho P, Poulin F, Sonenberg N. 2005. Contrasting mechanisms of regulating translation of specific *Drosophila* germline mRNAs at the level of 5'-cap structure binding. Biochem Soc Trans. 33(Pt 6):1544–6.

Lee Y, Kim M, Han J, Yeom KH, Lee S, Baek SH, Kim VN. 2004. MicroRNA genes are transcribed by RNA polymerase II. EMBO J. 23(20):4051–60.

- Leffers H, Dejgaard K, Celis JE. 1995.** Characterisation of two major cellular poly(rC)-binding human proteins, each containing three K-homologous (KH) domains. *Eur. J. Biochem.* 230 (2), 447-453.
- Lim LP, Lau NC, Garrett-Engele P, Grimson A, Schelter JM, Castle J, Bartel DP, Linsley PS, Johnson JM. 2005.** Microarray analysis shows that some microRNAs downregulate large numbers of target mRNAs. *Nature.* 433(7027):769-73.
- Liu J, Valencia-Sanchez MA, Hannon GJ, Parker R. 2005a.** MicroRNA-dependent localization of targeted mRNAs to mammalian P-bodies. *Nature Cell Biol.* 7 719-723.
- Liu J, Rivas FV, Wohlschlegel J, Yates JR 3rd, Parker R, Hannon GJ. 2005b.** A role for the P-body component GW182 in microRNA function. *Nat Cell Biol.* 7(12):1261-6.
- Lowell JE, Rudner DZ, Sachs AB. 1992.** 3'-UTR-dependent deadenylation by the yeast poly(A) nuclease. *Genes Dev.* 6(11):2088-99.
- Lykke-Andersen J. 2002.** Identification of a human decapping complex associated with hUpf proteins in nonsense-mediated decay. *Mol Cell Biol.* 22(23): 8114-21.
- Lykke-Andersen J, Wagner E. 2005.** Recruitment and activation of mRNA decay enzymes by two ARE-mediated decay activation domains in the proteins TTP and BRF-1. *Genes Dev.* 19(3):351-61.
- Mader S, Lee H, Pause A, Sonenberg N. 1995.** The translation initiation factor eIF-4E binds to a common motif shared by the translation factor eIF-4g and the translational repressors 4E-binding proteins. *Mol. Cell. Biol.* 15, 4990-4997.
- Mahowald AP. 1962.** Fine structure of pole cells and polar granules in *Drosophila melanogaster*. *J. Exp. Zool.* 151 201-215.
- Marcotrigiano J, Gingras AC, Sonenberg N, Burley SK. 1999.** Cap-dependent translation initiation in eukaryotes is regulated by a molecular mimic of eIF4G. *Mol Cell.* 3(6):707-16.
- Mendez R, Murthy KG, Ryan K, Manley JL, Richter JD. 2000.** Phosphorylation of CPEB by Eg2 mediates the recruitment of CPSF into an active cytoplasmic polyadenylation complex. *Mol Cell.* 6(5):1253-9.
- Metschnikoff E. 1865.** Veber die Entwicklung der Cecidomyienlarven aus dem Pseudovum. *Arch. Furr Naturg.* Bd 1.

Micklem DR, Adams J, Grunert S, St Johnston D. **2000**. Distinct roles of two conserved Staufen domains in oskar mRNA localization and translation. *EMBO J.* 19, 1366–1377.

Minshall N and Standart N. **2004**. The active form of Xp54 RNA helicase in translational repression is an RNA-mediated oligomer. *Nucleic Acids Res* 32(4), 1325–1334.

Miyawaki A, Tsien RY. **2000**. Monitoring protein conformations and interactions by fluorescence resonance energy transfer between mutants of green fluorescent protein. *Methods Enzymol.* 327: 472–500.

Morino S, Hazama H, Ozaki M, Teraoka Y, Shibata S, Doi M, Ueda H, Ishida T, Uesugi S. **1996**. Analysis of the mRNA cap-binding ability of human eukaryotic initiation factor-4E by use of recombinant wild-type and mutant forms. *Eur J Biochem.* 239(3):597–601.

Mühlemann O. **2005**. Applying the brakes on gene expression. *Nat Struct Mol Biol.* 12(12):1024–5.

Muhlrad D, Decker CJ, Parker R. **1995**. Turnover mechanisms of the stable yeast PGK1 mRNA. *Mol Cell Biol.* 15(4):2145–56.

Muhlrad D, Decker CJ, Parker R. **1994**. Deadenylation of the unstable mRNA encoded by the yeast MFA2 gene leads to decapping followed by 5'→3' digestion of the transcript. *Genes Dev.* 8(7): 855–66.

Mukherjee D, Gao M, O'Connor JP, Raijmakers R, Pruijn G, Lutz CS, Wilusz J. **2002**. The mammalian exosome mediates the efficient degradation of mRNAs that contain AU-rich elements. *EMBO J.* 21(1–2):165–74.

Naegele S and Morley SJ. **2004**. Molecular cross-talk between MEK1/2 and mTOR signaling during recovery of 293 cells from hypertonic stress. *J. Biol. Chem.* 44: 46023–46034.

Nakamura A, Amikura R, Hanyu K, Kobayashi S. **2001**. Me31B silences translation of oocyte-localizing RNAs through the formation of cytoplasmic RNP complex during *Drosophila* oogenesis. *Development.* 128(17): 3233–42.

Nakamura A, Sato K, Hanyu-Nakamura K. **2004**. *Drosophila* cup is an eIF4E binding protein that associates with Bruno and regulates oskar mRNA translation in

oogenesis. *Dev Cell*. 6(1):69-78.

Navarro RE, Shim EY, Kohara Y, Singson A, Blackwell TK. 2001. CGH-1, a conserved predicted RNA helicase required for gametogenesis and protection from physiological germline apoptosis in *C. elegans*. *Development*. 128(17): 3221-32.

Navarro RE and Blackwell TK. 2005. Requirement for P granules and meiosis for accumulation of the germline RNA helicase CGH-1. *Genesis* 42, 172-180.

Nelson MR, Leidal AM, Smibert CA. 2004. *Drosophila* Cup is an eIF4E-binding protein that functions in Smaug-mediated translational repression *EMBO J*. 23 (1), 150-159.

Okamura K, Ishizuka A, Siomi H, Siomi MC. 2004. Distinct roles for Argonaute proteins in small RNA-directed RNA cleavage pathways. *Genes Dev*. 18(14):1655-66.

Orban TI, Izaurralde E. 2005. Decay of mRNAs targeted by RISC requires XRN1, the Ski complex, and the exosome. *RNA* 11(4):459-69.

Ostareck DH, Ostareck-Lederer A, Wilm M, Thiele BJ, Mann M, Hentze MW. 1997. mRNA silencing in erythroid differentiation: hnRNP K and hnRNP E1 regulate 15-lipoxygenase translation from the 3' end. *Cell* 89(4):597-606.

Ostareck DH, Ostareck-Lederer A, Shatsky IN, Hentze MW. 2001. Lipoxygenase mRNA silencing in erythroid differentiation: The 3'UTR regulatory complex controls 60S ribosomal subunit joining. *Cell* 104(2):281-90.

Parker JS, Barford D. 2006. Argonaute: A scaffold for the function of short regulatory RNAs. *Trends Biochem Sci*. 31(11):622-30.

Parvinen M. 2005. The chromatoid body in spermatogenesis. *Int. J. Androl*. 28, 189–201.

Patterson GH, Piston DW and Barisas BG. 2000. Förster distances between green fluorescent protein pairs. *Anal. Biochem*. 284: 438-440.

Peng SS, Chen CY, Xu N, Shyu AB. 1998. RNA stabilization by the AU-rich element binding protein, HuR, an ELAV protein. *EMBO J*. 17(12):3461-70.

Pestova TV, Lomakin IB, Lee JH, Choi SK, Dever TE, Hellen CU. 2000. The joining of

ribosomal subunits in eukaryotes requires eIF5B. *Nature* 403, 332–335.

Pfaffl MW. 2001. A new mathematical model for relative quantification in real-time RT-PCR. *Nucleic Acids Res.* **29:** e45.

Pillai RS, Bhattacharyya SN, Artus CG, Zoller T, Cougot N, Basyuk E, Bertrand E, Filipowicz W. 2005. Inhibition of Translational Initiation by Let-7 MicroRNA in Human Cells. *Science* 309: 1573-6.

Ramirez CV, Vilela C, Berthelot K, McCarthy JE. 2002. Modulation of eukaryotic mRNA stability via the cap-binding translation complex eIF4F. *J. Mol. Biol.* 318: 951-962.

Rehwinkel J, Behm-Ansmant I, Gatfield D, Izaurralde E. 2005. A crucial role for GW182 and the DCP1:DCP2 decapping complex in miRNA-mediated gene silencing *RNA* 11:1640–1647.

Rhoades MW, Reinhart BJ, Lim LP, Burge CB, Bartel B, Bartel DP. 2002. Prediction of plant microRNA targets. *Cell* 110(4):513-20.

Richter JD, Sonenberg N. 2005. Regulation of cap-dependent translation by eIF4E inhibitory proteins. *Nature.* 433(7025):477-80.

Rivas FV, Tolia NH, Song JJ, Aragon JP, Liu J, Hannon GJ, Joshua-Tor L. 2005. Purified Argonaute2 and an siRNA form recombinant human RISC. *Nat Struct Mol Biol.* 12(4):340-9.

Rom E, Kim HC, Gingras AC, Marcotrigiano J, Favre D, Olsen H, Burley SK, Sonenberg N. 1998. Cloning and characterization of 4EHP, a novel mammalian eIF4E-related cap-binding protein. *J. Biol. Chem.* 273, 13104–13109.

Sachs AB, Sarnow P and Hentze MW. 1997. Starting at the Beginning, Middle, and End: Translation Initiation in Eukaryotes. *Cell* 89, 831–838.

Sachs AB, Varani G. 2000. Eukaryotic translation initiation: there are (at least) two sides to every story. *Nat Struct Biol.* 7(5):356-61.

Schmitter D, Filkowski J, Sewer A, Pillai RS, Oakeley EJ, Zavolan M, Svoboda P, Filipowicz W. 2006. Effects of Dicer and Argonaute down-regulation on mRNA levels in human HEK293 cells. *Nucleic Acids Res.* 34(17): 4801-15.

Schwartz DC, Parker R. 1999. Mutations in translation initiation factors lead to increased rates of deadenylation and decapping of mRNAs in *Saccharomyces cerevisiae*. *Mol Cell Biol.* 19(8):5247-56.

Schwartz DC, Parker R 2000. mRNA decapping in yeast requires dissociation of the cap binding protein, eukaryotic translation initiation factor 4E. *Mol Cell Biol*, 20:7933-7942.

Sen GL and Blau HM. 2005. Argonaute 2/RISC resides in sites of mammalian mRNA decay known as cytoplasmic bodies *Nature Cell Biol.* 7 633-636.

Shatkin AJ. 1976. Capping of eukaryotic mRNAs. *Cell* 9, 645–653.

Sheth U, Parker R. 2003. Decapping and decay of messenger RNA occur in cytoplasmic processing bodies. *Science.* 300(5620): 805-8.

Sheth U, Parker R. 2006. Targeting of aberrant mRNAs to cytoplasmic processing bodies. *Cell* 125(6):1095-109.

Smillie DA and Sommerville J. 2002. RNA helicase p54 (DDX6) is a shuttling protein involved in nuclear assembly of stored mRNP particles. *J.Cell Sci.* 115, 395-447.

St. Johnston D, Brown NH, Gall JG, Jantsch M. 1992. A conserved double-stranded RNA-binding domain. *Proc. Natl. Acad. Sci. USA* 89, 10979–10983.

Stebbins-Boaz B, Cao Q, de Moor CH, Mendez R, Richter JD. 1999. Maskin is a CPEB-associated factor that transiently interacts with eIF-4E. *Mol Cell* 4(6):1017-27.

Stoecklin G, Mayo T, Anderson P. 2006. ARE-mRNA degradation requires the 5'-3' decay pathway. *EMBO Rep.* 7(1):72-7.

Strome S, Wood WB. 1982. Immunofluorescence visualization of germ-line-specific cytoplasmic granules in embryos, larvae, and adults of *Caenorhabditis elegans*. *Proc. Natl. Acad. Sci. USA* 79 1558-1562.

Tanaka KJ, Ogawa K, Takagi M, Imamoto N, Matsumoto K, Tsujimoto M. 2006. RAP55, a Cytoplasmic mRNP Component, Represses Translation in *Xenopus* Oocytes *J. Biol. Chem.* 281 (52), 40096-40106.

Tang G, Reinhart BJ, Bartel DP, Zamore PD. **2003**. A biochemical framework for RNA silencing in plants. *Genes Dev.* 17(1):49-63.

Tarun S and Sachs AB. **1995**. A common function for mRNA and 3' ends in translation initiation in yeast. *Genes Dev.* 9, 2997–3007.

Tarun SZ, and Sachs AB. **1996**. Association of the yeast poly(A)- tail binding protein with translation initiation factor eIF-4G. *EMBO J.* 15, 7168–7177.

Teleman AA, Chen YW, Cohen SM. **2005**. Drosophila Melted modulates FOXO and TOR activity. *Dev Cell* 9(2):271-81.

Tharun S, He W, Mayes AE, Lennertz P, Beggs JD, Parker R. **2000**. Yeast Sm-like proteins function in mRNA decapping and decay. *Nature.* 404(6777):515-8.

Tharun, S. and Parker, R. **2001**. Targeting an mRNA for decapping: Displacement of translation factors and association of the Lsm1p–7p complex on deadenylated yeast mRNAs. *Mol. Cell.* 8: 1075–1083.

Tharun S, Muhlrads D, Chowdhury A, Parker R. **2005**. Mutations in the *Saccharomyces cerevisiae* LSM1 gene that affect mRNA decapping and 3' end protection. *Genetics.* 170(1):33-46.

Tucker M, Valencia-Sanchez MA, Staples RR, Chen J, Denis CL, Parker R. **2001**. The transcription factor associated Ccr4 and Caf1 proteins are components of the major cytoplasmic mRNA deadenylase in *Saccharomyces cerevisiae*. *Cell* 104(3):377-86.

Ullmannova V, Haskovec C. **2003**. The use of housekeeping genes (HKG) as an internal control for the detection of gene expression by quantitative real-time RT-PCR. *Folia Biol (Praha).* 49(6):211-6.

Unterholzner L and Izaurralde E. **2004**. SMG7 acts as a molecular link between mRNA surveillance and mRNA decay. *Mol. Cell* 16, 587–596.

Van Dijk E, Cougot N, Meyer S, Babajko S, Wahle E, Seraphin B. **2002**. Human Dcp2: a catalytically active mRNA decapping enzyme located in specific cytoplasmic structures. *EMBO J.* 21: 6915-6924.

Vilela C, Velasco C, Ptushkina M, McCarthy JE. **2000**. The eukaryotic mRNA decapping protein Dcp1 interacts physically and functionally with the eIF4F translation initiation complex. *EMBO J.* 19:4372-4382.

- Villaescusa** JC, Allard P, Carminati E, Kontogiannea M, Talarico D, Blasi F, Farookhi R, Verrotti AC. **2006**. Clast4, the murine homologue of human eIF4E-Transporter, is highly expressed in developing oocytes and post-translationally modified at meiotic maturation. *Gene* 15; 367:101-9.
- Wang** Z, Kiledjian M. **2000**. The poly(A)-binding protein and an mRNA stability protein jointly regulate an endoribonuclease activity. *Mol Cell Biol.* 20(17):6334-41.
- Wang** Z, Jiao X, Carr-Schmid A and Kiledjian M. **2002**. The hDcp2 protein is a mammalian mRNA decapping enzyme. *Proc Natl Acad Sci U S A.* 99(20) 12663–12668.
- Wells** SE, Hillner PE, Vale RD. and Sachs AB. **1998**. Circularization of mRNA by eukaryotic translation initiation factors. *Mol. Cell* 2, 135–140.
- Westhof** E, Filipowicz W. **2005**. From RNAi to epigenomes: how RNA rules the world. *Chembiochem.* 6(2):441-3.
- Weston** A, Sommerville J. **2006**. Xp54 and related (DDX6-like) RNA helicases: roles in messenger RNP assembly, translation regulation and RNA degradation. *Nucleic Acids Res.* 34 (10) 3082-3094.
- Wilhelm** JE, Hilton M, Amos Q, Henzel WJ. **2003**. Cup is an eIF4E binding protein required for both the translational repression of oskar and the recruitment of Barentsz J. *Cell Biol.* 163 (6), 1197-1204.
- Wilczynska** A, Aigueperse C, Kress M, Dautry F, Weil D. **2005**. The translational regulator CPEB1 provides a link between dcp1 bodies and stress granules. *J Cell Sci.* 118(Pt 5):981-92.
- Wilusz** CJ, Wormington M, Peltz SW. **2001**. The cap-to-tail guide to mRNA turnover. *Nat. Rev. Mol. Cell Biol.* 2:237–246.
- Yamashita** A, Chang TC, Yamashita Y, Zhu W, Zhong Z, Chen CY, Shyu AB. **2005**. Concerted action of poly(A) nucleases and decapping enzyme in mammalian mRNA turnover. *Nat Struct Mol Biol.* 12(12):1054-63.
- Yang** Z, Jakymiw A, Wood MR, Eystathioy T, Rubin RL, Fritzler MJ, Chan EK. **2004**. GW182 is critical for the stability of GW bodies expressed during the cell cycle and cell proliferation. *J Cell Sci.* 117(Pt 23): 5567-78.

Yang W H, Yu J H, Gulick T, Bloch K D, Bloch D B. **2006**. RNA-associated protein 55 (RAP55) localizes to mRNA processing bodies and stress granules. *RNA* 12, 547–554.

Zack GW, Rogers WE, Latt SA. **1977**. Automatic measurement of sister chromatid exchange frequency. *J. Histochem. Cytochem.* **25**: 741–753.

Zaessinger S, Busseau I, Simonelig M. **2006**. Oskar allows nanos mRNA translation in *Drosophila* embryos by preventing its deadenylation by Smaug/CCR4. *Development* 133(22):4573-83.

Zappavigna V, Piccioni F, Villaescusa JC, Verrotti AC. **2004**. Cup is a nucleocytoplasmic shuttling protein that interacts with the eukaryotic translation initiation factor 4E to modulate *Drosophila* ovary development. *Proc Natl Acad Sci U S A.* 101(41):14800-5.

Appendix

List of figures

Figure 2.1	Current model of mammalian 5' to 3' mRNA degradation pathway	7
Figure 2.2	Biogenesis of and post-transcriptional gene regulation by siRNAs and miRNAs	9
Figure 2.3	The closed loop model of cap-dependent translation	13
Figure 2.4	Translational repression mediated by eIF4E binding proteins	15
Figure 5.1	The translation initiation factor eIF4E localizes to the cytoplasm of HeLa cells and is enriched in foci containing LSm1.	42
Figure 5.2	The eIF4E- Homologous Protein localizes to the cytoplasm of HeLa cells and is enriched in foci containing LSm1.	43
Figure 5.3	Stress granules are structures distinct from the Processing bodies.	44
Figure 5.4	Consensus sequence of eIF4E interacting proteins	45
Figure 5.5	The rck/p54 protein is enriched in the cytoplasmic Processing bodies.	46
Figure 5.6	The eIF4E-Transporter protein is enriched in the cytoplasmic Processing bodies.	47
Figure 5.7.	eIF4E and eIF4E-T proteins interact directly in vivo as demonstrated by FRET.	48
Figure 5.8.	Efficient knockdown of Ccr4, LSm1, eIF4E-T, Dcp2 and rck/p54 mRNA levels is achieved by RNA interference as demonstrated by real-time RT-PCR.	50
Figure 5.9	eIF4E-T, LSm1, rck/p54, are required for the accumulation of each other and of eIF4E and Ccr4 in P bodies.	52
Figure 5.10	Ccr4, but not Dcp2, is required for the accumulation of P body components.	53
Figure 5.11	Effect of cycloheximide on the accumulation of LSm1, eIF4E, rck/p54, and eIF4E-T in P bodies	54

Figure 5.12	Effect of puromycin on the accumulation of eIF4E and LSm1, in P bodies	55
Figure 5.13	Fluorescence recovery after photobleaching indicates that P bodies have a highly dynamic nature.	56
Figure 5.14	Accumulation of eIF4E in P bodies is negatively affected upon loss of cap binding.	57
Figure 5.15	Accumulation of eIF4E in P bodies does not occur following removal of the eIF4E-T binding site.	58
Figure 5.16	Accumulation of a mutant eIF4E-T protein in P bodies is not affected upon loss of eIF4E binding.	59
Figure 5.17	On a cellular substrate depleted of endogenous eIF4ET, only the wild-type, externally provided eIF4ET is able to restore de novo formation of P bodies.	60
Figure 5.18	Structural and functional features of the eIF4E-T molecule	61
Figure 5.19	Schematic representation of the eIF4E-T molecule and several of its deletion constructs generated in order to define a P body localization signal	62
Figure 5.20	Cellular distribution of N- terminal fragments of the eIF4E-T molecule	64
Figure 5.21	Cellular distribution of constructs expressing central domains of the eIF4E-T molecule	65
Figure 5.22	Cellular distribution of C- terminal fragments of the eIF4E-T molecule	67
Figure 5.23	Dual affinity purification of P body components	68
Figure 5.24	Expression pattern of the Polycytosine binding protein 1	69
Figure 6.1	Proposed models for translational repression mediated by recruitment of the eIF4E-binding protein eIF4E-T or by sequestration of the m ⁷ G cap by eIF4E HP, in mammals	75

List of tables

Table 2.1	Protein composition of P bodies	5
Table 4.1	Primers used to amplify the ORF of several P body resident proteins	28
Table 4.2	Primers used to amplify eIF4E-T deletion constructs with the full-length eIF4E-T protein serving as template	28
Table 4.3	Primers used to insert point mutations in the ORF of eIF4E and eIF4E-T	29
Table 4.4	siRNA oligonucleotides (forward strand) used for knockdowns in HeLa cells	31
Table 4.5	Primers used in qRT-PCR to verify efficiency of mRNA reduction upon treatment of HeLa cells with the respective siRNAs	32

Curriculum vitae

Personal information

Name: Maria Alexandra Andrei
Date and place of birth: 27 May 1979, Bucharest, Romania

Education

- 1997** School Leaving Examination at “Stefan cel Mare” High School, Suceava, Romania
- 1997-2001** Study of Biochemistry, Faculty of Biology, University of Bucharest
Bachelor of Science: July 2001
- 2001-2002** Molecular Biology Graduate Program, Göttingen, Germany
- 2002-2003** Master Thesis at the Max-Planck-Institut for Biophysical Chemistry, Göttingen, Gene Expression Laboratory, under supervision of Dr. R. Rivera-Pomar
Project: “*siRNA screen of human translation initiation factors*”.
Master of Science: September 2003
- Since 2003** PhD Thesis in the Graduate College 521
at the Max-Planck-Institut for Biophysical Chemistry, Göttingen,
Department Cellular Biochemistry, under supervision of Prof. Dr. R. Lührmann
Project: “*Characterization of cytoplasmic bodies involved in 5' to 3' mRNA degradation in human cells*”.

Publications

- 2005** Andrei, M.A., Ingelfinger, D., Heintzmann, R., Achsel T., River-Pomar, R., Lührmann, R. A role for eIF4E and eIF4E transporter in targeting mRNPs to mammalian processing bodies. *RNA* **11**: 717-727
- 2006** Donnert G, Keller J, Medda R, Andrei MA, Rizzoli SO, Lührmann R, Jahn R, Eggeling C, Hell SW. Macromolecular-scale resolution in biological fluorescence microscopy. *Proc Natl Acad Sci U S A*. 103(31): 11440-5.

Conference contributions

- 2004** Minisymposium of the Graduate College “Membrane transport/ Protein-Protein interactions”, held in Bad-Münster am Stein-Ebernburg, Germany: Oral presentation.
- 2004** ELSO 2004 and the 8th International World Congress of Cell Biology, held in Nice, France: Poster “Targeting of mRNAs to human Processing bodies”.
- 2005** Eukaryotic mRNA Processing Meeting, Cold Spring Harbor Laboratory/ USA: “eIF4E-T interacts with the cap-binding protein eIF4E inside the Processing bodies and is required for their assembly”